ABSTRACT

NORTON, TAYLOR MONTGOMERY. 3D Orthogonal Woven Glass Fiber Reinforced Polymeric Bridge Deck: Fabrication and Experimental Investigation. (Under the direction of Dr. Sami Rizkalla and Dr. Amir Mirmiran.)

Rapid deterioration of civil infrastructure has created one of the major challenges facing the construction industry. In recent years, fiber reinforced polymers (FRP) have emerged as a potential solution to the tribulations associated with deficient bridge decks. The main objective of the proposed research is to adapt the 3-D orthogonal 3Weaving™ process to develop an innovative completely woven fiber reinforced polymeric bridge deck.

The research accomplished fabricating a unique 3Weaving™ loom capable of weaving an E-glass preform which "puffs out" into an open cell truss-like structure aimed to overcome each the weaknesses of its predecessors. The project succeeded in providing fiber reinforcement through the connection of the truss core components with the outer composite deck skins. The loom provided continuous fiber reinforcement through these top and bottom skins. And the innovative fiber architecture provided in-plane fiber reinforcement in each of the structural components. Two 5' long by 15" wide deck preforms were produced: the first 1 ½" thick and the second 3" thick. In addition, a 2' long by 12" wide by 1 ½" thick non-truss composite deck was produced for comparison. The truss oriented decks utilized triangular cut shafts of Balsa as core inserts, and the non-truss deck maintained a rectangular block of Balsa core; each deck was infused with an epoxy resin; and concrete was cast atop. Each of the decks was tested for stiffness and strength in three-point bend. The stiffness tests comprised loading and unloading the deck in 2 kip increments up to 22 kips and using linear regression analysis to ascertain any degradation in stiffness. The strength tests consisted of loading the deck until failure. The testing exemplified the importance of the attachment of the core structural components to the outer composite deck skins and demonstrated a resistance of delamination of the core to the outer skins and the outer skins to themselves.

3D Orthogonal Woven Glass Fiber Reinforced Polymeric Bridge Deck: Fabrication and Experimental Investigation

by

Taylor Montgomery Norton

A thesis submitted to the Graduate Faculty of
North Carolina State University
in partial fulfillment of the
requirements for the Degree of
Master of Science

Civil, Construction, and Environmental Engineering

Raleigh

August 11, 2004

APPROVED BY:

_____ _____

_____ _____

(Chair of Advisor Committee) (Co-Chairman)

DEDICATION

I dedicate this thesis to my wife Kristin Usner Norton.
Thank you for always supporting me.
You inspire me in my work and in my life.
I love you, you are my angel.

Biography

Taylor Montgomery Norton was born in New Orleans, Louisiana on December 7, 1979. Raised in New Orleans, he graduated from the elite Jesuit High School in N.O.L.A. He attended Louisiana State University where he received his Bachelor of Science in Pure Mathematics in the spring of 2002.

In the fall of 2002, the author enrolled in the department of Civil Engineering at North Carolina State University in Raleigh pursuant to the degree of Master of Science. While at North Carolina State University, he was offered the IGERT Fellowship which involved an interdisciplinary approach to advanced research. As part of this Fellowship, he attended Virginia Polytechnic Institute and State University in Blacksburg, Virginia in the spring of 2003 where he studied Macromolecular Engineering for use in civil infrastructure. Returning to North Carolina, the author then utilized this knowledge with his research of Fiber Reinforced Polymeric Bridge Decks.

Taylor Norton received his Master of Science from North Carolina State University with an emphasis in Structures and Mechanics in 2004. He then accepted a notable scholarship to Campbell University School of Law where he is a candidate for the degree of Juris Doctor in 2007.

Acknowledgements

The author would like to thank the following people and organizations:

-Dr. Sami Rizkalla, my committee chair. Dr. Rizkalla taught me how to compose myself as a professional and how to effectively interact with various personalities. This is the most valuable lesson I take with me as I leave Raleigh. Dr. Rizkalla is distinguished engineer and a leader in the world of civil engineering. I must also thank Dr. Rizkalla for his guidance, patience, and support he showed with the completion of this project and thesis.

-Dr. Amir Mirmiran, my committee co-chair, for his knowledge and support he provided me over the scope of the project. Dr. Mirmiran is one of the most intelligent and technically thorough persons I have ever met, and as such, he had a significant impact on the quality of my project.

-Dr. Emmett Sumner, committee member, for his overall engineering knowledge. Dr. Sumner is a well learned structural engineer who facilitates an "easy going" atmosphere. I have enjoyed being able to stop by his office "any time" for quick advice on the project.

-Dr. John J. "Jack" Lesko, committee member, for the opportunity he provided me in going to Virginia Tech. as part of the IGERT Research Fellowship. Jack is one of the most knowledgeable people I know, and his guidance at Virginia Tech. ignited my interest in research of advanced composite materials. Thank you for making me feel "at home" while in Blacksburg, it was one of the best times of my life.

-Robert W. "Bob" Schartow, engineer at 3Tex, Inc. Cary, North Carolina, for his unending assistance and advice in the fabrication of the composite bridge deck. I thank you Bob for the early mornings and late nights you spent with me at 3Tex from "resin calculations" to "trying to infuse a porcupine." It has been a pleasure brainstorming composite deck ideas in your office for the last two years.

-**Mr. Brad Dickinson**, textile engineer at 3Tex, Inc. Rutherfordton, North Carolina, for the extra effort he always gave in keeping this 3Tex project going. Brad stands to be one of the hardest working persons I know as well as a great engineer and machinist. I thank him for his many drives into Cary to work on the project.

-**Joey and Steve**, textile engineers at 3Tex, Inc. Rutherfordton, North Carolina for the long hours we pulled in weaving the first preform off the loom.

-Dr. Mansour Mohamed, Dr. Dmitri Mungalov, Dr. Alex Bogdanovich, Mr. Donald E. Wigent III, Mr. Patrick Duke, the Engineering Research and Development Team at 3Tex, Inc. in Cary, North Carolina, for the time, effort, and resources provided to bridge deck project. These gentlemen introduced me to the world of textile engineering and its capabilities. I have enjoyed my time working at 3Tex, yet I further enjoy the knowledge I take with me.

-Ms. Suzanne Anderson, international graduate student intern, for the tremendous effort in assisting me with the weaving process. I enjoyed our morning coffee, friendship, and hard work, not to forget your Danish culture.

-Mr. Tarek Mohamed, graduate student, for your help with the weaving and our good conversations.

-Mr. Lee Nelson, Research Engineer and Laboratory Manager of the Constructed Facilities Laboratory at North Carolina State University, for his outstanding expertise in the testing laboratory. Lee is technically precise, and I thank him for the help in the lab.

-**Dr. Tarek Hassan**, Post Doctoral Research Associate at North Carolina State University, for his assistance with the test setups, data acquisitions, and engineering advice throughout the research.

And finally, I would like to thank **Sidney** and **Leslye Usner** for being such wonderful support through my graduate program.

TABLE OF CONTENTS

List of Tables

List of Figures

Chapter 1: Introduction and Literature Review

1.1 Introduction

Deterioration of civil infrastructure and cost of rehabilitation are major challenges facing the construction industry. It has been well documented by the Federal Highway Administration that approximately half of the nation's 600,000 Federal, state, county and city bridges were built before 1940 (to load classification designs) and that approximately 200,000 bridges are either structurally deficient or functionally obsolete (Zureick et al. 1997). A study indicated that almost 132,000 of those bridges are deficient by poor decking conditions attributable to deterioration or sub standardization. Traditional rehabilitation of these structures is expensive and time consuming. The National Science Foundation is reacting to this dilemma by facilitating research of improved methods and materials of rehabilitating these bridge decks.

In recent years, fiber reinforced polymers (FRP) have emerged as a potential solution to the tribulations associated with civil infrastructure. The aerospace industry has capitalized the use of reinforced composites, known for their extensive outstanding material properties, for decades. The high strength to weight ratio, stiffness to weight ratio, and corrosion and fatigue resistance of FRP composites make them an attractive structural component for use in the construction of new bridges and retrofitting of existing bridges (Harik et al 1999). Well established industrial corporations such as Martin Marietta Materials and Creative Pultrusions have just recently begun fabricating and manufacturing Glass Fiber Reinforced Polymeric Bridge Decks (GFRP) such as "Duraspan" and "Superdeck" in response to this growing demand of long-lasting civil infrastructure.

Composites using glass reinforcing fibers are called glass fiber reinforced polymers (GFRP). Fiber types can vary and include E-glass, S-glass, Carbon, Kevlar, Graphite, Boron and others. The preference of a specific reinforcing fiber depends on the desired mechanical properties of the composite, such as strength and modulus of elasticity, and the relative cost. Fiber reinforcement appears in several forms including chopped strands, continuous strands, or woven fabrics with fibers in defined directions. In order to maximize the material properties, careful attention must be given to fiber

orientation and the resulting fiber architecture. One primary concern for this present research to optimize fiber orientation of a GFRP bridge deck panel by inducing a new textile engineering weaving process originated and patented at the Textile Engineering Department at North Carolina State University and licensed to the textile engineering company 3TEX™ located in Cary, North Carolina.

The author assisted 3TEX™ in building a machine capable of utilizing the innovative 3WEAVE™ weaving technique in fabricating a completely woven continuous glass fiber bridge deck preform. This preform will "puff out" into a modular 3 inch thick bridge deck panel with V-shaped (truss-like) cell orientation. The cells will be packed with triangular cut shafts of lightweight Balsa wood, and the deck will be vacuum resin infused. The initial target is to develop a product that will meet AASHTO HS-20 standard specifications.

This research will encompass testing the new bridge deck along with the material properties of the components comprising the specimen. The deck will be tested in three-point bend and analyzed. Particular attention will be given to the connection points of the structural components of the truss-like bridge deck as the new weaving technique introduces a continuous fiber continuity never achieved or built before by the composite industry.

1.2 Objectives

The primary goal of this project is to utilize the advancements in the three-dimensional weaving technology in developing an innovative GFRP deck system that satisfy AASHTO HS-20 performance specifications. The specific objectives of this research are as follows:

1. Generate appropriate modifications to the 3-D weave fabrication process to develop a viable FRP deck with improved strength and stiffness properties and most importantly which delays the common delamination failure observed in other GFRP decks.
2. Fabricate and experimentally characterize the skin and core of the deck system for optimization of fiber content.

3. Assess the feasibility and evaluate the implications of using the 3-D weaving process on the structural behavior of FRP bridge decks by scaled model tests prior to full-scale prototype tests.

1.3 Literature Review

1.3.1 Design Live Loads and Tire Contact Area

The design of elements of a bridge is governed by requirements of the American Association of State Highway and Transportation Officials (AASHTO) LRFD specifications (1998) and the AASHTO standard specifications (1996). The LRFD specification defines the reliability-based limit states to be considered in bridge deck design and provides load combinations and load factors. The design live loads consist of standard truck or lane loads that are equivalent to truck trains. Figure 1.1 shows the standard H truck loading, while figure 1.2 shows the standard HS truck loading giving wheel spacing and load distribution. Figure 1.3 gives the equivalent lane loading for both the H and HS20-44 and the H and HS 15-44 categories. These loads are placed at critical locations to produce maximum load effects. The configuration that produces the greatest stress is the design load.

AASHTO defines the finite surface area of the deck beneath the AASHTO truck wheel as the "tire contact area." The method governing the computation of this area is for reinforced concrete bridge decks. Most researchers have opted to apply this technique since there is currently no provision related to FRP decks in AASHTO's specifications. AASHTO LRFD Bridge Design Specifications (1998, 2nd Edition, Vol. 1, Section 3.6.1.2.5) states the tire contact area of a wheel consisting of one or two tires shall be assumed to be a rectangle, whose width is 20.0 inches and whose length in inches shall be taken as:

$$l = \gamma(1 + IM/100)P/2.5$$

where:

$\gamma =$ load factor

$IM =$ dynamic load allowance percent

$P =$ design load

The actual distribution of tire pressure is so small that the variation can be safely neglected in practical design.

1.3.2 Legal Truck Loads

The design truck load is not an actual weight of a truck but rather a conceptual demonstration guiding the requirements of construction to ensure safety. The truck loading is defined as the weight induced by each individual axle of the vehicle. Thus, axle weight limits are set forth by law to prevent a vehicle from overstressing the bridge structure. The Federal-Aid Highway Amendments of 1974 increased the weights allowed on the Interstate System to 20,000 pounds on a single axle, 34,000 pounds on a tandem axle, and 80,000 pounds gross weight (23 U.S.C. 127) (USDOT 1994).

The H truck load is a model representative of all trucks while the HS truck load is representative of a truck with a semi-trailer. The proposed 3Weave^{TM} GFRP bridge deck is deigned to achieve HS20-44 performance requirements. Illustrated in figure 1.3, the legal design per axle is 32,000 lbs., and thus the legal wheel weight shall be assumed to be 16,000 lbs (50% of legal axle).

1.3.3 Live Load Deflections

AASHTO LFRD Bridge specifications state there are as yet no simple definitive guidelines for the limits of tolerable static deflection or dynamic motion. Rather, these provisions permit the use of past practice for deflection control. Designers are permitted to exceed these limits at their discretion. In the absence of other criteria, the deflection limit to be considered for steel, aluminum, and/or concrete construction for "General Vehicular Load" is Span/800 (or L/800 where L is the length of the effective span or center-to-center distance between supports). Without specific guidelines for the deflection limits of FRP composite bridge decks, most researchers cite L/800 as their deflection criteria. This can also be referred to as a deflection index, and moreover, researchers are known to compare their experimental deflection indices against the L/800 deflection index.

1.3.4 Previously Conducted Research

Interest in fiber-reinforced polymeric bridge decks began almost 20 years ago. With recent advances in manufacturing techniques, multiple research papers and reports have been published pertaining to a true FRP bridge deck structure. A true FRP deck structure is defined as being made solely out of FRP (without regard to the wearing surface).

To the author's knowledge, the first published document of the subject was written by John Henry in 1985. Since then, a number of research papers have been published including but not limited to those by Shih (1995), Karbhari et al. (1997), Lopez-Anido et al. (1997a, 1997b), Harik et al. (1999), and Zureick et al (1997). In addition to these papers exist actual FRP deck systems in use today, namely "Duraspan" by Martin Marietta Materials and "Superdeck" by Creative Pultrusions.

At North Carolina State University, John Henry analyzed five single-span E-glass/epoxy deck panels using the computer program SAP IV. He investigated several cross sectional configurations (*Figure 1.4*) of the deck panel. Each deck was 8 inches long (in the direction of traffic), 9 inches thick, and comprised an effective span of 7 feet.

Henry researched the deflection of the deck beneath an HS-20 44 wheel load of 16 kips distributed over an 8 inch (traffic direction) by 20 inch area. The deck system consisted of a span equal to that of the roadway (assumed to be 28 feet) and the width of which is equal to the tire contact dimension of 8 inches (*Figure 1.5*). The load was placed at the critical section of each of the four 7 foot spans to achieve the largest deflection. Only lateral distribution of loads was assumed, or the load was carried to the supports by one-way (lateral) action only. The deck is assumed to behave as a one-way slab as the longitudinal span length is more than twice the lateral (perpendicular to the direction of traffic flow) span length.

Henry first analyzed the system as 4 simple supported spans and then a second time as a continuous system.

In the analysis computation, only wheel loads were considered, i.e., no additional loads like wind, creep, and dynamic effects were considered. Henry assumed a modulus of elasticity of 3,000 ksi since his composite was composed of E-glass with a

fiber orientation of 0, +-45^0 n, 0^0. Within the model, the top plates of the deck panels were managed as truss members even though they experience loads between nodes.

The largest deflections in these composite deck sections occurred directly under the center of the load (at center span). Table 1.1 depicts the live load deflections for the 5 different configurations illustrated in Figure 1.4. Although the deflections exceeded the L/800 (.105 inches for 7 foot span) deflection limit, the X-shaped deck panels (deck 1 and 2) were closest to meeting deflection criteria having deflected .144 inches each.

Henry then continued the research on the X-shaped deck panels with four primary objectives: 1) to determine the effects of the panel width on deflections, 2) to optimize the SAP program using truss elements in place of plate elements, 3) to explore the influence of boundary conditions, and 4) to determine the stresses and deflections of a 28 foot four-span continuous FRP deck system.

Shih (1995) also researched four various design configurations, shown in figure 1.6, of fiber reinforced polymeric bridge decks subjected to AASHTO HS-20 44 loading. He used an optimization algorithm along with his finite element technique to analyze strength and serviceability. His research concluded that V-shaped configuration was the most efficient design for various effective span lengths ranging from 4-12ft. Shih proposed minimum plate and element thicknesses that meet serviceability criteria.

In the *Proceeding of the International Composites Exposition* of 1997, Karbhari et al. presented the results of testing 8 different FRP bridge deck configurations varying cell orientation and core structures shown in figure 1.7. The three primary objectives for the development of these decks include: 1) the development of stiffness through the use of face sheets and internal core configurations that would fall in the range between the uncracked and cracked stiffness of reinforced concrete decks, 2) the development of equivalent energy levels at acceptable displacement levels as a means of building in a factor of safety due to the elastic behavior of composite materials, and 3) the development of processing methods that would be cost effective and which would ensure repeatability and uniformity. Deck components were manufactured by several industrial partners (as listed in *Figure1.7*) and were produced using Pultrusion, Hand Lay-up, and Resin Transfer Infusion techniques. The depth of the specimens was 9 inches to enable direct replacement with existing concrete decks, and the length varied from 3 ft. to 15 ft.

The truss core configuration consisted of triangular foam cores wrapped with fabric and inserted between face sheets to form the structure. In order to assess the effectiveness of additional reinforcements at the nodes formed by the adjacent triangles, the second configuration used a woven fabric insert that strengthened the node area. This is particularly important as one primary factor of the proposed 3Weave^{TM} FRP bridge deck of this thesis is the effect of additional strength at nodal points through continuity of fibers, capable solely with the innovative weaving technique. The effect of the reinforcement of the second configuration is illustrated in the load-displacement profiles of figure 1.8 as the response appears to shift from linear elastic to "pseudo-ductile" with the ductility being afforded by matrix cracking and gradual separation between fabric layers at internal nodes and along inclined webs.

All the deck specimens were tested, and the experimental results were compared with control mild steel reinforced concrete (RC) slabs. It was reported that the fiber reinforced composite deck specimens showed failure loads far in excess of that shown by the reinforced concrete specimen. The authors showed that the stiffness of the FRP decks was between two values, that of an uncracked RC slab and that of a cracked RC slab. Overall, the ultimate strength capacities of the FRP deck panels were higher than those of the reinforced concrete slabs, and the composite deck were 3 to 4 times lighter than the reinforced concrete deck panel which weighed about 12,500 lbs.

Three composite and one reinforced concrete deck panels were placed at a test site at University of California at San Diego for field monitoring of actual behavior.

The *Proceeding of the International Composites Exposition* of 1997, Lopez-Anido et al. presented also the experimental characterization of a cellular FRP bridge deck (H-deck) with multi-axial fiber architecture. This deck section was composed of pultruded hexagonal tubes and double trapezoidal sections (*Figure 1.9 and 1.10*) bonded by adhesives and rivets. There was no direct reinforcement continuity through the transverse direction of the structure, relying only on the adhesives and rivets to form the FRP deck modules. The materials comprising the deck were E-glass triaxial stitched fabrics [+-45/90^0] with binderless chopped strand mats and a vinylester resin matrix. The fabrics were manufactured by Brunswick Technologies Inc. (BTI).

The H-deck modules were placed transversely to the traffic direction and are supported by longitudinal beams. This system was designed to meet AASHTO 1994 highway bridge design requirements. The dimensions of the test specimen were 8 inches, 45 inches, and 108 inches for depth, width, and span respectively. The prototypes were fabricated using Vacuum Assisted Resin Transfer Molding (VARTM) by HardCore-DuPont, L.L.C.

The H-deck was evaluated for stiffness, strength, and fatigue resistance. Two types of loading were applied to the panels: 1) a patch load 10 inches by 20 inches, with the larger dimension perpendicular to traffic flow to simulate the action of a wheel load; and 2) a transverse line load with a width of 11.5 inches to establish longitudinal stiffness properties under cylindrical bending. Each panel was loaded up to 90 kips while strains and deflections were measured on the uppermost and bottommost surfaces. The analytical flexural rigidity of the FRP bridge deck was reported to be 74,500 kip-in. This major orthotropic bending stiffness, along with other mechanical properties of the composite laminate, was computed based on macro-mechanics, i.e., lamination theory.

Using finite element analysis (ANSYS TM 5.0) to predict the deflections and strains, the authors illustrated they were able to obtain a close relation with the experimental results: 4% to 9% proximity with the deflections and 2.4% to 33% proximity for the strains. The deck elements are modeled using eight-node layered shell elements (SHELL99). Each composite layer represents a multi-axial fabric with elastic properties that were obtained experimentally. A simply supported deck module with length 108 inches under a central patch load was modeled using 368 shell elements with 1026 nodes.

The authors indicated that the deck did not experience stiffness degradation due to fatigue. The design of FRP H-decks is controlled by deflection limit states. The H-deck met AASHTO requirements for highway bridges.

Lopez-Anido, Gangarao, Trovillion, and Busel (1997) next presented the preparation and installation of the H-decks for two secondary roads in West Virginia. A polymer concrete topping surface was applied to the bridge deck.

Zureick (1997) performed finite element analyses on FRP deck panels with box-shaped cells (*Figure 1.11, Deck 1*). The dimensions of the prototype models were 11

inches in depth and 8 feet in length (traffic direction). Each panel was simply supported with a 40 foot span and subjected to one "wheel line" (not an axle) of an AASHTO HS20-44 truck. Within the analyses, Zureick portrayed the materials properties to be consistent with E-glass/vinylester matrix with a fiber-volume fraction of 45%. Zureick studied four different configurations with various fiber directions and cell orientations. His test showed that stresses were less than 4 ksi in each case. Similar to most FRP decks, he found that deflection controlled. He also noted that deflections were less for decks with cell orientations perpendicular to traffic flow.

Zureick next optimized his ANSYS (finite element software) utilizing four different models, each comprising its own cell orientation, illustrated in figure 1.11. In his analyses, the deck widths (traffic direction) ranged from 9 to 10 cells or 72 to 80 inches respectively. The objective of the optimization was the minimum volume (by weight) FRP deck. There were four design variables of the optimization program: 1) top plate thickness, 2) bottom plate thickness, 3) web thickness, and 4) "theta" for two of the six plies in the laminate. Several constraints were imposed so that strength, stability, stiffness, and serviceability were not compromised. The constraints were as follows: 1) L/800 maximum deflection, where L is the center-to-center distance between supports (.12 inches at L=8 feet); 2) relative deflection between adjacent webs less than or equal to .1 inch; 3) max Tsai-Wu failure criteria is .6; 4) top plate thickness greater or equal to .5 inches; and 5) bottom plate and web thickness greater or equal to .25 inches. The author again portrayed the material properties to be E-glass/vinylester. The FRP decks were loaded by one HS20-44 axle on each span, for a total of 4 wheel loads-each of which was applied to the deck over a 6 inch (traffic direction) by 20 inch area. Optimum decks were found for 6 different deck depths (from 7 inches to 12 inches at 1-inch increments). Zureick found the box-celled deck and the V-celled deck to be the most efficient sections. The trapezoidal-celled deck converged to the box-cell at the optimum design. At every length, the X-cell deck was heavier than the V-cell deck. At smaller depths (7 to 10 inches) the V-cell deck was lighter than the box-cell deck, but at 11 and 12 inches, the box-cell deck was lighter.

After concluding that the box-cell and V-cell deck were optimum, Zureick tested these designs at larger stringer spacing. At 10-foot and 12-foot stringer spacing, neither

of the deck configurations were able to meet the deflection limit criteria of L/800 (.15 inches for L=10 feet and .18 inches for L=12 feet).

Brown and Zureick (1999) developed a modular glass fiber deck panel for the Landing Ship Quay/Causeway and Mobile Offshore Base programs funded by DARPA (Defense Advanced Research Projects Administration). Illustrated in Figure 1.12, this 9 inch thick deck panel consisted of pultruded triangular components interlockingly placed between two hand laid-up composite plates. The triangular elements were fabricated using a single ply of 3-D Through-the-Thickness^{R} E-glass braided fabric, produced by Atlantic Research, pulled through a pultrusion die. The face sheets comprised E-glass knitted fabrics, supplied by Johnson Industries, embedded in a vinylester resin. The deck modules produced for the LSQ/C application were 10 ft long in the traffic direction and 30 feet wide. Prior to application, a 9.84 square foot panel was produced and tested under 3-point bending. The deck was loaded to 140 kips without failure and experienced a maximum deflection of .7 inches, a max tensile strain of approximately 2300 microstrain and a max compressive strain of approximately 1600 microstrain. Upon completion of the test program, the Virginia Department of Transportation (VDOT) placed the two 10 feet by 20 feet deck panels test pit at the Troutville, Virginia weigh station on I-81 in order to conduct a durability demonstration of this deck panel concept.

Harik et al. (1999) carried out static tests of pultruded FRP deck panels manufactured by Creative Pultrusions. The panels comprised double trapezoid and hexagonal pultruded components bonded and interlocked (*Figure 1.13*). Under a three-point bending test, a rectangular patch load representing an AASHTO standard HS25 truck wheel load was applied to the center of each deck. The depth and width of all panels were 8 inches and 36 inches, respectively. The span lengths of the deck panels were 86 inches, 120 inches, and 144 inches. This comprised CPD1, CPD2, and CPD3, respectively.

In testing, the load was transmitted through a rectangular plate of size 22 in x 9 in x 2 in at the center of the deck panel in order to represent the AASHTO H25 wheel load. In order to minimize abrasions between the steel plate and the FRP panel surface, a rubber pad of .5 inch thickness was placed beneath the steel. Electrical resistance strain

gauges were placed on the top and bottom surfaces in order to measure the tensile and compressive strains.

The test method consisted of four steps. First, the specimen was loaded from zero to 26 kips and back to zero to establish a baseline curve. This 26 kip load represented the factored load (20 kip + 30% for impact) for the AASHTO HS25 truck wheel load. Second, the specimen was loaded from zero to 12 kips and back to zero, and this was repeated for a cycle of five times. The 12 kip load represented the service load for an HS25 truck (4 kips/ft width). Third, the specimen was loaded from zero to 26 kips back to zero. This was repeated five times. Fourth, the specimen was loaded from zero until failure. The details of the deflections and failure loads for the FRP deck panels can be seen in table 1.2.

The measured deflections were compared with the allowable deflection limits. It was found that all of the FRP deck panels produced by Creative Pultrusions satisfied deflection criteria. The factor of safety against collapse was greater than 5 for each panel. It is important to note that at failure of the deck, delamination of the panel at the end of the section was observed for specimens CPD2 and CPD3, and this is displayed in figure 1.14. Since there is no continuity of axial fiber along the top or bottom surfaces of the deck, this Creative Pultrusion FRP deck exhibits its major weakness of delamination between the pultruded components. One strong suit of the proposed 3TEX bridge deck is the continuity of the warp or axial fiber within this primary region.

1.3.5 Innovative Fiber Architecture

1.3.5.1 Introduction

Composite preforms are made from woven, braided, or stitch-bonded textile reinforcements such as carbon fiber, glass fiber, or Teflon filaments. Different from the use of chopped random fiber for reinforcement, preforms have acquired much interest for their many advantages including improved performance and low cost. These advantages are capitalized by using continuous, automated machines to place the fibers in the orientation needed.

There have been many publications on the use and design of “3D woven” composite materials, yet much of the available commercial products are formed by a 2D

weaving process that is used to build up a preform with fibers orientated in three dimensions. Recent advances in textile engineering have lead to a multiple insertion 3D weaving process, i.e. 3D fabric formation with each cycle, or multi-layers at one time, known as 3Weaving™ (Mohamed et al 2000). The distinctions of the processes will be detailed in this thesis in addition to the advantages of the 3Weave process in terms of economics, manufacturing, and performance of 3D woven textile preforms for composites.

1.3.5.2 2D and 3D Weaving

Weaving is the formation of fabric by the interlacing of two sets of yarns, the warp yarn (x-direction) and the weft yarn (y-direction, or filler yarn). The structure of a 2D woven fabric is illustrated in figure 1.15. The 2D weaving process is known to be relatively fast and economical. Yet the drawback is the inherent crimp, or waviness, of fiber orientation. It is this out-of-plane fiber orientation that prohibits its utilization of maximum fiber mechanical properties. Examples of 3D woven orientations are shown in figure 1.16. Most preform weavers use traditional 2D weaving with single filling (y-direction)in their 3D woven products, thus these fabrics are built up one insertion (one "layer") at a time (Mohamed et al 2000). A multiple insertion 3D weaving process with multiple filling insertions at one time has been developed at the North Carolina State University College of Textiles and the Mars Mission Research Center (Mohamed 1996). Inherently 3D orthogonal, this process does not involve the building up of multilayers. A unit of arbitrarily thick multilayer fabric is the product of this innovative process. The simultaneous filler insertion from one or both ends of the preform is the essence of the patent/invention. 3TEX Inc. is commercializing this patented technology under the trademarks 3Weaving™ or 3Weave™. The multi-weft insertion per weaving cycle allows for a fiber architecture unachievable by conventional weaving, and it is this unique process that will enable the open core structure of the 3TEX Bridge Deck.

The 2D and 3D weaving processes are illustrated in figures 1.17 and 1.18. In ordinary 2D weaving cycles, warp yarn (the primary yarn) is let off supply packages, potentially rollers on a creel, and is drawn through the weaving machine. The warp is then split into two layers forming a v-shaped opening called a shed. Filling yarn is then

inserted through/between this shed. This is done using rapiers, or long slender rods. This filling yarn is then "beaten" or packed into the forming fabric by a comblike device called a reed. The point where the fibers are formed into the fabric is called the "fell." The shed is then closed/crossed about the filling insertion locking the yarn into place. The fiber is now interlaced. The small uniform unit of new fabric is then "taken up" or shifted forward. This ends the weaving cycle, and the cycle is repeated. The use of multiple cycles to insert one filling (or pick) at a time without taking-up can create a multi-layer fabric from 2D weaving. With multiple filling insertions, the fabric is then built up in thickness.

The innovation of the 3Weaving^{TM} process involves a simultaneous multiple filling insertion from one or both sides of the shed in one weaving cycle. Thus, an increment or unit of fabric of arbitrary thickness is the result of a "three dimensional" weaving technique utilizing a Z-directional yarn interlacing the warp and the weft. The Z-yarn is orthogonal to both the filling and the warp. The inherently multiple layer increment is the result of not one, but multiple layers of straight warp pulled from the supply and interlaced with the multiple filling yarn. Thus, there are not one, but multiple sheds of warp for the innovative insertion process. The resulting fabric structure is free of crimp internally. Refer to figure 1.19 to perceive the 3Weave^{TM} process with the multiple warp layers and sheds. It is important to note that it is this multi-weft insertion that permits the formation of the innovative bridge deck.

1.3.5.3 Resulting Fiber Architecture

Unique from older 3D weaving processes architecture, the resulting architecture of the new 3D weaving process 3Weave^{TM} is illustrated in figure 1.20. The warp, the weft, and the Z-yarn are uniquely orthogonal to each other on the Cartesian coordinate system. This differs from other 3D, or multi-axial, strand orientations in other literature. The warp and the weft make up the x-y plane respectively, and the Z-yarn then integrates the fabric by traveling essentially perpendicular to the mid-plane inside the fabric and parallel to the warp on the surface. This through thickness reinforcement provides advances in composite performance.

1.3.5.4 Economics of Production: Cost

The productivity of a weaving machine withstanding a constant width is measured in picks per minute (ppm). A pick is considered a single filler insertion of fiber strand. Machine speed is measured by the number of filler insertion actions within a given minute. Thus, if 3Weave^{TM} is capable of multiple insertions within a single cycle of the process, a higher productivity is inherent. The productivity of 2D weaving machines versus 3D weaving machines is illustrated in figure 1.21 with "ppm" as a function of the numbers of layers (Mohamed et al 2000). Constant width, constant warp, and constant filling density were assumed.

An inexpensive, automated process is the only way to break the cost barrier that has limited the use of high strength composite materials for use in civil infrastructure. Thus, for instance, for a 10 filling layer fabric, a 3Weaving^{TM} machine running at 10 weaving cycles per minute will produce 100 filling insertions per minute. Whereas a 2D weaving machine would need to run at 100 weaving cycles per minute to equals the 100 filling insertions per minute. And since the 3Weave^{TM} machine will run fewer cycles than the traditional 2D weaving machine while maintaining a higher productivity, there will be less "beat-up" actions of the comb-like reed facilitating less fiber damage and better quality of product. This aids in maximizing the mechanical properties of the load bearing member, the fiber. Overall, the innovative process reduces the complexity and labor intensity of the expensive composite fabrication process and thus reduces the cost of the product.

In addition to being more economical in the machining fabrication, the ease and speed of wetting out these preforms has shown to be more viable in various resin infusion processes. 3Weave^{TM} preforms will show to wet-out more easily than stack of 2D preforms in Figure 1.22 (Bogdanovich et al 2001).

1.3.5.5 Advantages of 3Weave^{TM} Fabric Preforms

The 3Weave^{TM} process and resulting fiber architecture demonstrate superior in-plane mechanical properties along with significantly improved impact damage tolerance and ballistic performance over their laminated 2D fabric preform counterparts (Bogdanovich et al 2001). The primary in-plane fiber reinforcement, the warp, is

uncrimped due to the orientation of the weaving: the warp pulls straight through the machine and does not feed through the eyelets of the heddles. Thus there is no crossing of warp layers as utilized in 2D weaving. The Z-yarn provides through thickness reinforcement and thus provides resistance to crack propagation and eliminates delamination as a failure mode.

The weaving process also provides significant improvement in the resin infusion and resin transfer molding techniques. It is thought that the Z-yarn act as channels which accelerates the resin through the preform. This effect of higher permeability has been demonstrated by several independent investigators and figure 1.22 illustrates this higher processing speed (Bogdanovich et al 2001). In this VARTM wet out of E-glass preforms (figure 1.22), there are 4 plies plain woven rovings, 3 plies BTI style 3205 0/90 biaxial-reinforced warp knits, and one ply 3Weave™ woven rovings (left to right). All preforms have equal areal weight and dimensions, and are fed and exhausted by common supply lines. Left: flow fronts shortly after test start. Right: 3Weave™ fabric completely filled before plain woven or warp knitted fabrics were half filled.

The most significant aspect of utilizing the high performance capabilities of composites is high quality of product. This leads to the vital concern of fiber damage. Several aspects of the 3Weave^{TM} process preclude fiber damage.

First, as the warp yarns are pulled straight through the weaving machine, the multiple filler yarn insertion enables a formation of fabric without movement of the warp yarn. Thus, the warp fibers do not cross and break each other as seen in 2D weaving. Second, most 3D weaving machines utilize a stitching of the third direction, i.e., this strand is jabbed through the mid-plane fabric perceptibly breaking already woven fibers. 3Weaving^{TM} accomplishes Z-integration by a simple crossing of the Z-yarns about the filler insertion. Third, since the 3Weave^{TM} weaving machine achieves a multi-layer fabric fabricating pace above that of an equivalent design for a 2D weaving machine, it is able to physically operate slower. This comprises less “beating up” or packing of the fabric with the comb-like reed which gives way to less fiber damage. Operating slower, the machine also entails softer yanking/pulling on the fibers through the machine.

1.3.5.6 Designing with 3Weave™ Preforms

In designing with 3Weave™ preforms, there will always be a compromise between ultimate fiber volume content in each of the 3 orthogonal directions. The design volume content of in-plane and out-of-plane fiber reinforcement is directly contingent on the use of the fabric. A basic understanding of this balance is crucial in understanding the design utilized in the complex 3D bridge deck. Figure 1.23 illustrates the total fiber volume fraction and the in-plane fiber volume fraction variation for a balanced (i.e., having equal warp and filling yarn content) orthogonal XYZ reinforcement with changing Z-yarn content (Bogdanovich et al 2001). As Z-yarn content tends toward 0%, a cross-ply composite with reinforcement in the x-y plane is produced. As Z-yarn content tends toward 100%, a unidirectional composite with reinforcement in the Z-direction is produced. The goal is to use the minimal amount of through thickness reinforcement necessary to prevent delamination and meet damage tolerance. This allows maximum in-plane fiber content. Further analysis on through thickness fiber reinforcement is found in Dickinson 1999.

1.3.5.7 In-Plane and Out-of-Plane Properties of 3Weave™ Composites

Static strengths and directional moduli of elasticity for E-glass 3Weave™ composites are presented in comparison with 2D fabric composite materials in Singletary et al 2001. Strengths of 3Weave™ composites having around 2% Z-fiber content were experimentally tested and were generally better than those from comparable 2D weaves. The authors suggest the absence of in-plane crimp optimizes the mechanics of the materials, and the transverse (out-of-plane) strength and damage tolerance of the composites is dramatically improved by the through thickness reinforcement.

1.3.5.8 Application of Predictive Analysis to 3Weave™ Composites

With 3D orthogonal fiber architecture in their preforms, 3Weave™ composites allow a rather confident prediction of the fiber architecture and elastic constants (Bogdanovich et al 2001). The “Fabric Geometry Model” relates the principal processing parameters (i.e., characteristics of yarns in the x, y, and z directions; number of ends and picks per unit length, Z-yarn insertion parameters) with geometric hypotheses to

determine that part of the space which is occupied by all yarns in the manufactured fabric. Knowing the yarn locations and occupied space, one can then predict fiber volume fraction in each of the principal reinforcement directions, as well as fabric thickness and areal weight (Bogdanovich et al 2001). Examples of such models can be found in references Pastore 1996 and Bogdanovich 1996.

1.3.6 Research at North Carolina State University

North Carolina State University has worked with Martin Marietta Composites (Raleigh, N.C.) to develop an innovative 3D FRP sandwich panel for transportation and infrastructure, a project of the Center for Repair of Buildings & Bridges with Composites (RB^2C). Martin Marietta Composites first developed "Duraspan," a successful FRP bridge deck currently commercially available, which is comprised of pultruded FRP components ultimately laminated together. This new research introduces a new generation of composite panels that utilize a through-panel-thickness stitching of fibers (Z-tows). The panels consist of top and bottom GFRP pultruded skin layers attached by vertical pins of fiber. The skins are 2D woven fabrics, and the pins are jabbed through the 2 mid-plane fabrics consequently attaching them. A dense foam fills the volume between layers. The main variables in this study include the thickness of the panel, number of GFRP plies in the top and bottom skin layers, intensity of vertical pins, and type of loading. The researchers at NCSU aim to examine the structural performance of the innovative deck beneath various loadings; this is illustrated in figures 1.24-26. The behavior of the panels during testing are monitored using a combination of electrical strain gauges, string potentiometers, and PI gauges.

1.4 Summary

In the past few years, various fiber reinforced polymeric bridge deck panels have been designed and tested for use in civil infrastructure. The literature review has covered the most recent and successful ventures involving top researchers from around the country. And yet the innovative 3D woven bridge deck as the primary focus this thesis remains unique in several ways. It was illustrated by Henry (1985) and Shih (1995) that V-shaped cell orientation prevailed for FRP deck panels. Karbhari et al. (1997)

researched truss core configuration consisted of triangular foam cores wrapped with fabric and inserted between face sheets to form the structure. But gradual separation between fabric layers at internal node was demonstrated. Lopez-Anido et al. presented the H-deck, pultruded hexagonal tubes and double trapezoidal sections, in 1997. Harik (1999) also tested this configuration for a product of Creative Pultrusions. The pultruded sections were bonded and interlocked, thus they were ultimately laminated together. Failure in these laminated points was illustrated in figure 1.14. Brown and Zureick in 1999 demonstrated triangular pultruded components between laminated skins. Here, there was continuity of fiber in the top and bottom skins but ultimately lamination between the skins and the triangular pultruded cells. And thus no reinforcing continuity existed between the skins and the deck core.

Current weaving technology along with an illustration of 2D versus 3D weaving was given. Most researched FRP decks consist of pultruded components laminated between 2D woven fabrics or structured to interlock with the next.

It is the primary goal of this thesis research to demonstrate a fiber reinforced polymeric bridge deck that utilizes an innovative textile engineering weaving technology and creates an advanced composite bridge deck overcoming each of the weaknesses of its predecessors. Thus it will encompasses continuity of reinforcing fiber in both the top and bottom skins (x-direction), continuity of fiber between the outer skin and the inner core (y-direction), and uncrimped in-plane fiber architecture (throughout). As a woven preform, the deck skins are able to sustain continuous reinforcing fiber of arbitrary length. The open cell of the preform is viable by the unique weaving manner of the Z-yarn maneuvering/crossing above and below the filler yarn of adjacent mid-plane layers. This directly eliminates delamination of the skin layers from the deck core. Also, the orthogonal Z-reinforcement of each skin prohibits delamination of the skin from itself. Lastly, all in-plane reinforcement remains uncrimped, and is thus able to exhibit maximum mechanical properties, due to the innovative multiple filler insertion process of 3Weave^{TM} technology.

Much appreciation is noted for the engineers and resources associated with 3Tex Inc. in Cary, N.C. and the Constructed Facilities Laboratory at North Carolina State University in Raleigh, N.C. for devotion to the proof of concept of the new bridge deck.

3Tex, Inc. is a world leader in 3D woven and braided composite reinforcement materials that are increasing product performance, saving manufacturing costs and reducing weight. 3Tex's 3D weaving technology was developed in the 1990's at NC State University's College of Textiles. Under a NASA sponsored research program at the University's Mars Mission Research Center, Dr. Mansour Mohamed, Founder and now Chief Scientific Officer of 3Tex, and his colleagues invented a unique method of weaving three-dimensional fiber architectures and studied their properties and applications.

3Tex, Inc. and North Carolina State University sustain a strong affiliation deeply rooted in aiding students' research of advanced composite materials.

1.5 Tables and Figures

Table 1.1 Deflections of the five deck configurations analyzed by John Henry

Deck Type	Maximum Deflection (in)	Deflection Index
1	0.144	L/583
2	0.144	L/583
3	0.199	L/422
4	0.204	L/412
5	0.214	L/393

Table 1.2 Deflection and failure loads for the FRP deck panels tested by Harik et al

Specimen Identification	Centerline Deflection 12 kip Load (in)		Centerline Deflection 26 kip Load (in)	Load at Failure (kips)	Safety Factor	Maximum Deflection at Failure (in)	Mode of Failure
	Measured	Allowable					
CPD1	0.090	0.125	0.208	148	5.70	1.540	Punching
CPD2	1.160	0.170	0.362	147	5.65	2.408	Punching
CPD3	0.239	0.240	0.573	145	5.59	3.882	Punching

Safety Factor = Load at Failure/ 26kips

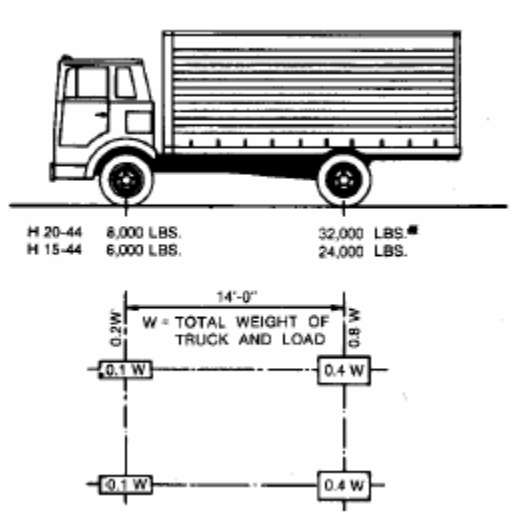

Figure 1.1: Wheel loads and geometry for H trucks

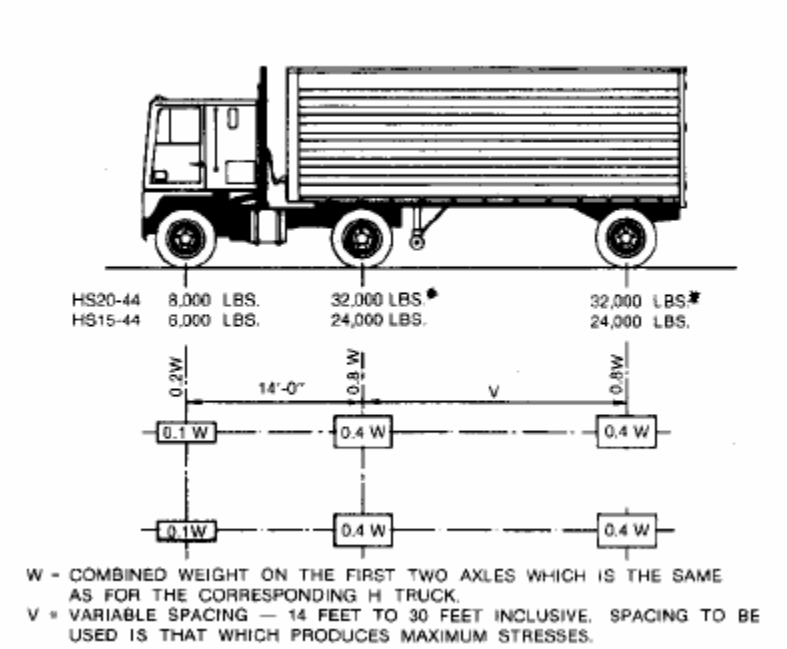

Figure 1.2: Wheel loads and geometry for HS trucks

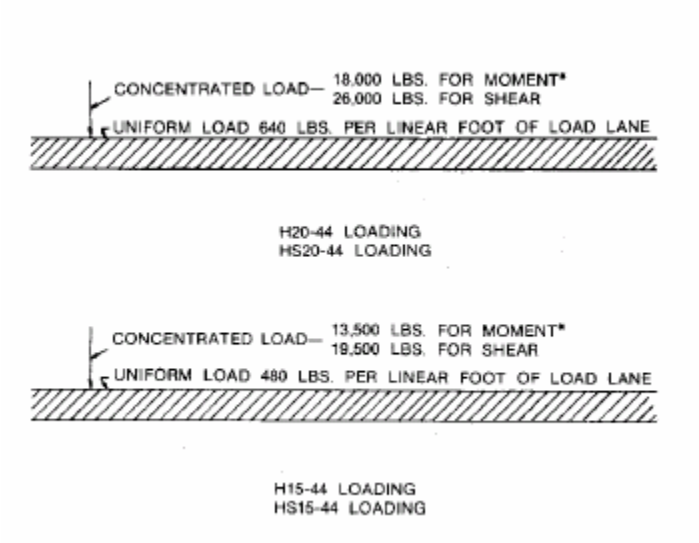

Figure 1.3 Equivalent lane loading for H and HS trucks

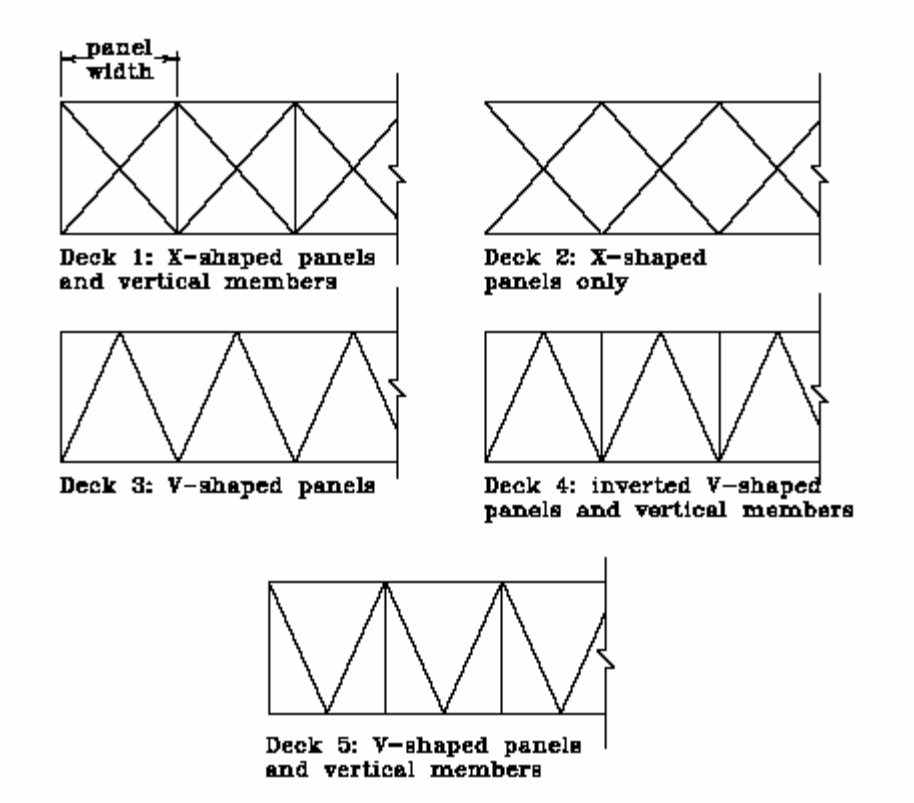

Figure 1.4 Sections of the FRP deck configurations analyzed by John Henry

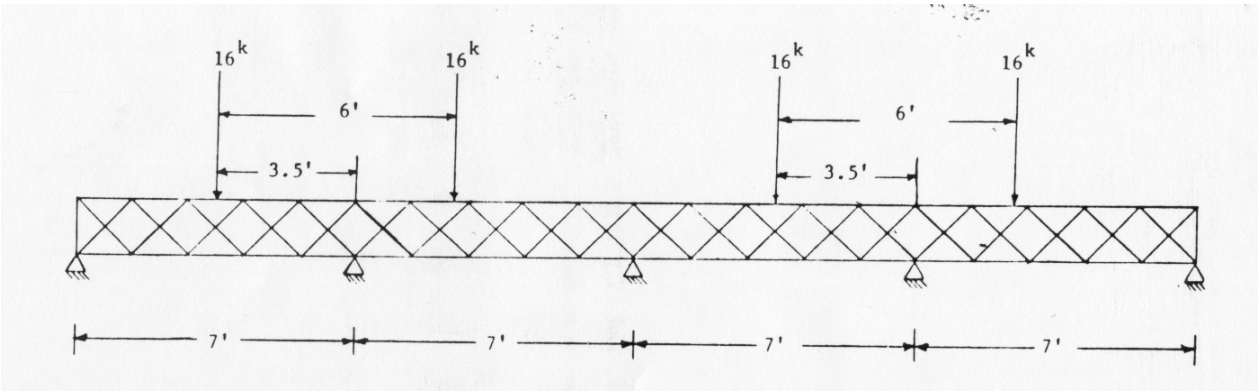

Figure 1.5 28 foot deck span analyzed by John Henry

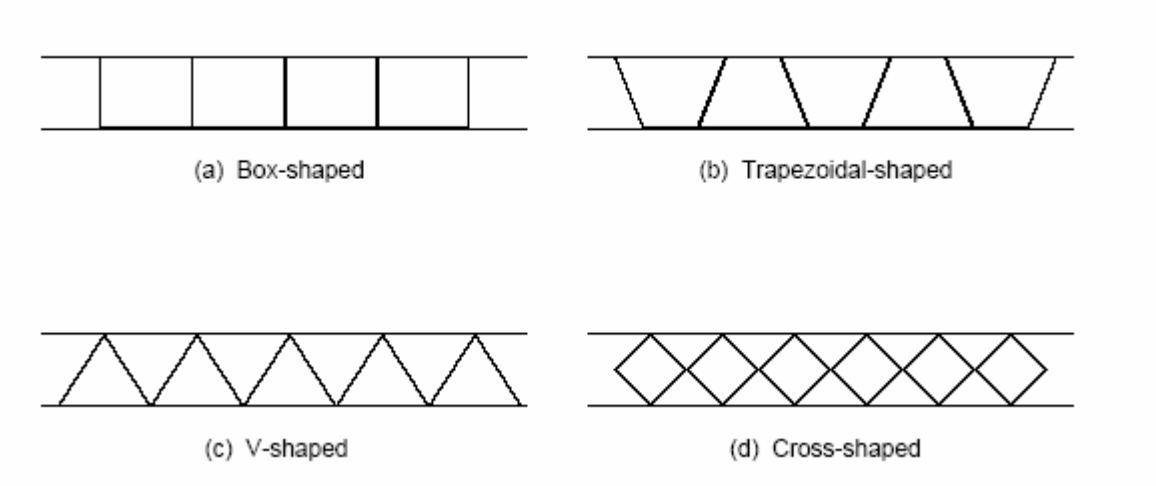

Figure 1.6 FRP bridge deck configurations studied by Shih (1995)

CONFIGURATION	COMPONENT SCALE			
	3' - 4'	6' - 8'	14'	15' x 7.5' Panels
Balsa Core (Dupont)	●			
Foam Filled Boxes (Dupont)	●		●	
Foam Filled Truss (Dupont)	●	●	●	●
Foam Filled Hat Sections (Dupont)			●	●
Pultruded Profiles With Face Sheets (Lockheed-Martin)	●	●	●	
Hybrids (Lockheed-Martin)				●
Corrugated Core (Core-Kraft)		●		
"Egg Crate" Core (Northrop-Grumman)			●	

Figure 1.7 Matrix of specimens tested by Kabhari

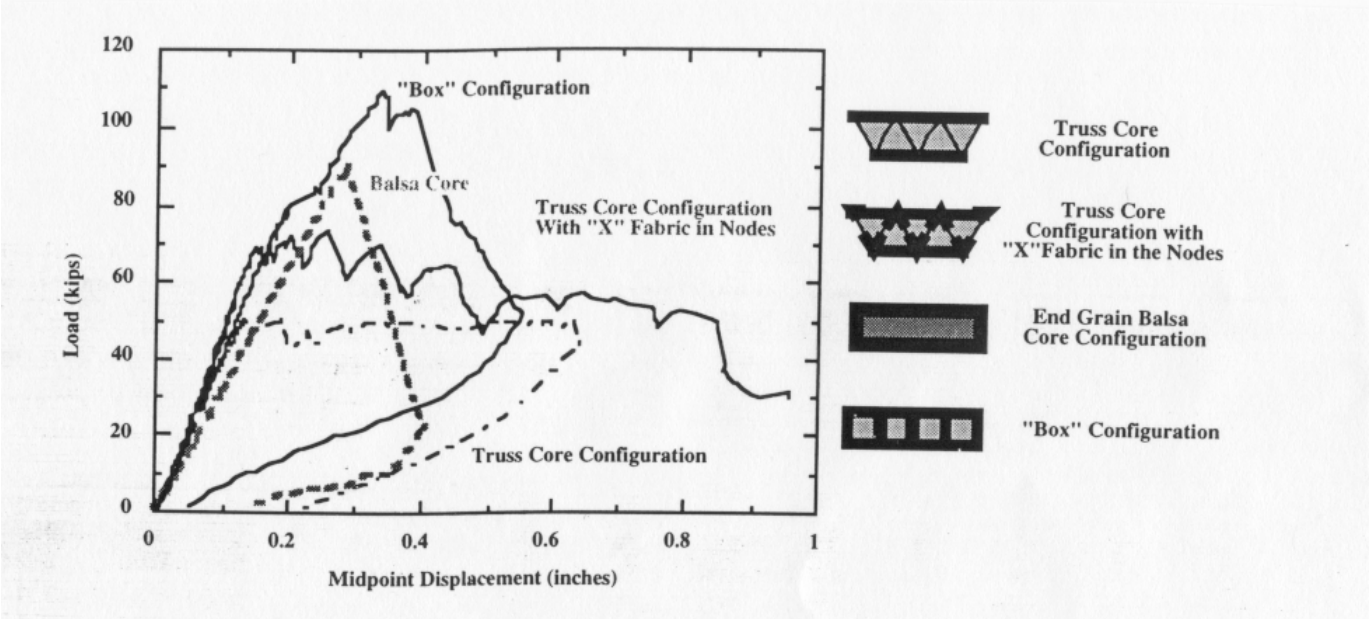

Figure 1.8 Karbhari Load displacement profiles

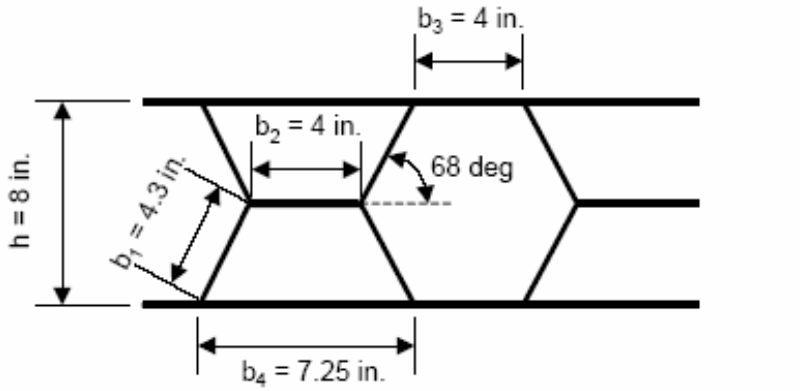

Figure 1.9 Cross-section with dimensions illustrating hexagonal tubes and trapezoidal sections of FRP bridge deck from West Virginia University (Lopez-Anido et al)

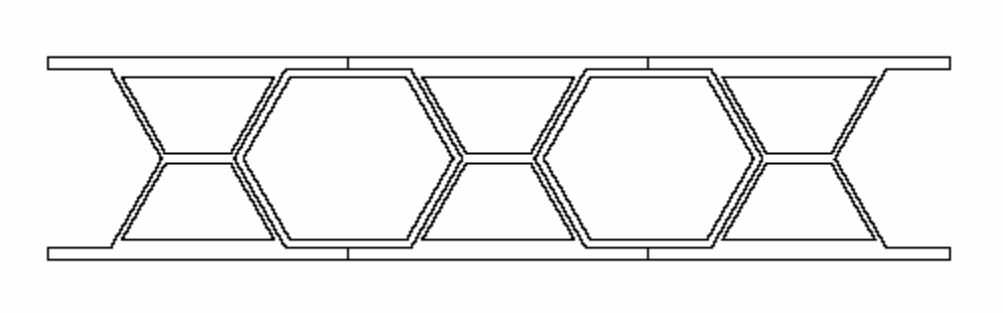

Figure 1.10 Cross-section illustrating elements of hexagonal tubes and trapezoidal sections of FRP bridge deck from West Virginia University (Lopez Anido et al)

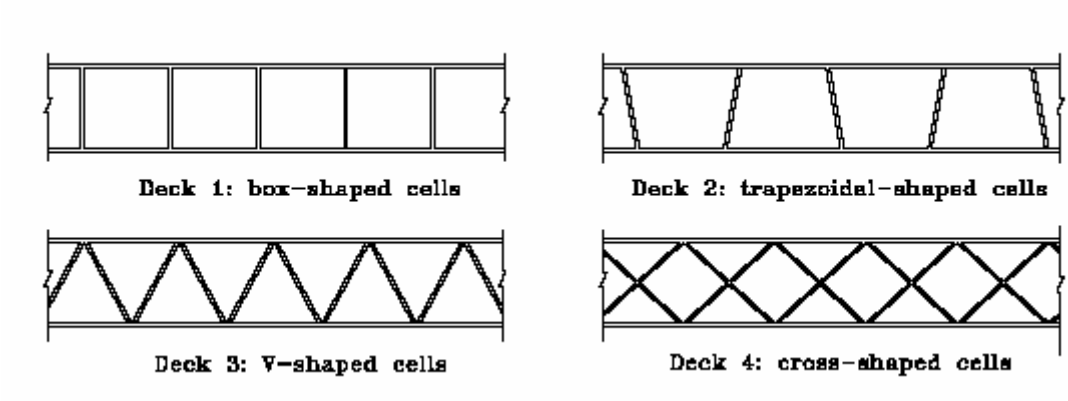

Figure 1.11 Sections of the four FRP deck panels analyzed by Zureick

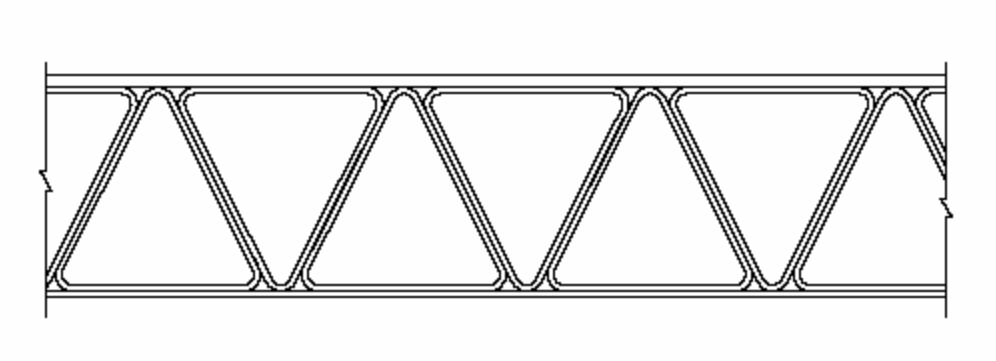

Figure 1.12 Section of FRP panel tested by Brown and Zureick

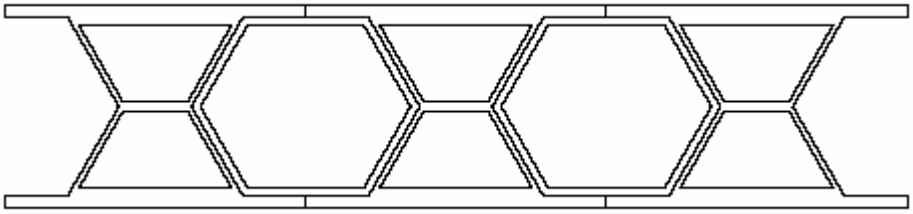

Figure 1.13 36 inch wide FRP deck panel tested by Harik et al produced by Creative Pultrusions

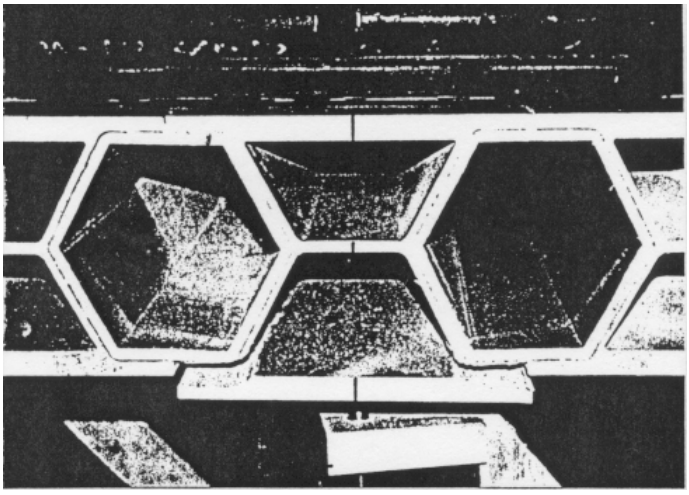

Figure 1.14 Delamination at the end section for specimen CPD2

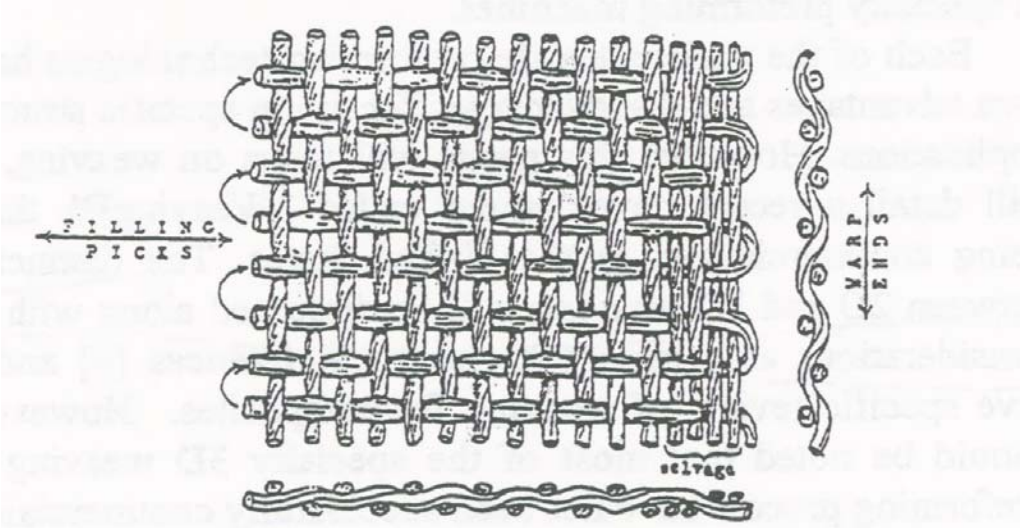

Figure 1.15 2D woven fabric structure

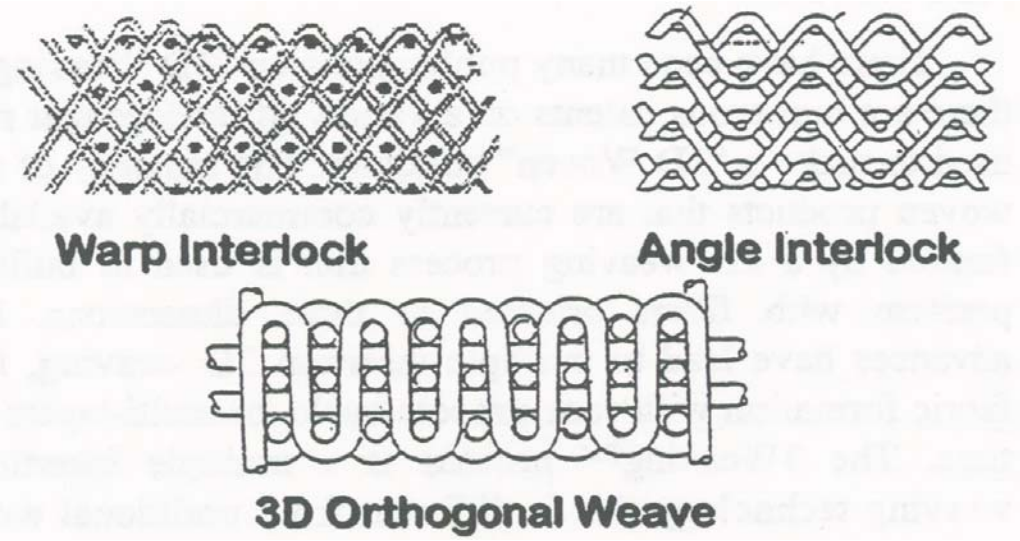

Figure 1.16 Examples of 3D orientations

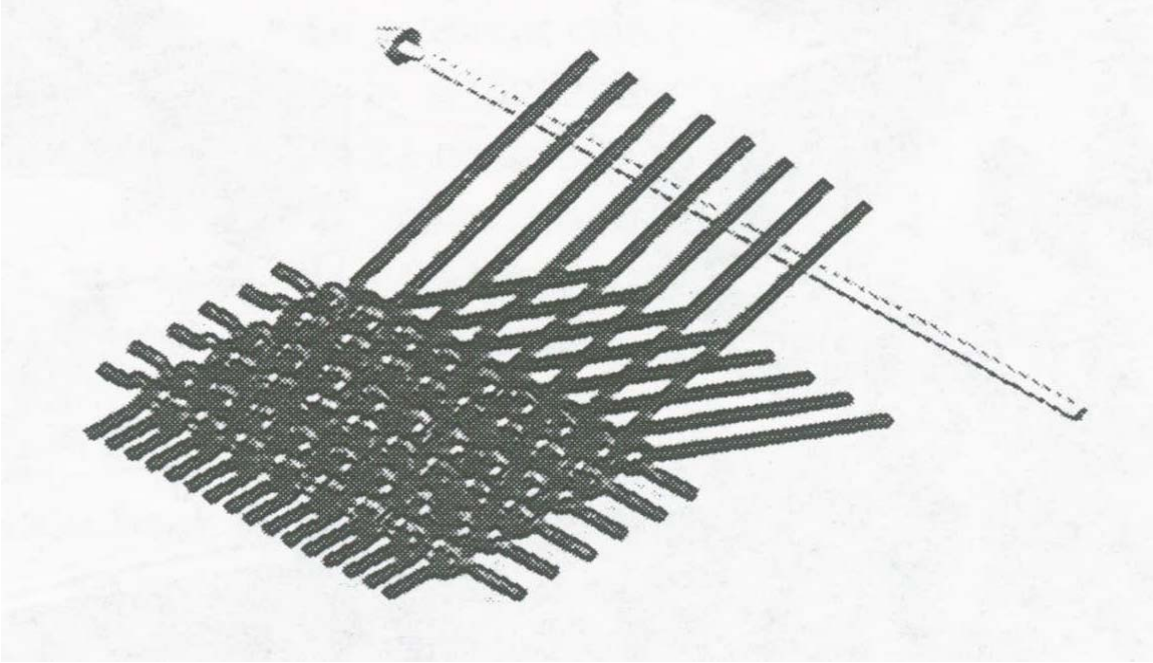

Figure 1.17 Conventional 2D weaving process

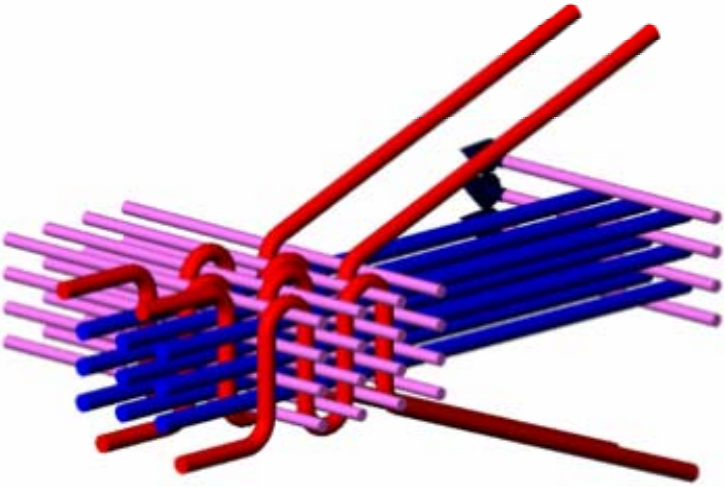

Figure 1.18 Innovative 3Weaving^{TM} process

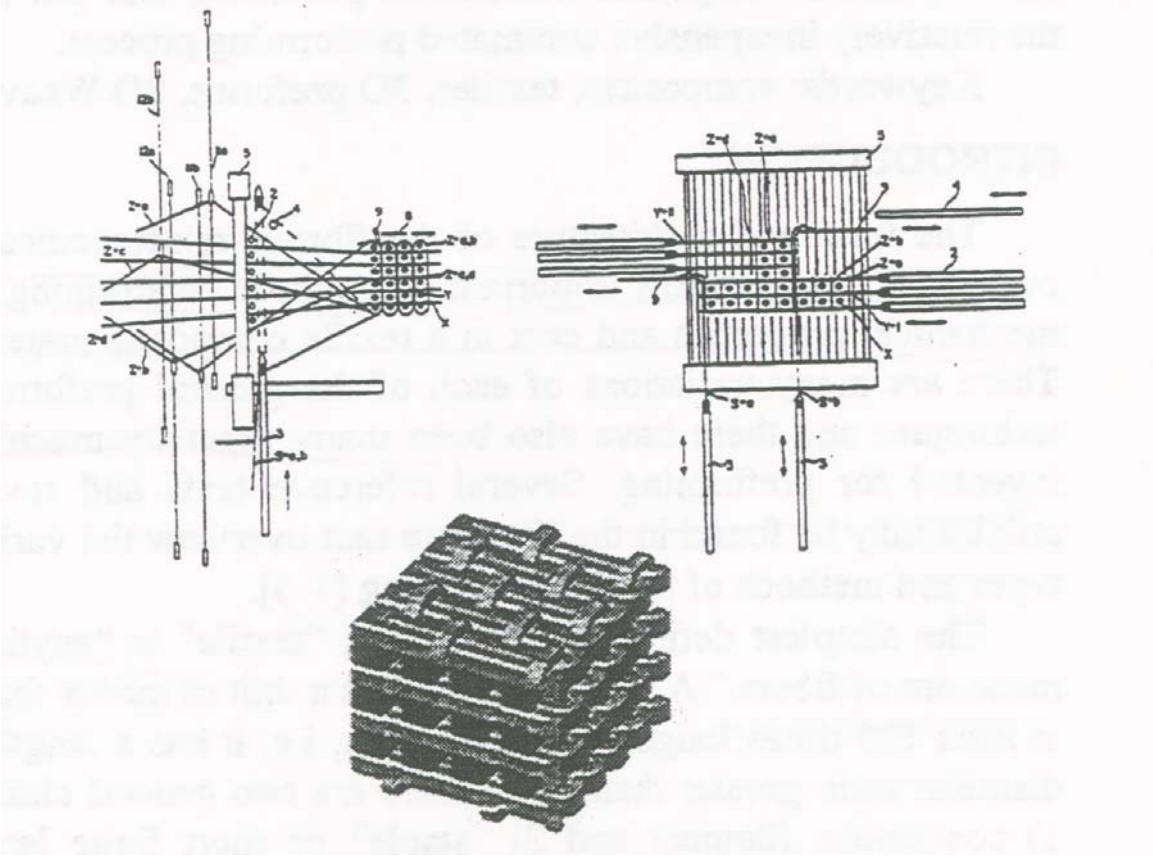

Figure 1.19 Schematics of 3Weaving™ process and one of the possible resulting 3D preform structures

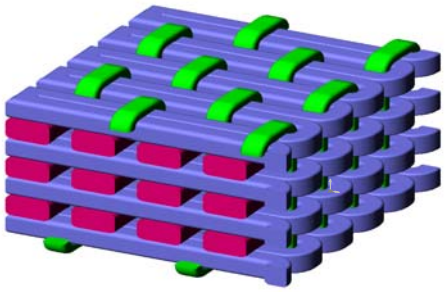

Figure 1.20 Resulting 3D orthogonal fiber architecture of 3Weave™ process

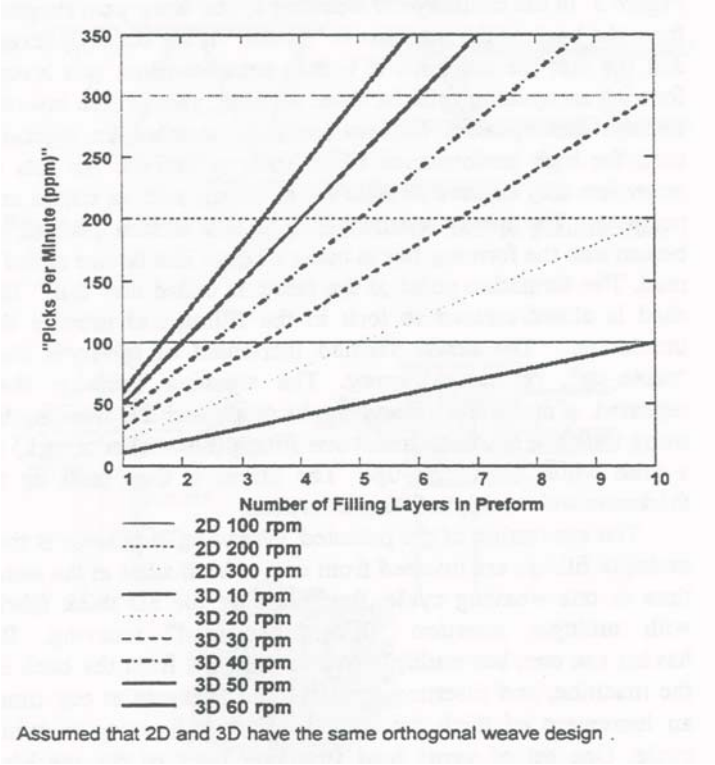

Figure 1.21 Productivity comparison between 2D weaving and 3Weaving™

Figure 1.22 VARTM wet out of E-glass preforms. Left: flow fronts shortly after test start. Right: 3Weave™ fabric completely filled before plain woven or warp knitted fabrics were half filled (Bogdanovich et al 2001).

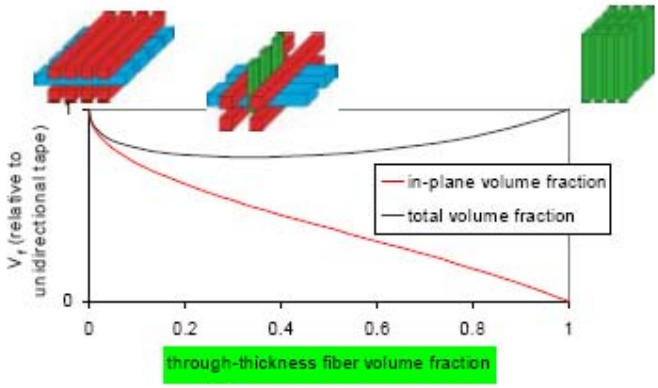

Figure 1.23 Total and in-plane fiber volume fractions as a function of Z-fiber volume fraction (Bogdanovich et al 2001)

Figure 1.24 Test setup for FRP sandwich panels using a concentrated truck tire loading at mid-span

Figure 1.25 Test setup for FRP sandwich panels using two line loads

Figure 1.26 Test setup for FRP sandwich panels using one line load at mid-span

Chapter 2: Materials and Fabrication of Bridge Deck Panel Skin

2.1 Introduction

Weaving is defined as the process of "interlacing" two sets of yarns, the warp and the weft (or filling). Before fabrication of the open cell 3D woven GFRP bridge deck, the research comprises optimizing the fiber orientation and resulting fiber volume fraction of the bridge deck panel skin. Thus, three preforms of various fiber weight fractions are woven and tested for material properties. This chapter illustrates the components of the 3D orthogonally woven GFRP skins as well as the material structures of these components. Fabrication of the skins and the difference in fiber weight fraction between each skin are discussed. The chapter concludes with the resin infusion process.

2.2 Components and Material Properties

The principal components of the FRP deck panel are three yarns woven in a unique weaving manner in an organized fashion in three-dimensional space. The yarns are a continuous E-glass fiber, Product Type HYBON 2022^{R}, produced by PPO Industries, Inc. and available in various size rolls (*Figure 2.1*). The material properties of this E-glass are given in table 2.1, and the PPG Industries product specification is posted in appendix C. The three yarns, the warp, the weft, and the Z-yarn, are defined by their weights 103 yards per pound, 218 yards per pound, and 675 yards per pound respectively (*Figure 2.2*). The fibers are pulled through the machine and woven into a 12" wide panel of continuous form. The paneling is cut into several arbitrary lengths and prepared for vacuum resin infusion.

The epoxy system for infusion utilizes Jeffco 1401-12/4101-17. This is a multifunctional epoxy and cycloaliphatic-amine blend hardener for high performance composite parts. This system has excellent fatigue and inter-laminar shear strength with rapid wetting of E-glass fiber reinforcements. The Jeffco Epoxy Resin is colored transparent ruby red for visual indication of infusion progress. Jeffco 1401-12 Epoxy Resin is formulated for highly increased E-glass fiber compatibility. Jeffco Products asserts an E-glass matrix with increased physical properties including: fiber pull-out strength, tensile strength and modulus, flexural strength and modulus, compressive

strength, impact resistance, and inter-laminar strength. Additionaly, Jeffco Products asserts this product asserts the retention of the above properties after exposure to heat, cycle fatigue, water, and expected adverse environmental reagents such as salt spray and acid rain.

The material properties of the E-glass fibers and the Jeffco Epoxy System are listed in *Tables 3.1 and 3.2*. Technical information given for Jeffco Products on the epoxy system is detailed in *Appendix B*.

The glass-fiber volume fraction of these skins is typically 50-60% of the total volume. Utilizing a 3D Weave Hybrid Composite software at 3Tex Inc., directional composite moduli of elasticity are predicted using a method of orientational averaging of stiffnesses and compliances. The assumed modulus of elasticity of E-glass HYBON 2022 is 10,500 ksi (72.5 GPa), and the shear modulus 4044 ksi (27.885 GPa). The assumed modulus of elasticity of JEFFCO Epoxy 1401-12/4101-17 is 660 ksi (4.5 GPa), and the shear modulus 242 ksi (1.667 GPa). Assumed Poisson's ratios were 0.300 and 0.350 for E-glass and resin, respectively. For each composite skin, x-directional, y-directional, and Z-directional moduli of elasticity were twice predicted using an assumed fiber volume fraction of 50% and of 60%. Illustrations of the orientational averaging and the resulting directional moduli are displayed in figures 2.3-2.8 for each of the three skins with different woven weight fractions. The preform product specification for each of the skins is illustrated in appendix A.

2.3 Innovative Fiber Architecture

Weaving is defined as the formation of fabric by the interlacing of two sets of yarns, the warp and the weft. The warp (x-direction) yarn is defined as the primary yarn within the deck panel. This yarn is pulled straight through the machine, eliminating out-of-plane fiber and fiber waviness. The weft (y-direction) yarn is orthogonal to the warp and is of double insertion above and below the warp (*Figure 2.9*). This is the essence of the patented 3Weave^{TM} process, that two or more filling yarns are simultaneously inserted from one or both sides. In this 3Weave^{TM} preforming, a third set of yarns, called *Z-yarns* (z-direction), then integrates all sets of yarns into the fabric. The Z-yarns take a path essentially perpendicular to the fabric mid-plane inside the fabric and parallel to the

warp direction on the fabric surfaces. An illustration of this process is given in *Figure 2.10.*

The resulting fiber architecture is demonstrated in *Figure 2.11*. Thus, the schematics of the yarns proceed along the three Cartesian orthogonal coordinates, and the idealized model can be assumed to have rectangular cross-sections of the yarns.

2.4 Woven Skin Preform Design

Woven composite cross-sections are defined in picks per inch (ppi). A pick is a unit strand of fibers pulled through a weave. The fiber weight fraction differs from skin #1 to #2 to #3. The design of skin #1 calls for a warp of 21 ppi and a weft insertion of 6 ppi. The reed is comprised of 7 dpi and thus 3 picks of warp feed through each dent. The amount of warp fiber is reduced by 1/3 for the design of skin #2. Thus, the warp is 14 ppi. The filler design maintains 6 ppi. The design of skin #3 entitles a reduction of the filler yarn by 1/3 and otherwise an equal design of skin #2. Thus, skin #3 comprises a warp of 14 ppi and a filler yarn insertion of 4 ppi. In defining the E-glass fiber, the warp is 108 yds/lb, the Z-yarn is 675 yds/lb, and the weft is 218 yds/lb.

Each skin comprises a Z shed of 7 ppi. Consequently, 1 Z pick feeds each reed dent across the preform. In order to fully "close off" the preform near the sides (outer four dents), the Z picks-per-dent were doubled and present 14 ppi.

2.4.1 Nominal Architectural Parameters

For skin preform #1, the width-in-reed is 12.00 inches (+/- 0.25 inches), the overall width is 13.50 inches (+/- 0.25 inches), the linear weight is 64.67 oz/yd (+/- 4.0%), and the areal weight is 194.00 oz/yd (+/- 4.0%). The thickness is 0.21 inches.

The weight fractions of warp (0^0), filling (90^0), and Z (thickness) are 60.3%, 32.7% and 7.0%, respectively. The fiber volume fractions are 27.9%, 15.1% and 3.3%, respectively.

For skin preform #2, the width-in-reed is 12.00 inches (+/- 0.25 inches), the overall width is 13.50 inches (+/- 0.25 inches), the linear weight is 51.19 oz/yd (+/- 4.0%), and the areal weight is 153.57 oz/yd (+/- 4.0%). The thickness is 0.17 inches.

The weight fractions of warp (0^0), filling (90^0), and Z (thickness) are 50.8%, 41.3% and 7.9%, respectively. The fiber volume fractions are 23.0%, 18.7% and 3.6%, respectively.

For skin preform #3, the width-in-reed is 12.00 inches (+/- 0.25 inches), the overall width is 13.50 inches (+/- 0.25 inches), the linear weight is 43.27 oz/yd (+/- 4.0%), and the areal weight is 129.80 oz/yd (+/- 4.0%). The thickness is 0.15 inches.

The weight fractions of warp (0^0), filling (90^0), and Z (thickness) are 60.1%, 32.6% and 7.3%, respectively. The fiber volume fractions are 26.7%, 14.5% and 3.3%, respectively.

The skin preform specifications can be found in appendix A.

2.5 Fabrication Process / Setup of Ordinary 3D Loom

Each of the yarns was purchased from PPO Industries, Inc. by 3TEX, Inc. in the form displayed in *Figure2.8*. This yarn would then be "rewound" onto individual rollers (*Figure 2.12*), each accounting for one particular yarn within the panel. The warp yarn was rewound to 60 yards on each roller, and the Z-yarn was rewound to 80 yards on each roller.

The width of the bridge deck panel was 12" and constituted 252 warp yarns uniformly distributed across the section. Thus, 252 individual rollers were rewound with 60 yards of 103 yd/lb yarn each. The Z-yarn constituted 100 yarns across the section and 100 rollers of 675 yd/lb yarn were rewound accordingly. These rollers were then placed on a creel as shown in *Figure 2.13*.

Each yarn is then drawn through the small eye-let boards at the end of the creel nearest the weaving machine. The yarns are then pulled from the creel through a structure containing three large eye-let boards (*Figure 2.14 and 2.15*). The yarns must be pulled through in a manner conducive to the designed "draw-in" of the machine. It is important to note that there must be no or minimum fiber contact between yarns as it will significantly reduce the course of production and the quality accordingly.

Of the three eye-let boards, the top eye-let board consisted of the Z-yarn. The Z-yarn was pulled through at two layers each spreading 50 holes across the board. The

middle and lower eye-let boards consisted of the warp yarn. Each of these two boards held yarn of three layers each spreading 42 holes across.

2.6 Fiber Draw-In

The design of the draw-in was created by Dr. Salama of 3Tex, Inc. and performed by the author. There are two steel harnesses on this weaving machine (*Figure 2.16*). A harness is a rectangular component consisting of wire heddles with eye-let holes through which individual Z-yarn will pass. Harness 1 and harness 2 will commence to shift upwards and downwards opposite each other creating a crossing scheme with the Z-yarn. In between each of the arms of the heddles will pull three warp yarns.

The design draw-in is as follows. A set of 3 warp picks will be drawn through each dent of the reed. With the reed at 7 dents-per-inch, the design of 21 ppi is achieved. Between each set of warp picks is a steel heddle from either of harness #1 or #2 in alternation. The outer four dents of each side of the reed have a slight difference in design. Between each set of warp picks are two heddles, one from each of the harnesses. This process leads to a cross-section depiction of 2 Z-yarn rotating opposite each other, then 3 warp yarns, then 2 Z-yarn rotating opposite each other, and so forth.

2.7 3Weaving™ Manner

The 3Weaving™ process involves three key aspects. A flat layer of warp fiber is pulled straight through the loom and meets the Z-yarn at the fell. The Z-yarn sheds-out above and below the warp layer. And filler yarn is inserted perpendicularly above and below the warp layer, from one side of the shed, in one weaving cycle. Between each weft insertion, the harnesses cross and the reed beats the new interlacing into newly formed fabric. Thus, an increment of fabric of .2 inch thickness is the result of a "three dimensional" weaving technique utilizing a Z-directional yarn interlacing the warp and the weft.

2.8 Resin Infusion Process

Three different skin preforms were 13 inches in width and cut to 36 inches in length. The infusion system comprised vacuum bag infusion above a flat high density polyethylene table (HDPE). See figure 2.17 for illustration. This is a process whereby

resin is pulled through the fiber materials by vacuum. Resin is inserted into the system through a tube under a vacuum. This tube then leads to three coiled tubes which release the resin. In order for the resin to bleed uniformly through the preforms, coiled tubes run the length of each of the skins. At the opposite end of the coiled tubes, bleeder cloth is placed to slow down the resin, prevent race-tracking of the resin through the vacuum system, and provide time for the rest of the fabric to wet-out. There is one resin exit tube at the end of each skin. The vacuum will be pulled by a pump connected to these exit tubes. The skins are being infused in Figure 2.18.

A Jeffco 1401-12/4101-17 epoxy system is a 100:30 resin to hardener mix. It is formulated for highly increased E-glass fiber compatibility and has a very long pot life. The resin has a cure time of 12 to 14 hours. A heating blanket was placed above the panels to generate a better cure. The epoxy resin is colored transparent ruby red for visual indication of infusion progress. The panels infused in 8 minutes.

2.9 Figures and Tables

Table 2.1 Material properties of E-glass Product Type HYBON 2022^{R}, produced by PPO Industries Inc.

E-glass, generic	
Tensile Strength	500 ksi
Elongation at Break	4.80%
Modulus of Elasticity	10,500 ksi
Shear Modulus	4350 ksi
Components	**Wt. %**
Al2O3	15.2
BaO	8
CaO	17.2
MgO	4.7
NaO2	0.6
SiO2	54.3

See also Appendix C Figure C

Figure 2.1 Glass Fiber Product Type HYBON 2022R manufactured by PPO Industries Inc. (218yd/lb.)

Figure 2.2 Z, Y, and X-yarns used at 3Tex for fabrication of bridge deck

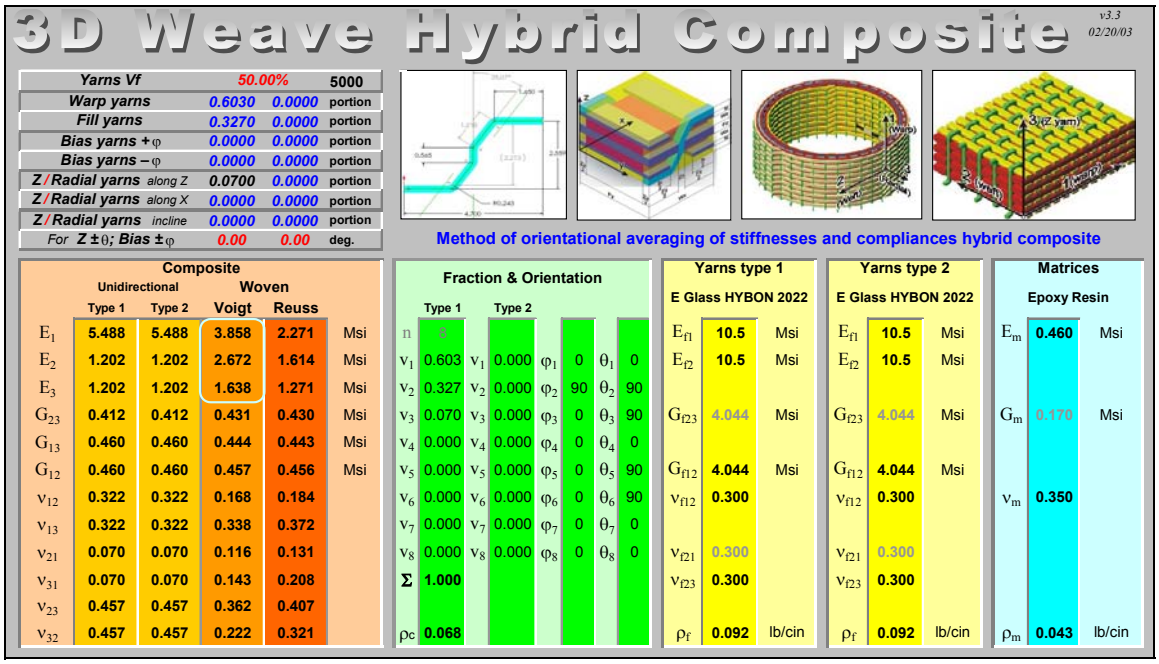

Figure 2.3 Method of orientational averaging of stiffnesses and compliances of skin #1 with assumed volume fraction of 50.0%

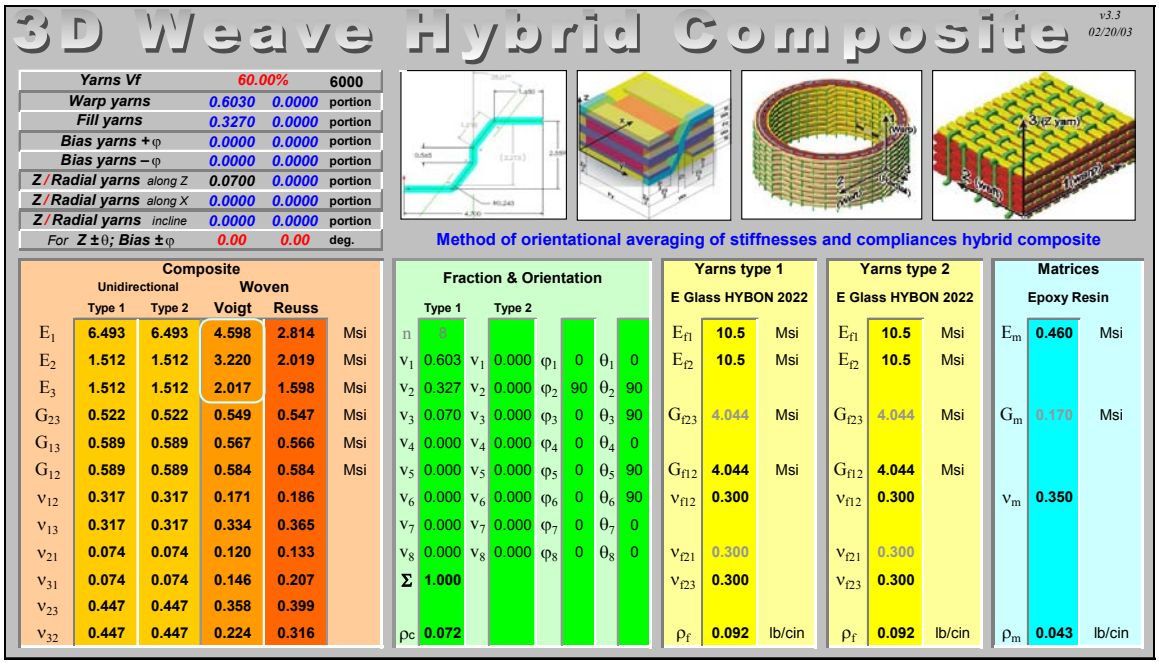

Figure 2.4 Method of orientational averaging of stiffnesses and compliances of skin #1 with assumed volume fraction of 60.0%

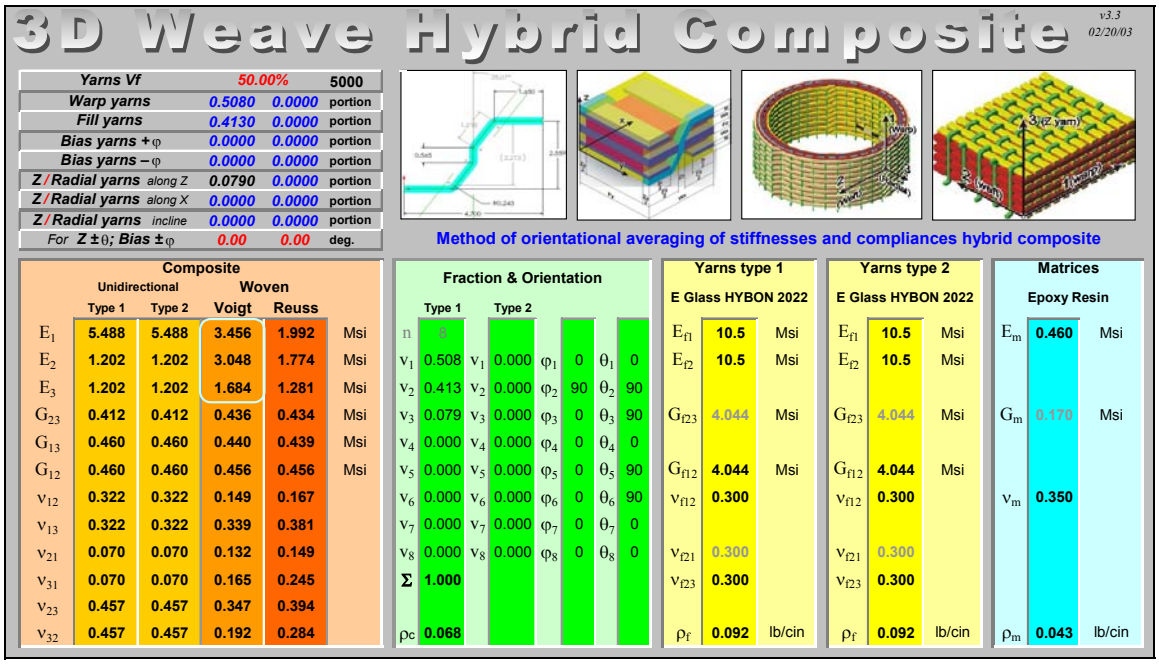

Figure 2.5 Method of orientational averaging of stiffnesses and compliances of skin #2 with assumed volume fraction of 50.0%

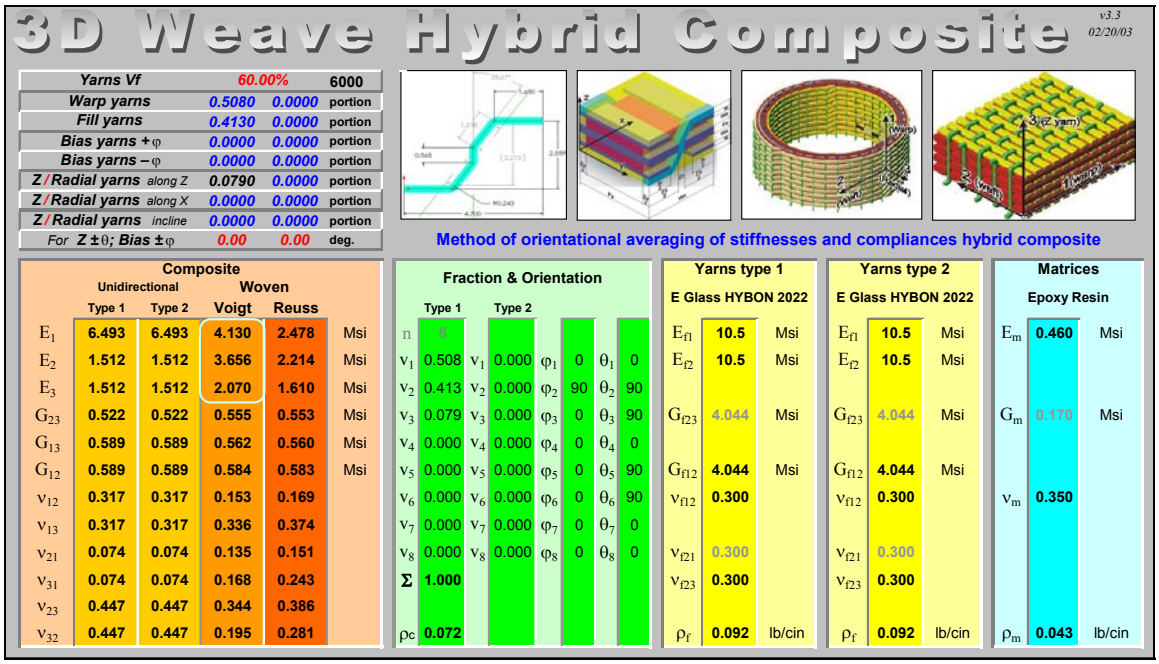

Figure 2.6 Method of orientational averaging of stiffnesses and compliances of skin #2 with assumed volume fraction of 60.0%

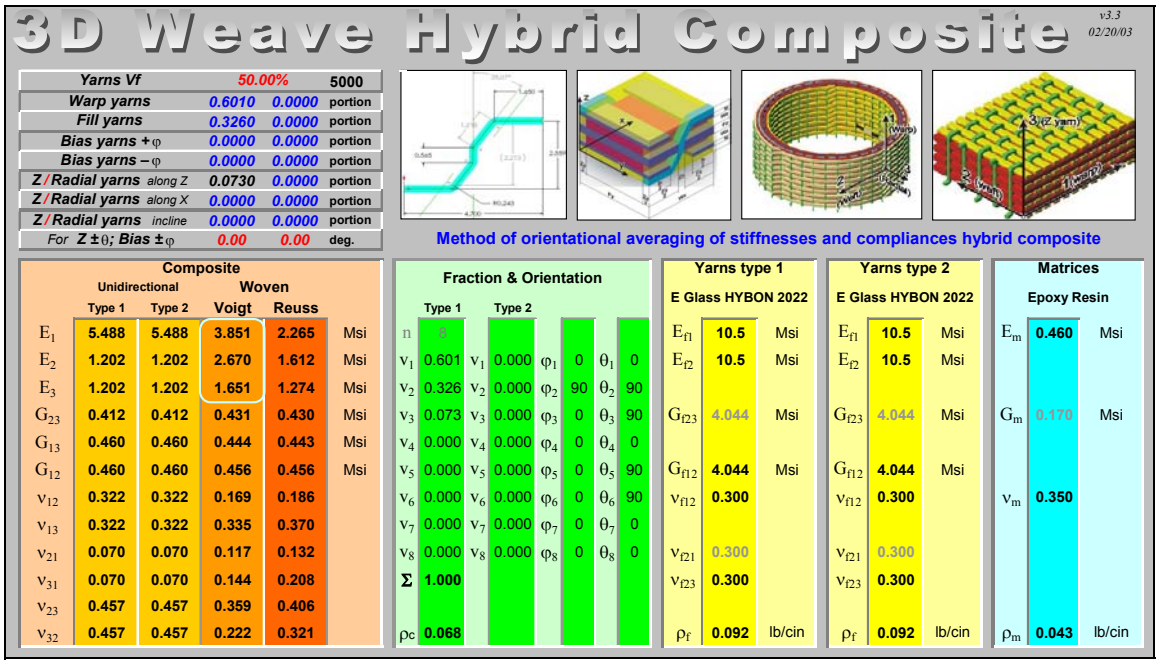

Figure 2.7 Method of orientational averaging of stiffnesses and compliances of skin #3 with assumed volume fraction of 50.0%

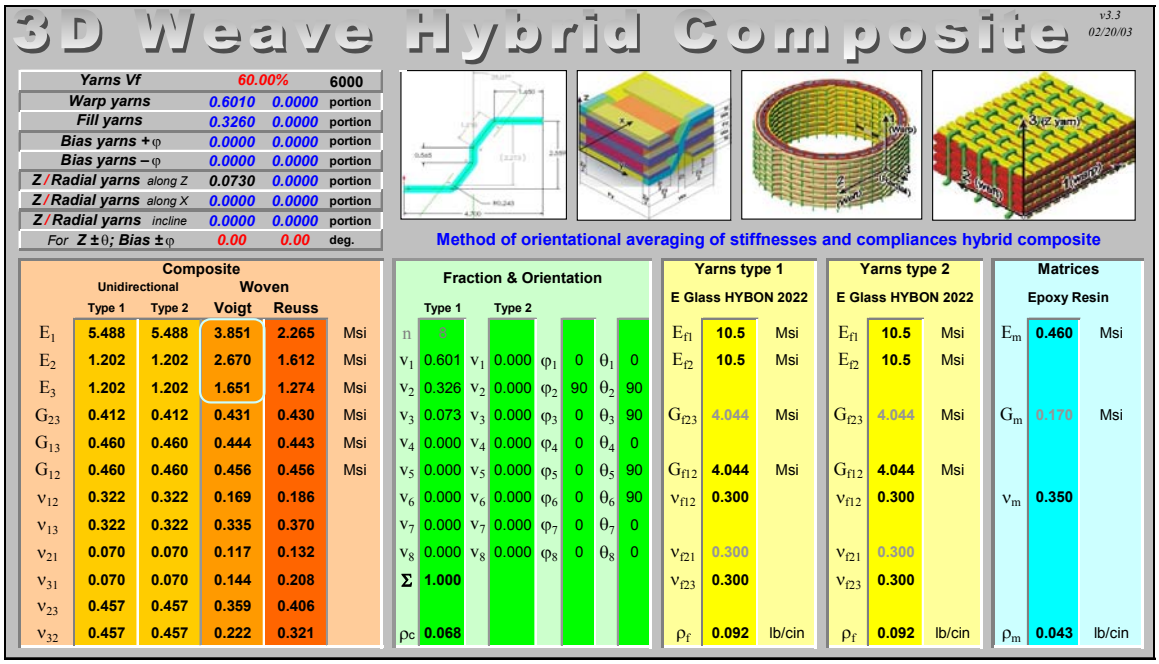

Figure 2.8 Method of orientational averaging of stiffnesses and compliances of skin #3 with assumed volume fraction of 60.0%

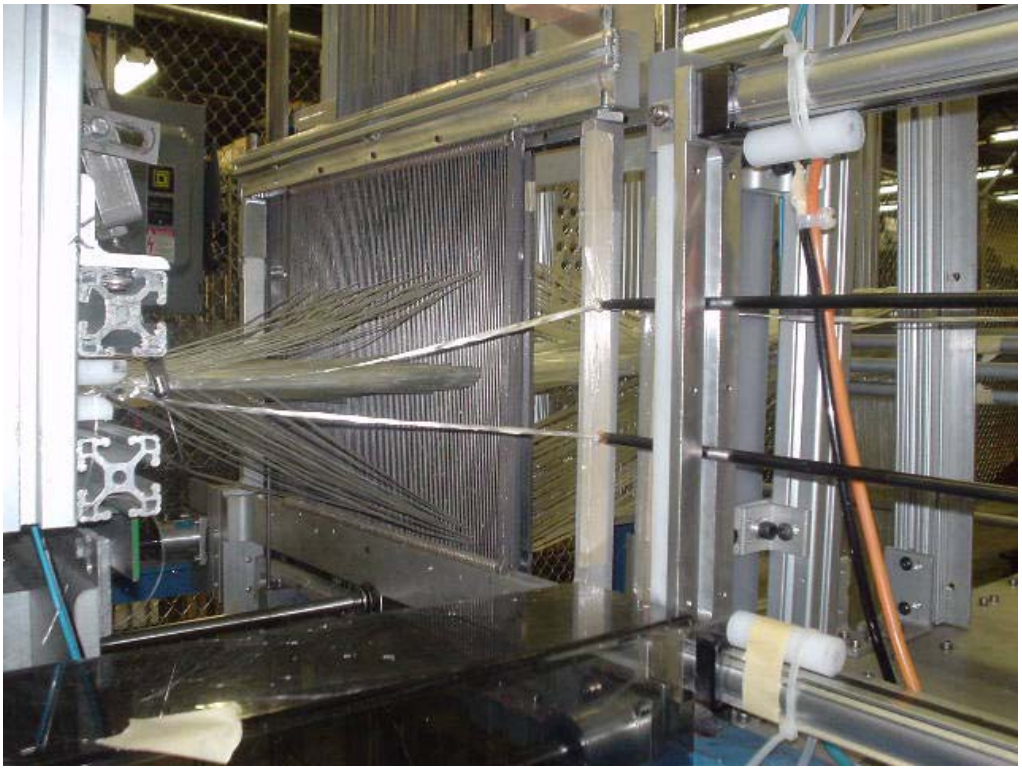

Figure 2.9 Straight fiber double insertion process above and below warp

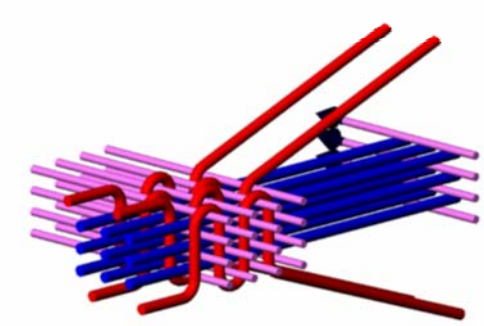

Figure 2.10 Illustration of 3WeaveTM multiple insertion process

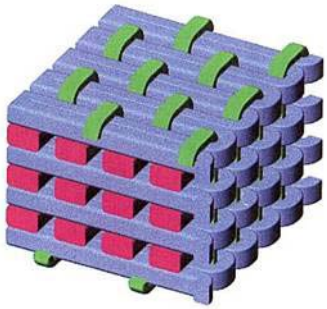

Figure 2.11 Resulting fiber architecture obtained through 3Weave process

Figure 2.12 Rewinding yarn on individual rollers

Figure 2.13 Yarn rollers aligned on creel in front large eye-let board structure

Figure 2.14 Yarn pulled through large eye-let boards

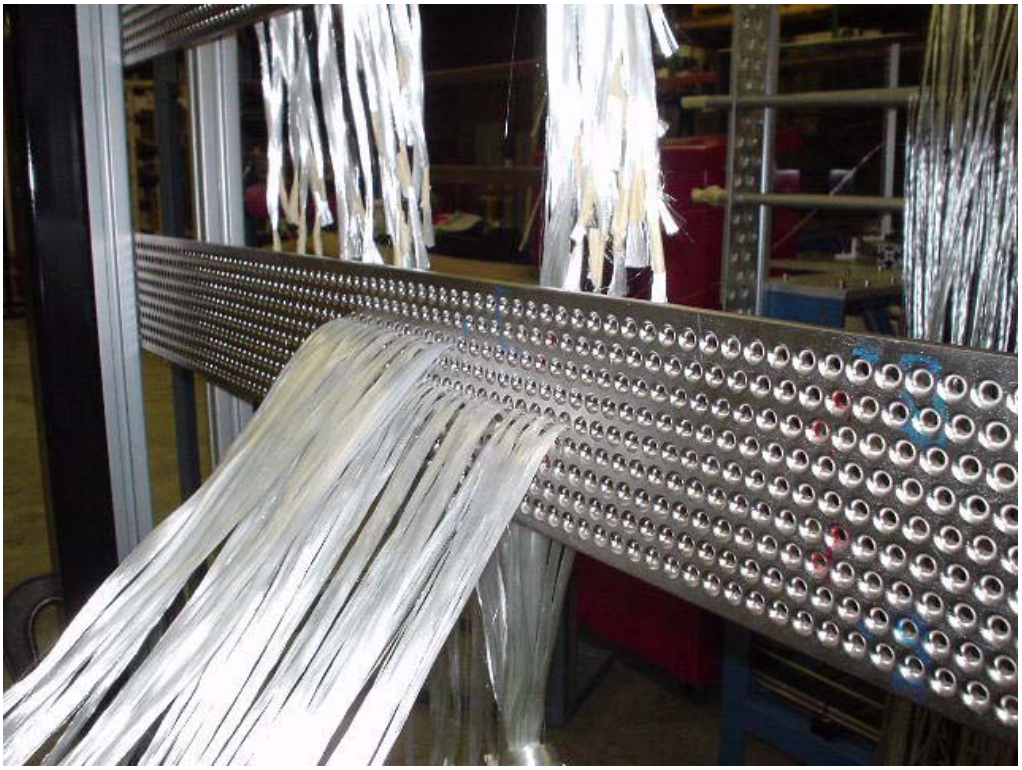

Figure 2.15 Close-up yarns through eye-let boards

Figure 2.16 Steel harness 1 in front of steel harness 2

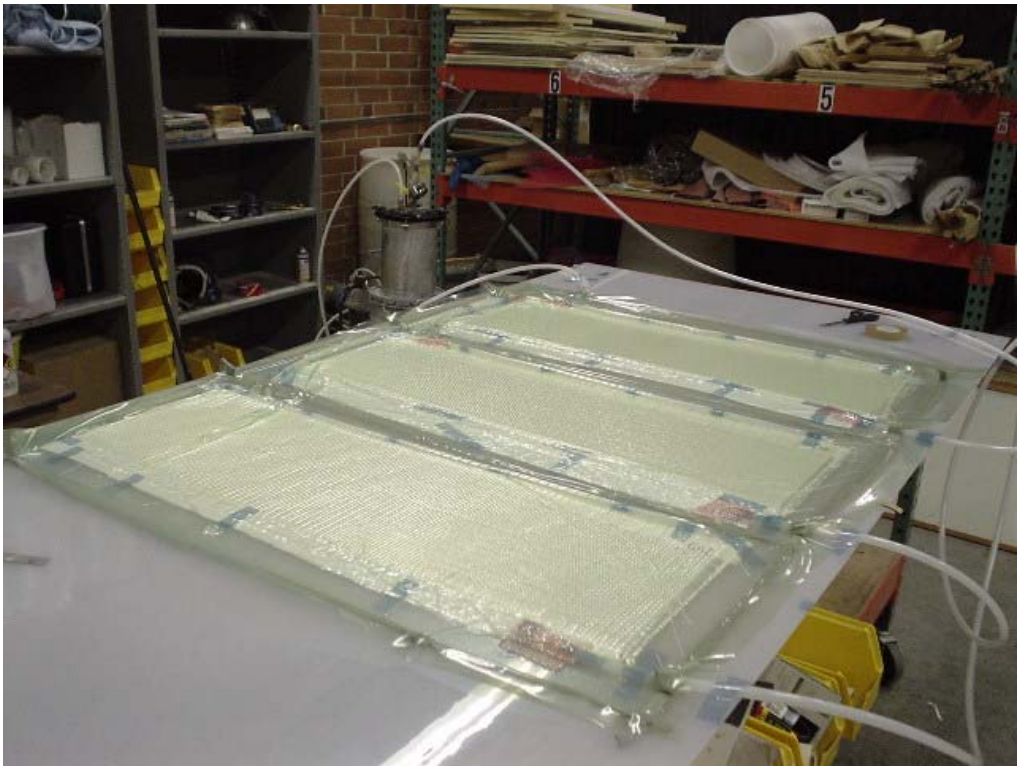

Figure 2.17 Infusion system: three dry fiber skin preforms setup for vacuum bag infusion

Figure 2.18 Skin 1, Skin 2, and Skin 3 preforms undergoing vacuum bag infusion

Chapter 3: Materials and Fabrication of Bridge Deck

3.1 Introduction

In this chapter, the author depicts the components of the three bridge deck panels as well as the material framework of these components. The author also illustrates the fabrication of the machine system theoretically capable of producing a 3D integrated woven structure expected to overcome the skin/delamination problems associated with 2D GFRP decks. The author then illustrates the complex fiber draw-in of the system and continues with the unique weaving manner thought to produce the appropriate preform. This chapter concludes with the resin infusion process and the placement of the concrete.

Deck 1 utilizes the textile engineered open-cell truss design. Deck 2 was produced as a control for Deck 1; it maintains the same thickness but sustains no woven mechanical reinforcement through its core. Deck 3 is a second generation open-cell truss preform utilizing an optimization of the fabricated 3D weaving machine system.

3.2 Components and Material Properties

The primary components of the FRP deck are woven textile reinforcements, specifically E-glass fiber, embedded in a Jeffco Products epoxy resin matrix. The yarns are a continuous glass fiber, Product Type HYBON 2022^{R}, produced by PPO Industries, Inc. and available in various size rolls (*Figure 2.1*). The fiber strands are oriented in the 3 orthogonal Cartesian coordinates and utilize the advanced 3Weave^{TM} process in producing three separate skin preforms. The glass-fiber fraction of these prefrom skins is typically 50-60% of the total volume.

The three yarns, the warp, the weft, and the Z-yarn, are defined by their weights 103 yards per pound, 218 yards per pound, and 675 yards per pound respectively (*Figure 2.2*). The 3 preform skins are connected at specified points to produce the open-cell preform structure envisioned. The preform skin product specification is in Appendix A.

This E-glass fiber is known for maximum wet-out consistency with good abrasion resistance and processing characteristics. RRG Industries boasts excellent package transfer efficiency through the use of an outer adhesive film. The product is manufactured in conformance to ISO 9002 requirements.

The epoxy system for infusion utilizes Jeffco 1401-12/4101-17 (figure 3.1). This is a multifunctional epoxy and cycloaliphatic-amine blend hardener for high performance composite parts. This system has excellent fatigue and inter-laminar shear strength with rapid wetting of E-glass fiber reinforcements. The Jeffco Epoxy Resin is colored transparent ruby red for visual indication of infusion progress. Jeffco 1401-12 Epoxy Resin is formulated for highly increased E-glass fiber compatibility. Jeffco Products asserts the production of an E-glass matrix with increased physical properties including: fiber pull-out strength, tensile strength and modulus, flexural strength and modulus, compressive strength, impact resistance, and inter-laminar strength. Additionaly, Jeffco Products asserts this product retains the above properties after exposure to heat, cycle fatigue, water, and expected adverse environmental reagents such as salt spray and acid rain.

The material properties of Jeffco Epoxy System are listed in *Tables 3.1 and 3.2*. Technical information given for Jeffco Products on the epoxy system is detailed in Appendix B. Product Description for the E-glass fibers, HYBON 2022, is given in Appendix C.

Each deck will comprise a concrete layer above the cured composite deck. The specifications for the material properties of concrete are given in Appendices D and E. Actual material properties of the concretes are obtained experimentally and illustrated in section 5.3.1.

3.3 Innovative Fiber Architecture

3.3.1 Introduction

Deck 1 and Deck 3 utilize the advanced fiber architecture of the completely woven open-cell design.

3.3.2 Innovation

As illustrated in latter figures, three 3Weave^{TM} fabrics are woven simultaneously on one weaving machine due to the 3Weave^{TM} multiple filler insertion technique. This 3D orthogonal fiber architecture was demonstrated in figure 2.11 of chapter 2. The innovative architecture of this preform is that the core fabric/skin attaches to the outer skin by the Z-yarn shed of the core wrapping around the filler insertion of the outer layer

at specified points. This introduces a fiber reinforcement through the connection point of the core to the skin. In addition, this core Z shed interlacing in alternation with the top and bottom skins is the mechanism that provides an open cell preform, a preform that can "puff out" into a three dimensional structure.

The core skin will attach to the outer skin for two weaving cycles thus producing two crossings about the filler strand. At 116 Z-strands per layer, two layers of Z-yarn shed provides 464 strands (2 crossings * 2 layers * 116 Z-strands per layer) of 675 yd/lb E-glass fiber reinforcement. Since crossing about the filler axis entails strands leading up to and hence coming from, the number of actual reinforcing strands in the connection is 2*464=928. More detail of the weaving method is covered in 3.6.

The continuous reinforcing fiber through the components connection provides direct elimination of the outer skin layers delaminating from the core. Additionally, the 3Weaving^{TM} of the individual skins provides direct reinforcement against skin delaminating from itself.

The 3Weaving^{TM} of the 3 individual skins allows non-crimped in-plane warp reinforcement which asserts higher static strengths and moduli of elasticity according to Singletary et al 2001. The Z-yarn may act as resin channels within the three skins and particularly to the center of the core of the "puffed out" preform during the resin infusion process.

3.3.3 Woven Preform Design

Woven composite cross-sections are defined in picks per inch (ppi). A pick is a unit strand of fibers pulled through a weave. The design of each skin calls for a warp of 21 ppi, a Z shed of 7 ppi, and a weft insertion of 7 ppi. The reed is comprised of 7 dpi and thus 3 picks of warp feed through each dent. Consequently, 1 Z pick feeds each reed dent across the preform. In order to fully "close off" the preform near the sides (outer four dents), the Z picks-per-dent were doubled and present 14 ppi.

The width of the preform comprises 108 dents of the reed. At 7 dpi, the preform width is approximately 15.4 inches. The warp of each skin is 3 picks-per-dent (ppd) and consequently 324 picks overall. Thus, for 3 skins there are 972 total picks. The Z of each skin is 1 ppd for 108 dents plus an additional 1 ppd for the outer four dents. Thus,

for 3 skins there are 348 total picks. Overall, 972 picks of warp yarn have to be back-wound on individual rollers for the supply along with 348 picks of Z-yarn.

Each of E-glass fiber, the warp is 108 yds/lb, the Z-yarn is 675 yds/lb, and the weft is 218 yds/lb.

3.4 Fabrication of Machine System

3.4.1 Introduction

The objective is to engineer a machine capable of producing a 3D integrated woven preform structure by utilizing the unique manner of the 3Weave^{TM} process. Photographs will assist in illustrating the system.

3.4.2 Fiber Feed System

Spools are "backwound" with E-glass fiber and placed on three aligning creels at the rear of the fabrication system. As illustrated in figure 3.2, the warp fibers are fed from the outer two creels while the Z-yarn is fed from one inner creel. Individual U-shaped compensation weights are hung at the creel to provide tension in the warp layers as they are pulled through the system.

3.4.3 Warp/ Z-Yarn Compensation System

This system will compensate the slack fibers produced when the machine necessitates reverse. The optimum compensator location was determined to stand between the fiber supply creels and the fiber partition. The designed and built system consisted of an "S" mechanism frame and a compensator mechanism frame within a welded steel rectangular support frame showed in figure 3.3. The "S Mechanism Frame," as labeled in figure 3.3, applies an "S" wrap to each of the 3 layers of warp and to each of the 3 layers of Z-yarn by utilizing a crossing movement of 1 steel rod upward between 2 permanent rods. This structure is illustrated in figure 3.4. The "action rod" is bolted to the S mechanism frame and is fired through the permanent rods upon exertion of four 4 inch air cylinders above the frame. In front the S mechanism frame is the "Compensator Mechanism Frame," also illustrated in figure 3.4. The fiber layers pass through this

compensator mechanism frame above each of the "Compensator Rods" bolted to this frame (Figure 3.5). The rods fire upward with the frame upon exertion of the 4 twelve inch air cylinders, illustrated in figure 3.6, to take up the slack of the fiber layers during the reverse portion of the weaving cycle. Overall, the S mechanism is fired to clench the fibers, and the compensator mechanism absorbs the slack induced by the machine reverse. This S mechanism prevents the compensator from pulling additional fiber from the supply creels. An image of the entire compensation system is displayed in figure 3.7.

Air throttles were used to control the thrust of the air cylinders on the compensation system frames. ¼ inch air tubing was used to fire the cylinders upon signal from the input/output of the computer.

3.4.4 Partition System

In front of the compensation system is the partition system that provides resistance to take-up of the fiber layers and positions these layers into an appropriate shed. "S" wraps of fiber layers are used to provide resistance to maintain tension in the warp and Z-yarn during the weaving process (Figure 3.8). After the major S wrap of figure 3.8, the top Z-yarn layer is divided into two by an alternation of two S wraps atop the partition system (Figures 3.9 and 3.10). Every other fiber strand utilizes the first S wrap, and the fiber strands between these utilize the second S wrap. U-shaped weight placement on individual fiber strands then follows this alternation accordingly. The weight placement is a means of small compensation of the Z-yarn during the crossing of the steel heddles, i.e., the weights attempt to provide constant tension of this Z-yarn (Figures 3.9 and 3.10). This weighted division setup exists for each of the three layers of Z-yarn. The front of the partition system then guides each of the warp and Z layers into the appropriate shed position as seen in figure 3.11.

3.4.5 Harness System

Six harnesses were installed with vertical sliding capability. Each of these harnesses is equipped with 108 plus steel heddles, 33 inches in length. A heddle is one of a set of parallel cords or wires in a loom used to separate and guide the warp threads and to provide an eyelet hole through which an individual Z-yarn passes. The vertical sliding of a pair of harnesses provides the crossing of the Z-yarn about the inserted filler

yarn. Since the filler insertion is perpendicularly above and below the warp plane, the crossing Z-yarn interlaces this mid-plane into a fabric. From the partition system, the warp fiber sheds are drawn between these steel heddles, through the reed, and into the clamp of the take-up system. The Z-yarn is drawn through eyelets of the steel heddles and then follows the same path (Figure 3.12). The detailed design of the fiber draw-in is covered in section 4.5. From back to front, the harnesses are numbered 6, 5, 4, 3, 2, and 1 (Figure 3.13). Harnesses 6 and 5, 4 and 3, and 2 and 1 operate the Z-yarn of the bottom skin, top skin, and middle skin (core), respectively.

The harnesses are activated to cross by compressed air operating on the two steel rods attached beneath the harnesses. The harness limiting system was designed to confer the optimum shed orientation of the Z-yarn with respect to the warp shed. This was accomplished by placing "stops" on the two rods pultruding above and below each harness. Optimal shed orientation and stops are illustrated in figures 3.14 and 3.15. Additional harness limits are provided for the core harnesses. These stops must be removable as the course of the cycle proceeds in order for the middle skin harnesses to raise the Z-yarn shed above/below the filler insertion of the adjacent skin (Figure 3.16). This action attaches the core skin to the outer skins.

Directly in front of the harnesses is the reed, a comb-like device used to pack the interlacing weft strands into the fabric. A reed is a frame having parallel flat strips of metal, between which the warp threads pass. The reed used was 20 inches wide and 12.5 inches tall with 7 dents per inch, i.e., there were 7 openings between strips every 1 inch. The size of the preform is limited by the size of the reed. The reed must withstand proper spacing of the sheds of the warp and the Z-yarn. This spacing is illustrated in previous figures 3.13 and 3.14. The density of the preform is determined by the dents-per-inch (dpi) of the reed. For instance, 7 dpi will pack in more warp fiber then 5 dpi.

3.4.6 Take-up System

The take-up system consists of a 20 inch wide fabric clamp cantilevered above a 1 ¼ inch diameter threaded bar attached to a rotary motor. With signal from the input/output, the rotary motor rotates the threaded bar in turn moving the fiber clamp forward. This action pulls the fibers from the supply creels and through the machine for

the weaving process. The motor must be capable of reverse as it is necessary for the design of the weaving process.

3.4.7 Rapier System

A rapier is a light cylinder with a small ring fixed on the end used for thrusting filler insertion yarn between the sheds of the warp and the Z-yarn. Adherent to the weave design, 2 rapiers encompass the filling insertion for each of the 3 layers of warp. Thus, 3 sets of rapiers were mounted on the left side of the 3 sheds of warp. This is rapier system #1. It is important to note that each of these sets of 2 rapiers must align only slightly above and below the corresponding shed to warrant a tight weave with the crossing Z-yarn. This and maintaining a tight shed affirm the rapiers not catching a Z-yarn during insertion of the weft. This multiple filler insertion is the essence of the patented 3Weave^{TM} process (Figures 3.17-3.18). The right side of the shed maintains a single rapier set aligned with the center of the shed. This is rapier system #2. This set provides the filler insertion to the middle skin layer during the portion of the weaving cycle that necessitates weaving additional length of the core skin. This additional length allows the preform to "puff out" into a truss form. See section 3.6 for weaving details.

Images of the mounted rapiers threaded with 218 yd/lb E-glass fiber are in figures 3.17 and 3.18. All rapiers are mounted on linear motor carriages, horizontally sliding brackets, which are shifted by compressed air. Selvedge holds are mounted near each side of the fell of the fabric. This actuated rod holds one end of the weft yarn as the rapiers insert the filler through the sheds.

3.4.8 Entire Machine

The necessary modifications were made to ensure the required number of outputs (control channels) were available through combining actions/motions. The program was written in Basic and contains functionality for all required motions: rapier cycles, take-up cycles, harness cycles, beat-up cycles, and compensator cycles. Careful planning and timing are noted to ensure sensitive management of the fiber strands. The basic weaving program is displayed in appendix D.

3.5 Intricate Fiber Draw-In of System

According to the design of section 3.3.3, 972 picks of warp yarn have to be back-wound on individual rollers along with 348 picks of Z-yarn. These rollers are then placed on the supply creel as illustrated in previous figure 3.2, and the individual picks must then be drawn to the front of the creels and through the creel eye-let boards. Prevention of pick intertwining will allow for less fiber damage and a cleaner weave. The potential skin layers are then formed by the designed division of the warp supply into 3 separated eye-lit plates on the eye-let board frame as demonstrated in figure 3.19. The Z supply is also divided up into three layers; each layer corresponds with one layer of warp.

Each of the layers is then drawn through the compensation system, which consists of the S wrap mechanism and the compensator mechanism. This is displayed in figure 3.7. As illustrated in figure 3.11, layers are then drawn through the partition system and into the assembled weaving machine. The rods separating and organizing the layers in the partition system were placed after the fibers had been drawn completely through the machine into the clamp of the take-up system.

The weaving system consists of six harnesses and a reed through which all fiber layers pass. The design draw-in of the weaving system is as follows. For one layer, 324 picks of warp must be drawn in sets of 3 picks-per-dent of the reed. Between each set of 3 warp picks exist 3 steel heddles, one from each of the 3 sets of harnesses (the six harnesses are devised in 3 sets of 2). This is consistent for each of the other layers of warp yarn.

More complicated, the Z-yarn is drawn through the eye-let holes of these steel heddles, one pick per eye-let hole (Figure 3.12). 2 Z sheds (upper and lower) correspond with 1 layer of warp as demonstrated in figure 3.14. The back 2 harnesses (6 and 5) weave the mid-plane of the bottom warp layer. The middle two harnesses (4 and 3) weave the mid-plane of the top warp layer. The front two harnesses (2 and 1) weave the mid-plane of the core layer and the attachment of the core layer to the outer layers. For one dent of the reed: for the bottom skin, 1 upper Z pick is drawn through the heddle eye-let of back harness 6; for the top skin, 1 upper Z pick is drawn through the heddle eye-let of middle harness 4; and for the core skin, 1 upper Z pick is drawn through the heddle eye-let of front harness 2. Each of these 3 Z picks feed through this same dent on

the reed. For the adjacent dent of the reed: for the bottom skin,1 lower Z-pick is drawn through the heddle eye-let of back harness 5; for the top skin,1 lower Z-pick is drawn through the heddle eye-let of middle harness 3; and for the core skin, 1 lower Z-pick is drawn through the heddle eye-let of front harness 1. Each of these 3 Z picks feed through this same adjacent dent on the reed.

The outer four dents of each side of the reed have a slight difference in design. For each one of these four dents: for the bottom skin, 1 upper Z pick and one lower pick are drawn through the heddle eye-lets of back harnesses 6 and 5, respectively; for the top skin, 1 upper Z pick and 1 lower Z pick are drawn through the heddle eye-lets of middle harnesses 4 and 3, respectively; and for the core skin, 1 upper Z pick and 1 lower Z pick are drawn through the heddle eye-lets of front harnesses 2 and 1, respectively.

All 9 sheds meet at the fell just before the fabric guide. As a preform, it feeds into the fabric/cloth clamp which is part of the take-up system.

3.6 Unique Weaving Manner

An innovative weaving manner was designed and utilized to fabricate a completely woven open cell preform with diagonal core members opposite each other, a truss-like orientation. The complete weaving cycle involves a total of four steps.

Step 1: The first step in this weaving process is to weave the two skins and core separately. For a 3" thick structure with 45 degree triangular core, the core length is 4.4". One half of that is 2.28" or equivalent of approximately 16 filler insertions (at 7 insertions/in. or 7 ppi).

As shown in figure 3.20, the two skins and the core are being woven at the same time for the first half (16 insertions) of this step. All 6 rapiers insert and all 3 pair of harnesses cross during this period. After this period, the process will weave the second half of the core only. For this section, only core rapiers # 3 and 4 (rapier system #2) and harnesses # 1 and 2 are in action. After weaving 16 insertions for the second half, the take-up will need to reverse a distance equivalent 16 insertions to move the fell of the fabric back. The process is then ready for the next step – connecting the core to one of the skins.

Step 2: As shown in figure 3.21, the core will be connected to the upper skin (skin#2) during this step. During this period, harnesses # 1 and 2 will have an asymmetric opening which will enclose rapiers # 3, 4, 5, and 6. All 6 rapiers and all 6 harnesses will be in action in this step. There are only two insertions in this step.

Step 3: Repeat step 1.

Step 4: As shown in Figure 3.22, the core will be connected to the lower skin (skin# 1) during this step. During this period, harnesses # 1 and 2 will have an asymmetric opening which will enclose rapiers # 3, 4, 1, and 2. All 6 rapiers and all 6 harnesses will be in action in this step. There are only two insertions in this step.

Completion of cycle.

3.6.1 Weaving of Deck 1

As illustrated in figure 3.23, all 9 sheds meet at the fell just before the fabric guide and feed into the fabric/cloth clamp which is part of the take-up system. This deck utilizes the unique weaving manner presented in section 3.6. Thus, three skins are woven simultaneously for 16 picks; then, the core is woven an additional 16 picks; the take-up system is reversed 2.3 inches (16 picks equivalent); and the core skin is connected to the top skin for two picks. The next 50 picks follow with the connection of core to the bottom skin. This 100 pick cycle/process is repeated with an end result of an open cell truss orientation.

The weaving design sanctions the core skin to buckle amidst the reversing of the take-up system and the connection of this core to the outer skin. This is a temporary fabric buckling as the preform is designed to "puff-out" into an open cell structure with straight diagonal core members. After a 5' section was woven and released from the fabric clamp, the preform puffed-out to 1 ½ inches in thickness. Observations proposed an explanation of this first generation truss deck.

First, the core fabric maintained to great of a stiffness of to buckle with the reverse of the take-up system and the connection of the skins. Second, a three skin preform comprising a buckled core fabric was too thick to pass through the opening of the fabric guide illustrated in figure 3.24. Third, the fabric clamp of the take-up system compressed all three skins together, and the tension induced by the take-up system

prevented the height levels of the outer skins to adjust to the buckling of a center core. In sum, since the core fabric was unable to buckle appropriately, the puffed-out height of the preform was limited to 1 ½ inches and did not meet the 3" design.

3.6.2 Weaving of Deck 2

The skins of deck 2 were woven on the ordinary 3D loom illustrated in chapter 2. Utilizing the 3Weaving^{TM} manner, one layer of warp yarn (including 2 corresponding Z sheds) is pulled straight through the machine to the fabric clamp of the take-up system. Thus, the two skins were woven individually and are ultimately laminated to the Balsa wood core. There are no fiber mechanical connections between these skins.

3.6.3 Weaving of Deck 3

This is a second generation truss bridge deck utilizing the unique weaving manner presented in section 3.6. As illustrated in figure 3.25, the fabric clamp and guide have been modified to obtain the designed 3 inch puffed-out preform. The fabric skins have been spaced open within the fabric clamp, and the fabric guide has been opened respectively. This facilitates a better weave by: 1) enabling a better shed-out of the fiber layers and thus less hairiness and 2) eliminating the need to buckle the core skin when connecting it to an outer skin. In addition, the triangular cut Balsa wood cores are inserted as the weaving cycles take place. This not only prevents buckling of the core skin but also assures a rigid fit of the core with the fabric. This tightness aids in maintaining the straight diagonal composite members desired in a truss. See figure 3.26 for the opened fabric guide and the insertion of Balsa triangular shafts. In sum, this composite preform is woven off the machine in open cell form.

3.7 Resin Infusion Process

Each of the composite decks was infused with a process whereby resin is pulled through the fiber materials by vacuum beneath a plastic bag. The system utilized a Jeffco 1401-12/4101-17 epoxy system with a 100:30 resin to hardener mix. It is formulated for highly increased E-glass fiber compatibility and has a long pot life of 120 minutes. The resin has a cure time of 12 to 14 hours. A heating blanket was placed above the deck to

generate a better cure. The epoxy resin is colored transparent ruby red for visual indication of infusion progress.

3.7.1 Infusion of Deck 1

The infusion system comprised vacuum bag infusion above a flat steel table. Metal truss connector plates, punched from hot-dipped galvanized sheet steel, are bent and devised as metal shear connectors for the composite bridge deck (figure 3.27). The teeth of these plates provide mechanical connection with the composite skin (figure 3.28). The truss plates are hammered into the dry preform and infused with the deck. Triangular cut Balsa wood shafts 1 inch in height and 6 ½ inches in length are inserted between the preform skins essentially puffing-out the preform to its 1 ½ inch height as illustrated in figure 3.27.

A blue sheet of peel ply was set atop the deck to produce a prepared surface ready for bonding with the concrete, eliminating the need for mechanical abrasion on composite top. It was assumed race-tracking would occur beneath the metal shear connectors, so red flow media was added between each connector to assist these areas in wetting out before the race-tracking would induce a channel out for the resin. Small strips of white bleeder cloth were taped above the ends of each metal shear connector to prevent puncturing of the vacuum bag. A 5' spiral tube ran the length of the deck to immediately transfer resin along the entire side of the deck aiming to provide a uniform flow of resin across the deck. And a 5'long rectangle of Balsa wood covered in white bleeder cloth ran the opposite side of the deck to act as a dam. This wall provided time for the entire composite to wet out before the resin could channel out of the system. This setup is illustrated in figure 3.29. The vacuum bag is set atop the composite deck and is bonded to the steel table with tacky tape (figure 3.30). Figure 3.31 shows the uniform flow of resin across the deck; figure 3.32 shows the infusion complete.

3.7.2 Infusion of Deck 2

The infusion system comprised vacuum bag infusion above a flat high density polyethylene table (HDPE). Metal truss connector plates, punched from hot-dipped galvanized sheet steel, are bent and devised as metal shear connectors for the composite

bridge deck (figure 3.33). The teeth of these plates provide mechanical connection with the composite skin (figure 3.34). The truss plates are hammered into the dry top skin and infused with the deck. A solid rectangle of Balsa wood is placed between the upper and lower skins. There is no mechanical connection between the outer skins and this Balsa core.

Figure 3.35 illustrates the setup for infusion. This infusion system is analogous with that of Deck 1. A blue sheet of peel ply was set atop the deck. Red flow media assists resin flow between each connector. Small strips of white bleeder cloth were taped above the ends of each metal shear connector. A 30" spiral tube ran the length of the deck to provide a uniform flow of resin across the deck. And a rectangle of Balsa wood covered in white bleeder cloth ran the opposite side of the deck to act as a dam. Illustrated in figure 3.36, the vacuum bag is bonded to the table with tacky tape, and the resin flowed uniformly across the system during the infusion. The completely infused deck is displayed in figure 3.37. Figure 3.38 points out the deck is ultimately laminated together with no mechanical connection between the outer skins and core.

3.7.3 Infusion of Deck 3

The infusion system comprised vacuum bag infusion above a flat steel table as illustrated in figure 3.39. 3D orthogonal woven 270 ounce dry fiber fabric (3/4 inch thickness) was cut into strips and nailed atop the truss preform with 1 inch Brad nails. These strips are added as shear connectors and are infused with the deck preform. Figure 3.40 shows these shear connectors.

A 5' spiral tube ran the length of the deck to immediately transfer resin along the entire side of the deck aiming to distribute a uniform flow of resin along the deck. Beneath this tube was red flow media, and beneath this media was black flow media. Each of these flow media aim to transfer the resin from the spiral tube up the side of the deck preform so that resin can flow uniformly across the top of the deck (figure 3.41 and 3.42). A 5'long white bleeder cloth dam ran the opposite side of the deck to provide time for the entire composite to wet out before the resin could channel out of the system. This setup is illustrated in figure 3.43. The vacuum bag is set atop the composite deck and is bonded to the steel table with tacky tape. The infusion system was given 3 resin

exit tubes by which the system could pull a vacuum. This cautious measure was taken in case the resin flowed across the mid-section of the preform and through the bleeder cloth dam before both ends of the preform wetted out. The two additional exit tubes were placed at opposite ends of the deck to potentially pull resin that direction.

Figure 3.44 illustrates Deck 3 completely cured with the bag removed. It is important to note that the same epoxy resin system is used for each of the three decks; Jeffco Products did not dye this batch of resin red.

3.8 Placement of Concrete

3.8.1 Deck 1

QUIKRETE® 5000 High Early Strength Concrete Mix is a commercial grade blend of stone or gravel, sand and cement specially designed for higher early strength. It achieves 3500 psi after 7 days and 5000 psi after 28 days.

After infusion and curing, the sides of Deck 1 were trimmed clean and prepared for formwork as shown is figure 3.45. The composite deck thickness was 1 ½ - 1 ¾ thickness. Thus, 2 x 4 wood formwork encapsulated the deck. 2 inch thickness of QUIKRETE® 5000 concrete was cast atop Deck 1 (total deck thickness - 3 ½ inches) (figure 3.46). The concrete was spread to fill the form, rodded, vibrated and then floated immediately. Deck 1 and Deck 2 were cast from the same batch of concrete.

3.8.2 Deck 2

The composite deck thickness was 1 ½ inches. 2 x 4 wood formwork encapsulated the deck, and 2 inch thickness of QUIKRETE® 5000 concrete was cast atop Deck 2. The concrete was spread to fill the form, rodded, vibrated and then floated immediately. Figure 3.47 displays the composite deck after infusion and curing, and figure 3.48 shows the casting of concrete. The total deck thickness was 3 ½ inches. Four 4” x 8” cylinders were cast from this batch of concrete to determine the compressive strength of the concrete atop each deck the day of testing. More information on concrete compressive strengths is located in section 5.3.1. QUIKRETE® 5000 High Early Strength Concrete Mix specification data is located in Appendix D.

3.8.3 Deck 3

SikaTop® 122 Plus is a two-component, polymer-modified, cementitious, trowel-grade mortar plus FerroGard 901 penetrating corrosion inhibitor and aggregate. This polymer concrete boasts high compressive and flexural strengths and high early strengths. Component "A" is 1 gallon plastic jug of activator, and component "B" is one 61.5 lb. bag of cementitious material. All of component "A" was poured into the mixing container. Then all of component "B" was added while mixing. Then 3/8 inch coarse aggregate (pea gravel) was added up to 42 lbs. This aggregate was in accordance to ASTMC1260.

Figure 4.49 displays Deck 3 completely cured with the sides trimmed clean. 2 x 6 wood formwork encapsulated the deck and lightweight reinforcement was set atop the composite deck. Figure 3.50 illustrates the formwork enabling a 1 inch layer of concrete to be set. The polymer concrete was worked into the formwork, vibrated, and then screed (figure 3.51). The concrete was moist cured with burlap as per Sika® recommendations. See Appendix E for technical information and recommendations. Two 4" x 8" cylinders were cast from this batch of concrete to determine the compressive strength of the concrete the day of testing the deck. SikaTop® 122 Plus Concrete Mix specification data is located in Appendix E.

3.9 Summary

Each of the three decks were woven and infused at 3TEX, Inc. in Cary, N.C. Deck 1 demonstrated that the machine built to produce the theoretical completely woven open-cell truss preform was successful. Deck 2 served as a non-truss control composite bridge deck. Deck 3 demonstrated the success in reaching the 3" open-cell truss design after optimizing the fabricated 3D weaving machine. The concrete surface cast atop each of the decks was performed at the Constructed Facilities Laboratory at North Carolina State University. It was this laboratory that demonstrated the testing of these bridge decks in three-point bending up to and beyond an AASHTO HS20 wheel load. The experimental program is illustrated in Chapter 5.

3.10 Tables and Figures

Table 3.1 JEFFCO PRODUCTS Epoxy System for Infusion liquid properties

JEFFCO PRODUCTS Epoxy System for Infusion		
Properties of 1401-12/4101-17 System Liquid Properties:	Minimum	Maximum
Resin Viscosity (Part "A") (cps) @77degree F	900	1000
Hardener Viscosity (Part "B") (cps)	10	10
Mixed Viscosity (cps)	140	140
Mix Ratio, Resin to Hardener (by weight)	100:30	100:30
Gel Time, minutes @ 77degree F	70	75
Weight Per Gallon, Resin (lbs.)	9.4	9.5
Weight Per Gallon, Hardener (lbs.)	7.9	8
Color, Resin	Transparency Ruby Red	
Color, Hardener	Clear - Amber	

Table 3.2 JEFFCO PRODUCTS Epoxy System for Infusion cured physical properties of neat resin

JEFFCO PRODUCTS Epoxy System for Infusion		
Neat Resin Cured Properties of 1401-12/4101-17 System:	Minimum	Maximum
Shore D Hardness	87D	87D
Tensile Strength, psi	83,000	83,000
Flexural Strength, psi	86,000	86,000
Compressive Strength, psi	14,500	14,500
HDT, Degree F	188	188
Elongation	7.5	8.5
*Jeffco 1401-1 Epoxy Resin, 100 Parts, Jeffco 4101-17 Epoxy Hardener, 30 Parts *Cured 2 hours at 35 Degrees C + 14 hours at 50 Degrees C		

Figure 3.1 The epoxy system for infusion utilizes Jeffco 1401-12/4101-17.

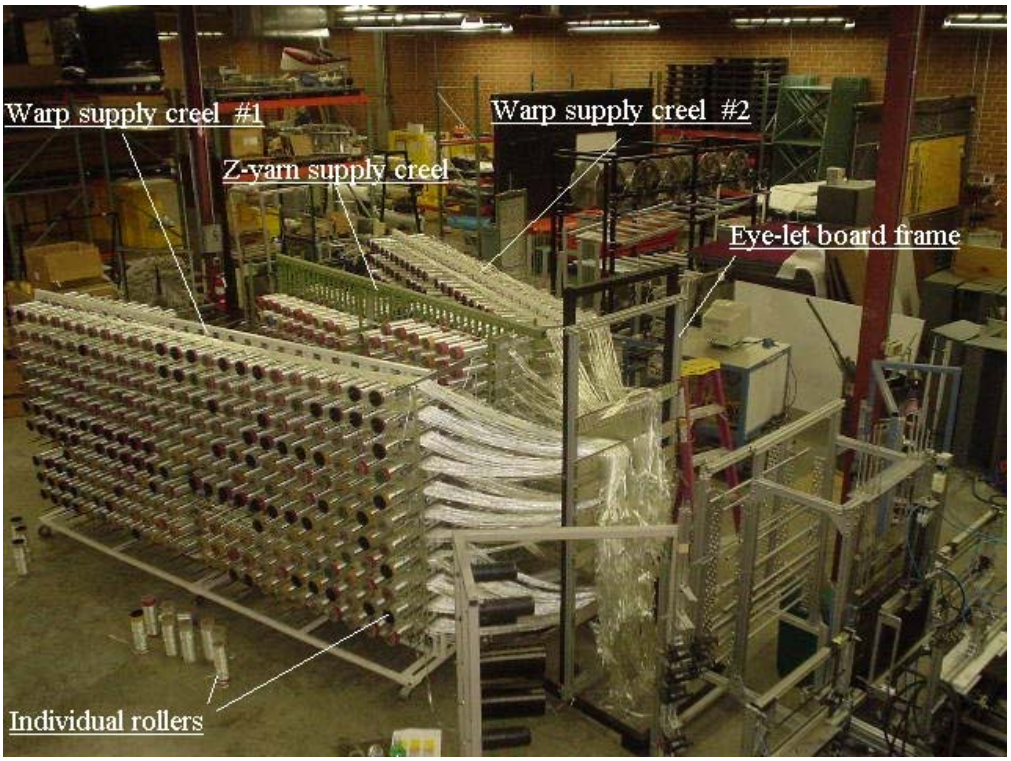

Figure 3.2 Image displays 3 supply creels holding 972 rollers of warp fiber and 358 rollers of Z-yarn. Picks are drawn through the front of the creel eye-lit boards to the eye-lit plate frame.

Figure 3.3 Frames of compensation system

Figure 3.4 S wrap induced by upward crossing movement of "action rod" (beneath fiber layer) between two "permanent rods" (left: demonstrates 1 layer; right: 2 layers close up)

Figure 3.5 Compensator mechanism rods

Figure 3.6 4 twelve inch stroke air cylinders used to activate compensation frame

Figure 3.7 Image of the supply fiber divided into layers at the eye-lit board frame and drawn through the compensation system.

Figure 3.8 Illustration of major S wrap imposed on Z-yarn of top skin

(fiber layers travel from right to left in this figure)

Figure 3.9 First and second S wraps divide the Z-yarn into 2 layers atop the partition system. U weights hang from fiber strands to provide tension.

Figure 3.10 Top view of first and second S wraps dividing the Z-yarn into 2 layers atop the partition system

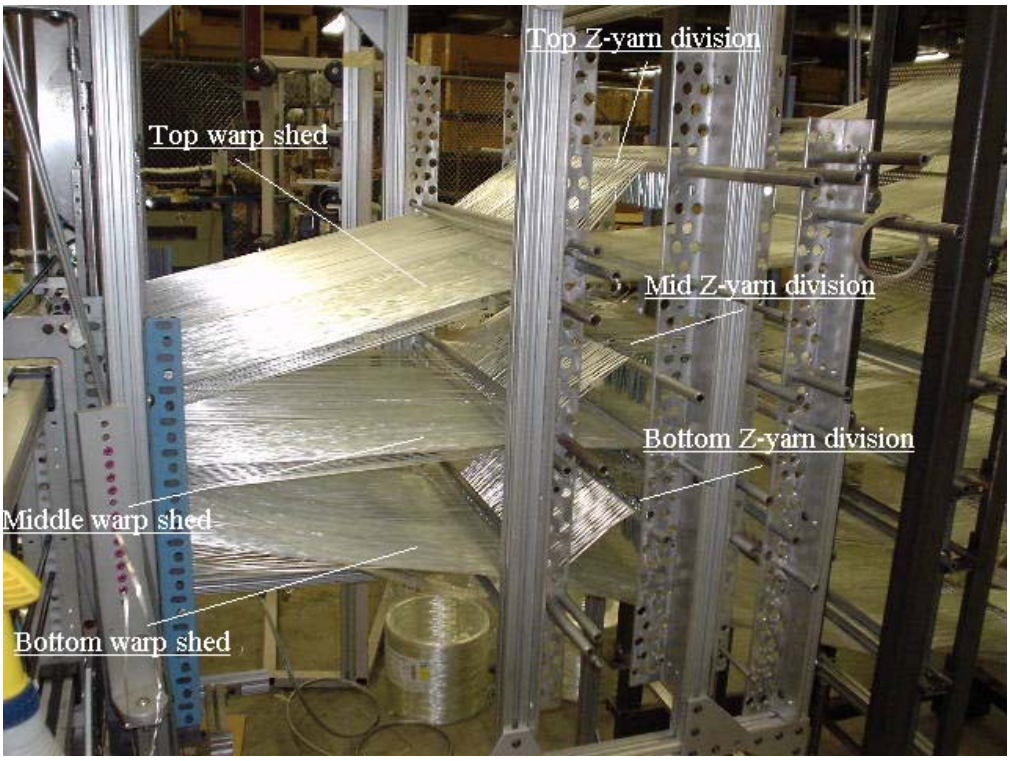

Figure 3.11 3 warp sheds and 6 Z-yarn sheds are guided from the partition system into the heddles and reed of the weaving machine

Figure 3.12 Individual Z-yarn are drawn through the eyelets of the steel heddles.

Figure 3.13 6 vertical sliding harnesses each with 108 steel heddles.

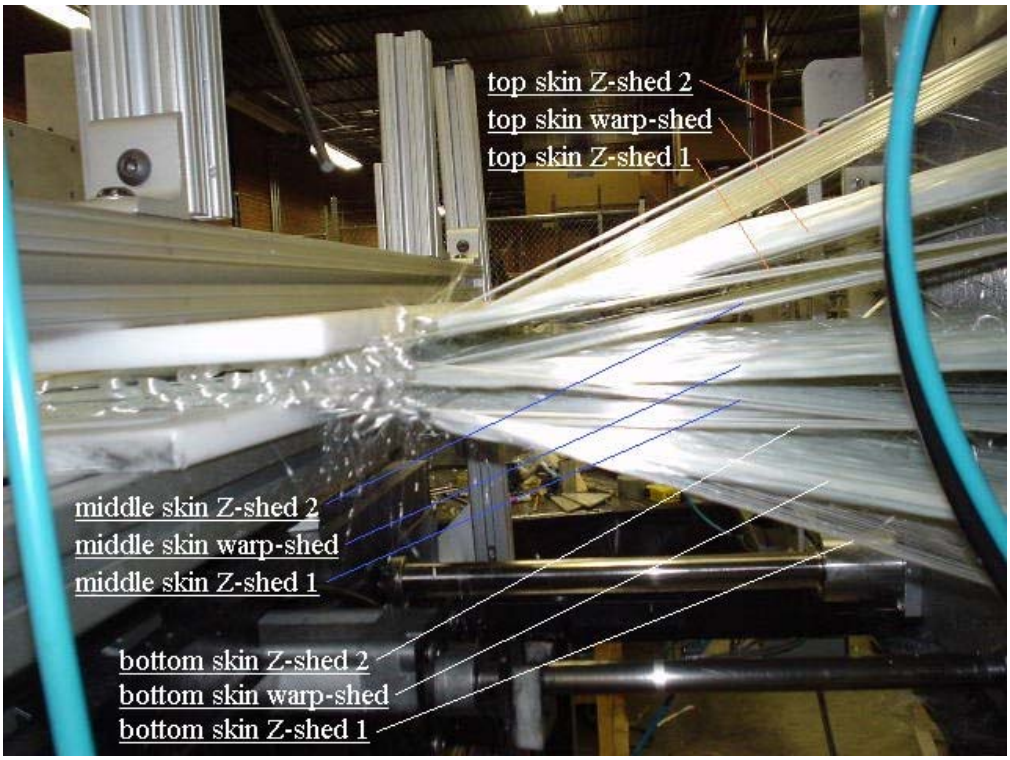

Figure 3.14 Optimum Z shed orientation with respect to warp shed

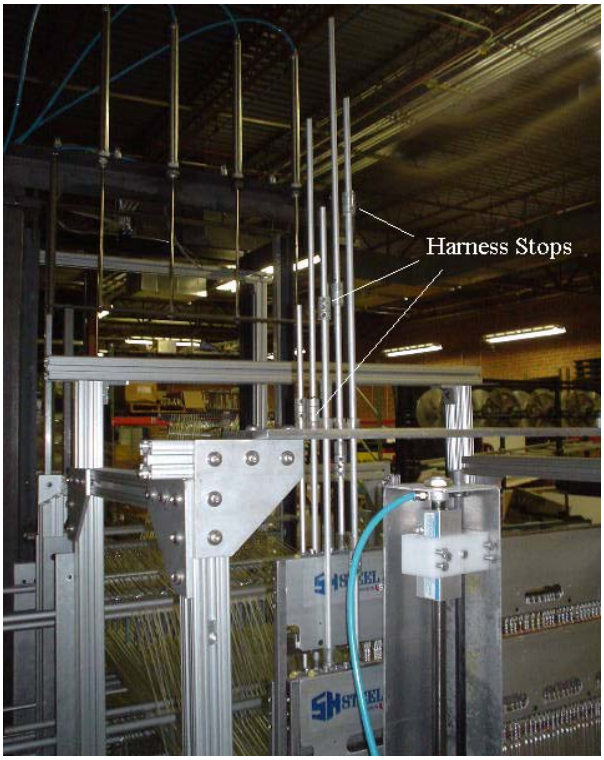

Figure 3.15 Harness limiting stops for the exterior skin harnesses

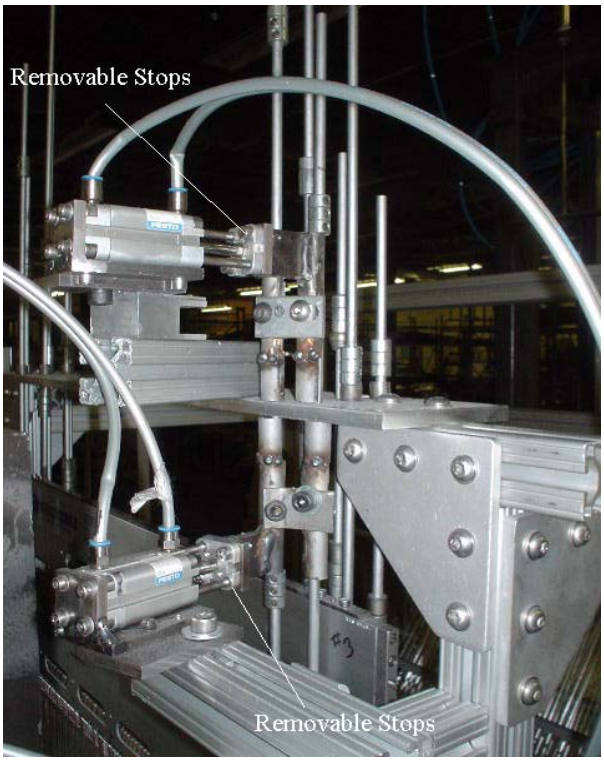

Figure 3.16 Removable harness stops which enable the core harnesses to shift the Z shed above the filler insertion of the adjacent skin layer

Figure 3.17 3 sets of rapiers mounted in alignment with its corresponding shed

(top set of rapiers are labeled in picture)

Figure 3.18 Single rapier set used for additional length of core skin

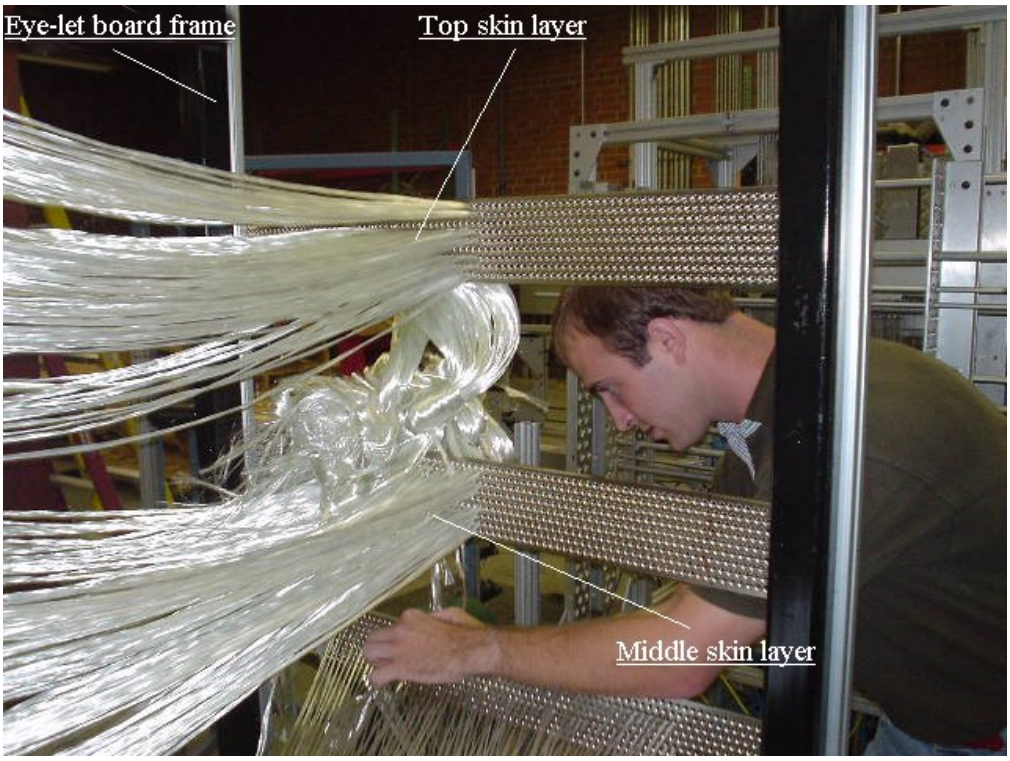

Figure 3.19 Division of fiber supply by draw-in of eye-lit boards on frame.
(Top and middle warp layers are 50% complete)

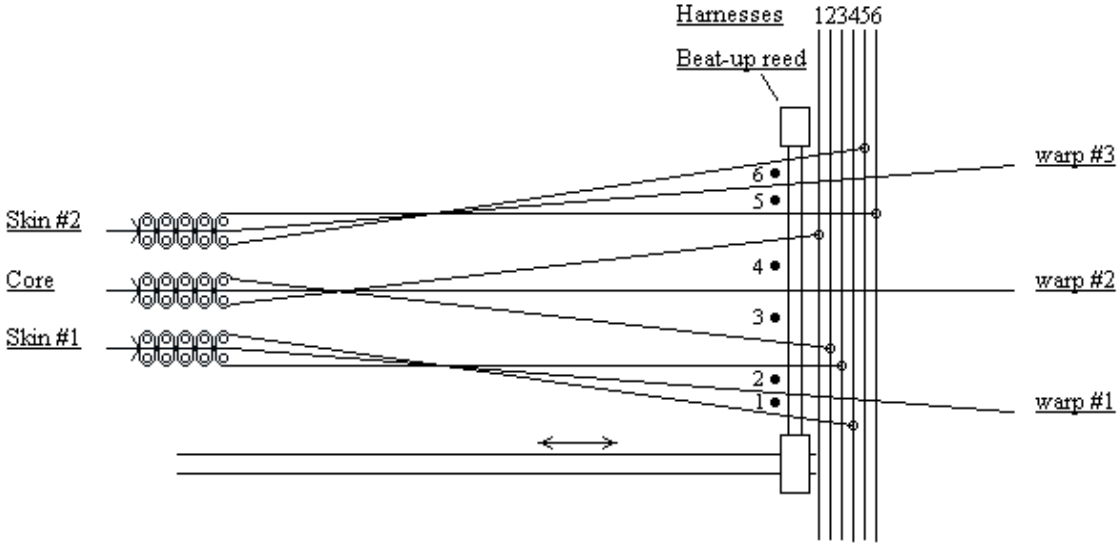

Figure 3.20 Schematic of weaving process of the 3D integrated sandwich structure for bridge deck.
Process step #1: weaving of individual skins and core.

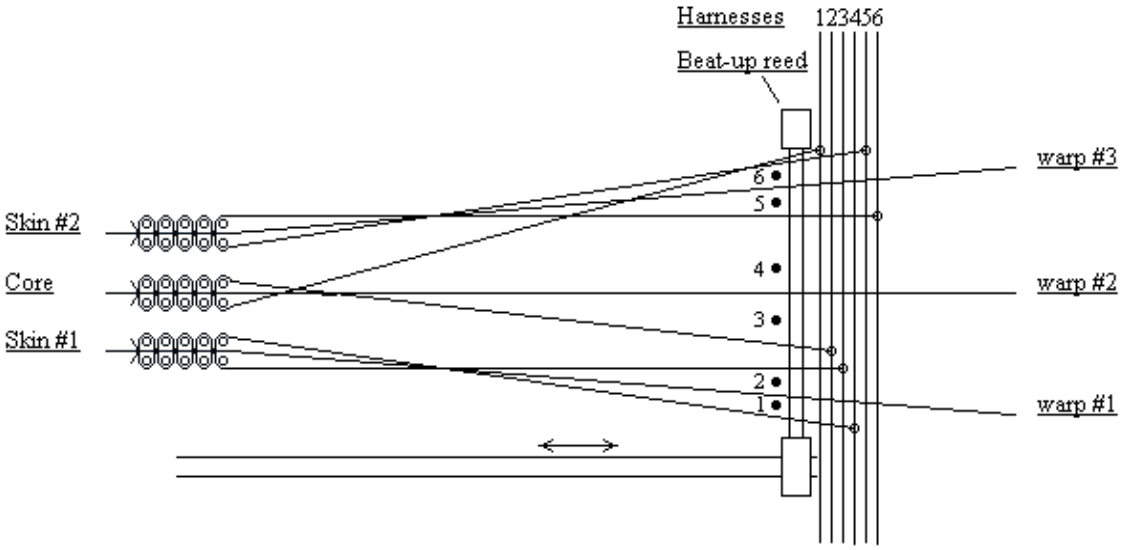

Figure 3.21 Schematic of weaving process of the 3D integrated sandwich structure for bridge deck. Process step #2: connecting the core with the upper skin (skin #2).

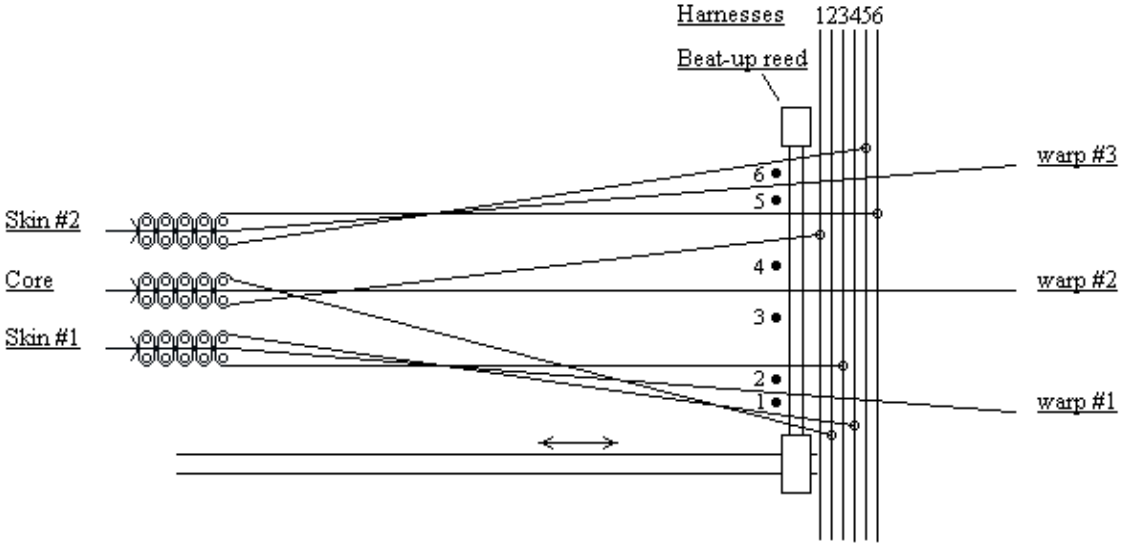

Figure 3.22 Schematic of weaving process of the 3D integrated sandwich structure for bridge deck. Process step #3: connecting the core with the lower skin (skin #1).

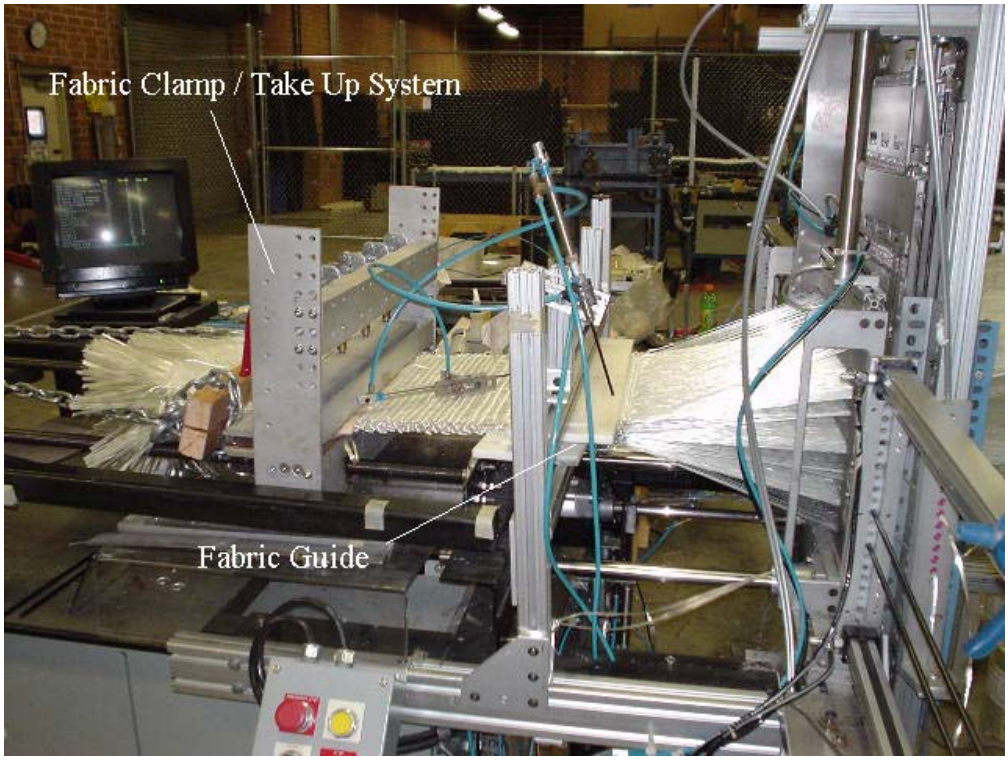

Figure 3.23 All 9 sheds meet at the fell just before the fabric guide and feed into the fabric/cloth clamp which is part of the take-up system.

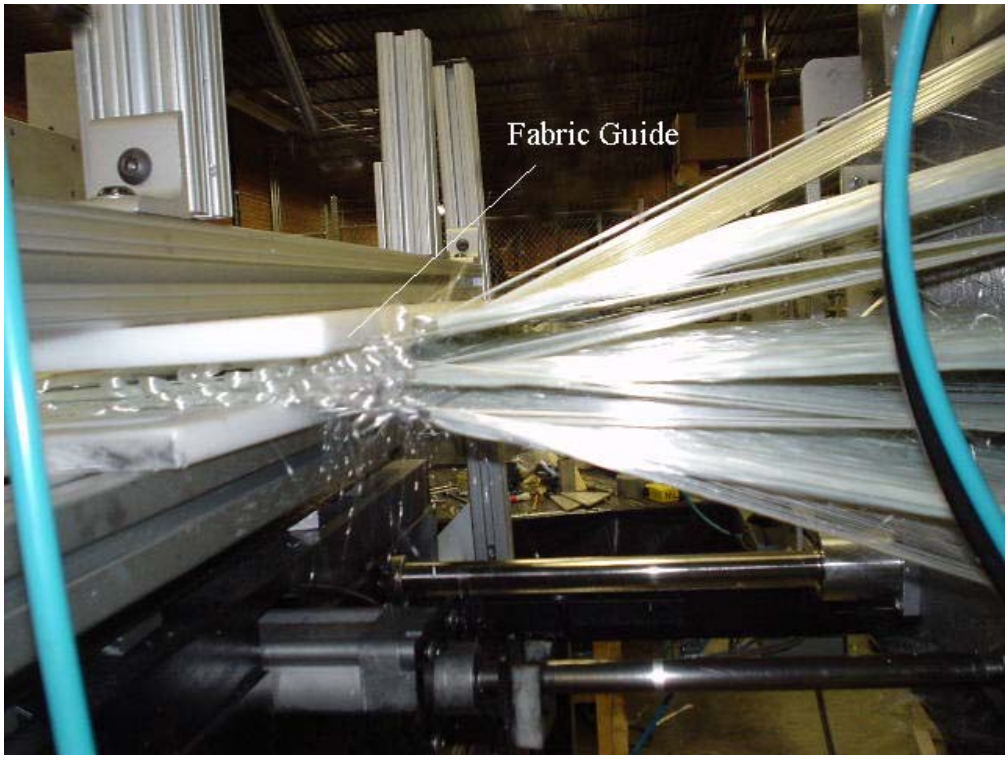

Figure 3.24 Close up of fabric guide illustrating the opening size

Figure 3.25 Second generation 3 inch truss deck. Note the 3 inch wood spacer between the skins layers of the fabric clamp.

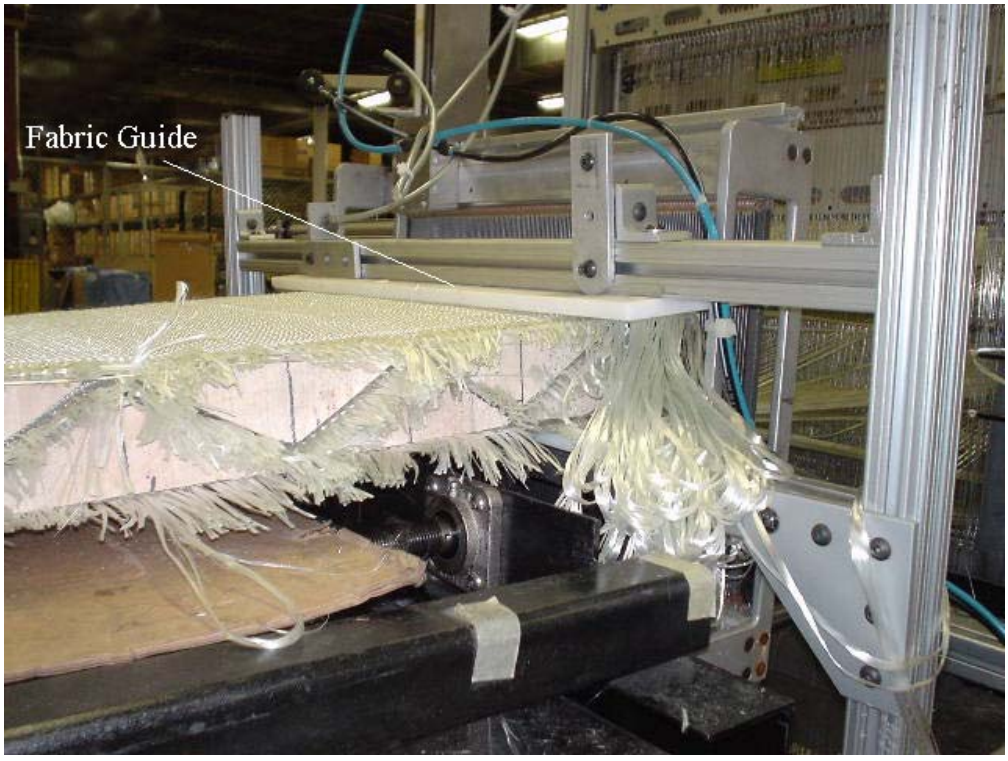

Figure 3.26 Close up of fabric guide modified for second generation truss deck. Note the insertion of the Balsa wood cores during the weaving process.

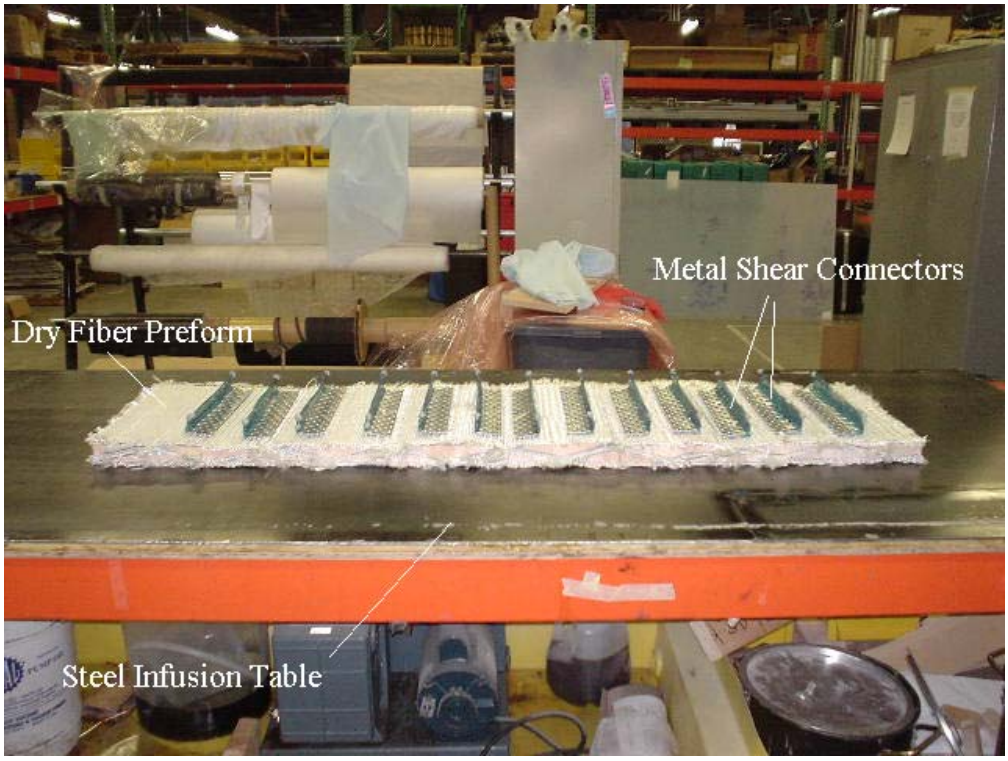

Figure 3.27 Puffed out dry fiber preform with metal shear connectors.

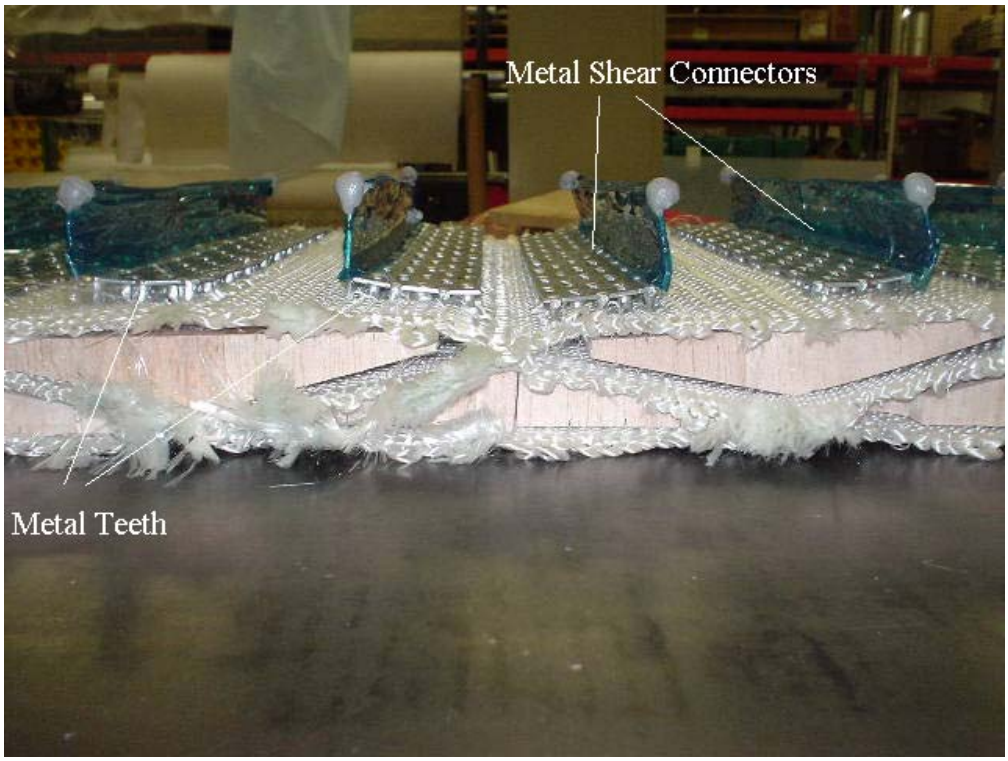

Figure 3.28 Teeth of metal shear connectors act as mechanical connection.

Figure 3.29 Deck 1 infusion setup prior to vacuum bag.

Figure 3.30 This figure illustrates the deck beneath a vacuum bag.

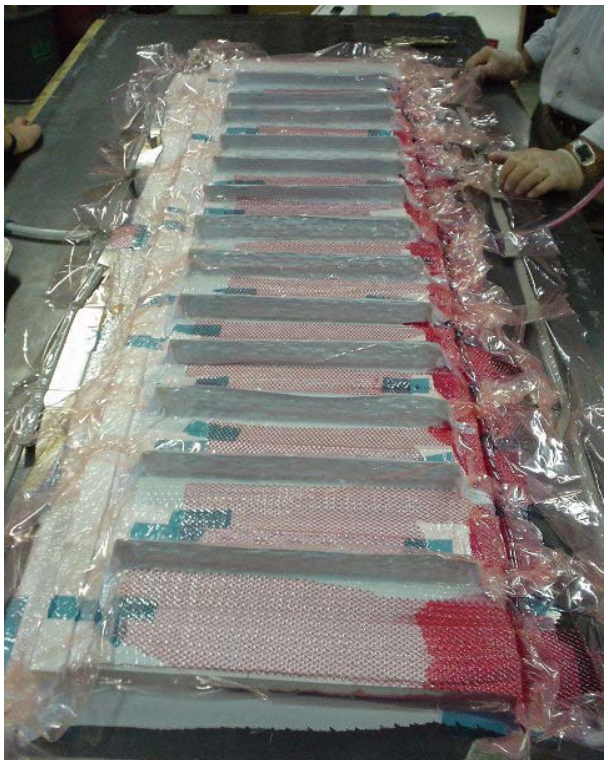

Figure 3.31 The resin flows uniformly across the system during the infusion. The vacuum is pulled by the resin exit tube on the left of the deck.

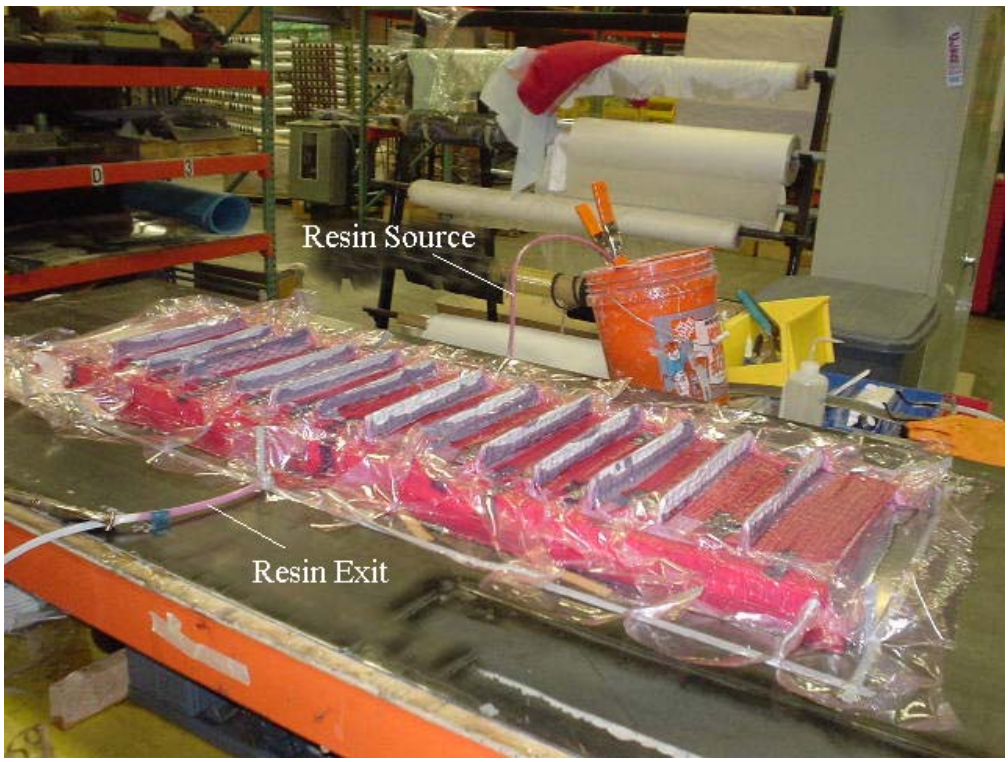

Figure 3.32 Deck 1 completely infused.

Figure 3.33 Deck 2 comprises a bottom skin, a rectangular Balsa core, an upper skin, and metal shear connectors.

Figure 3.34 Teeth of metal shear connectors act as mechanical connection to top skin.

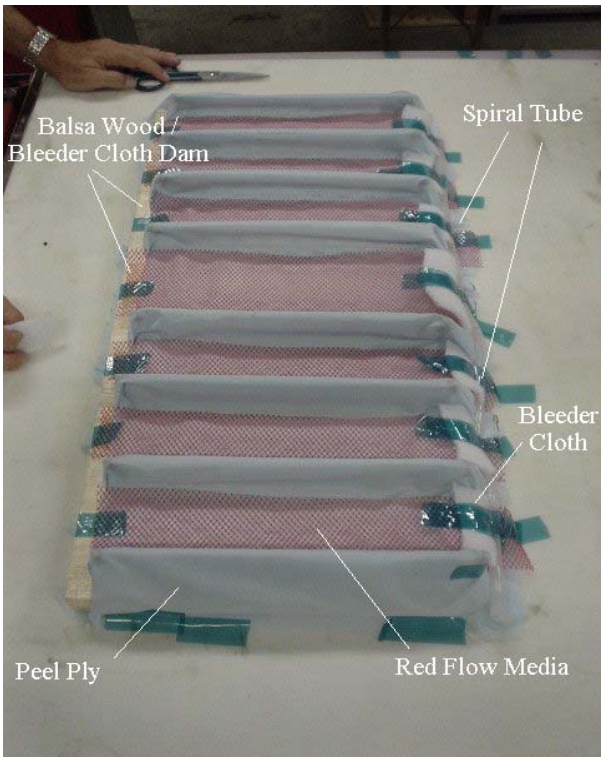

Figure 3.35 Deck 2 infusion setup prior to vacuum bag.

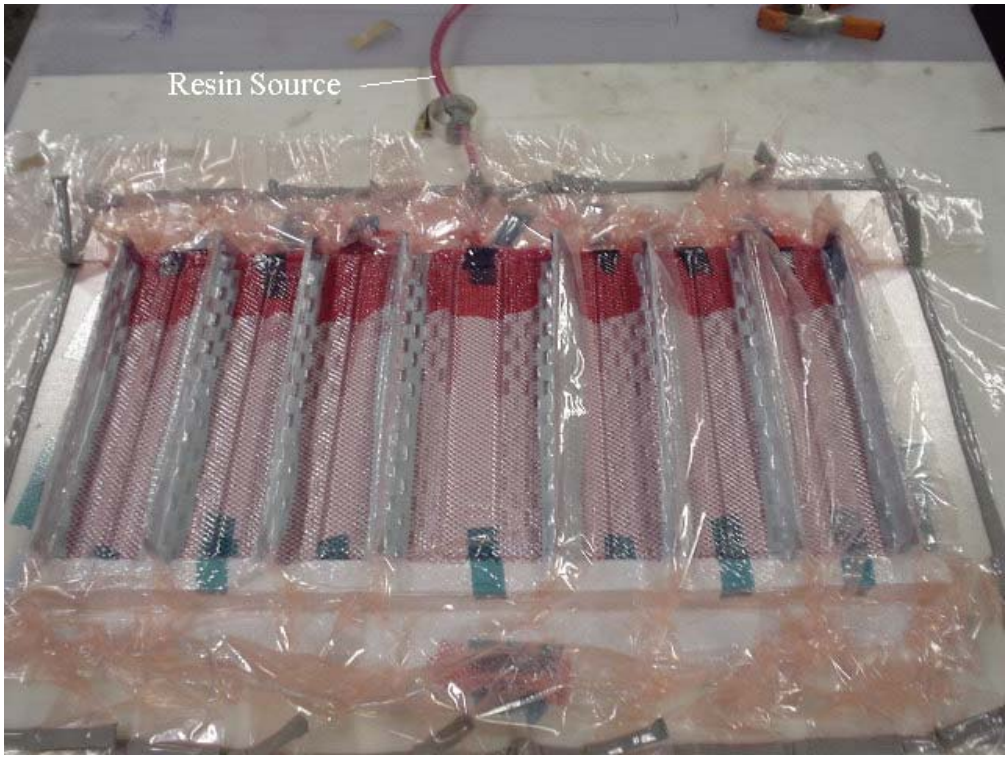

Figure 3.36 The resin flow uniformly across the system during the infusion.

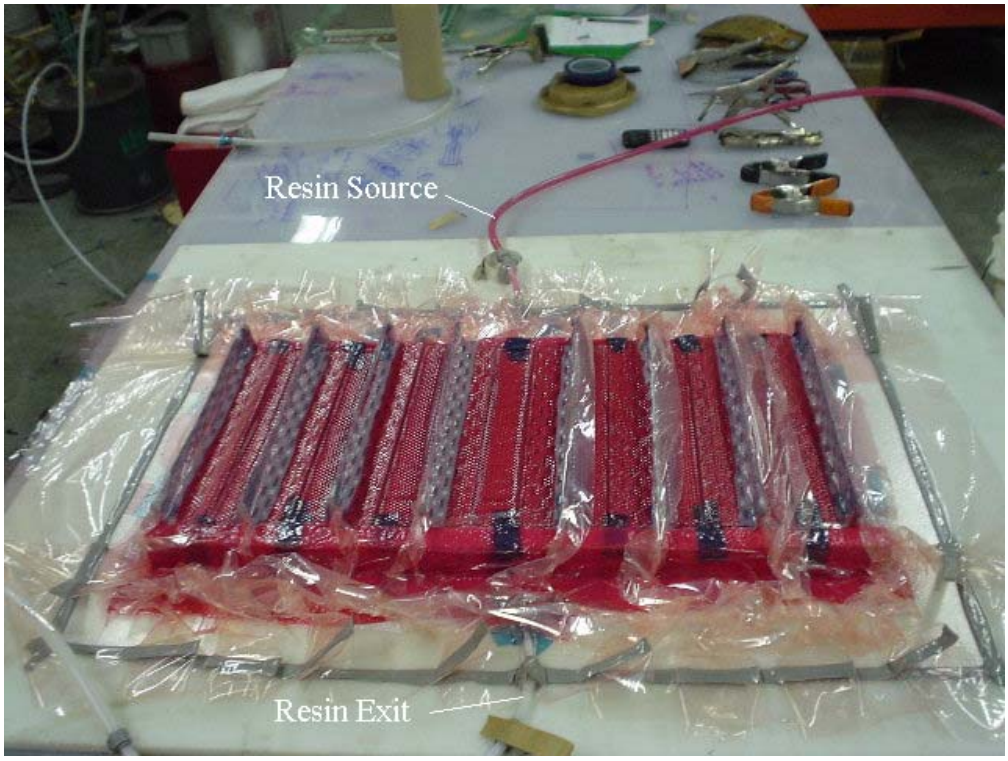

Figure 3.37 Deck 2 completely infused. The vacuum was pulled by the resin exit tube.

Figure 3.38 The composite deck is ultimately laminated together. There is no mechanical connection between outer skins and core.

Figure 3.39 Deck 3 dry fiber preform atop a steel table for infusion.

Figure 3.40 Dry fiber fabric (270 ounce / ¾ inch thickness) was cut to 1 ¼ inch strips and nailed atop the truss preform with 1 inch Brad nails. These strips are added as shear connectors. (Deck 3)

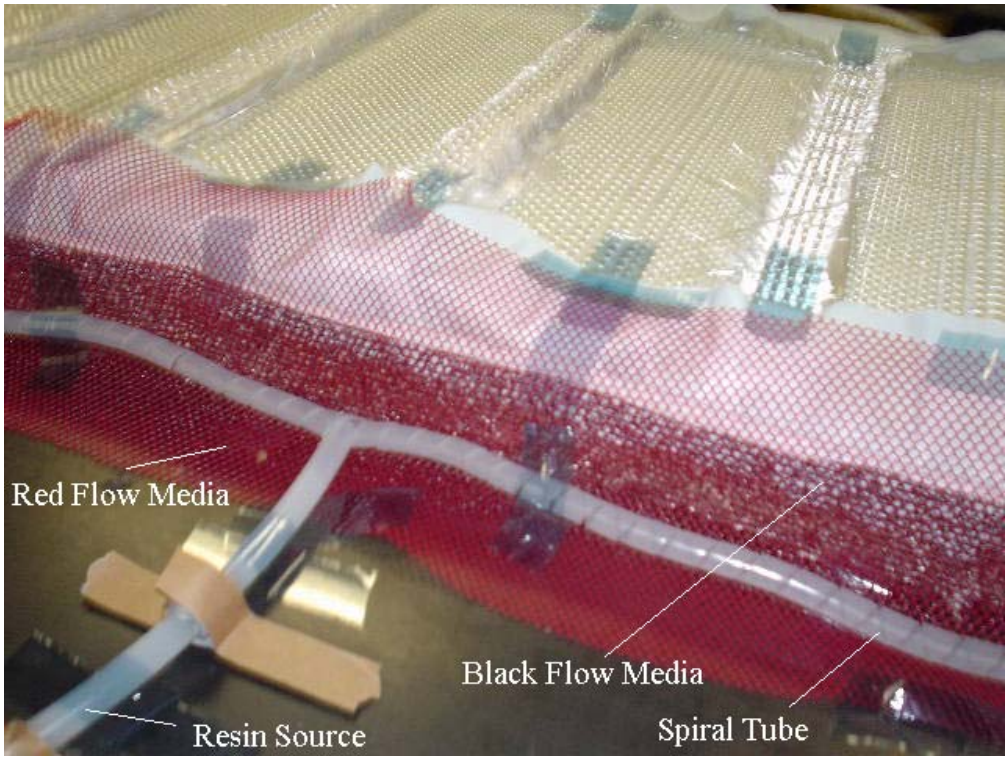

Figure 3.41 This figure illustrates the resin source tube entering the spiral tube at mid-section of the preform. Beneath the spiral tube is red flow media; beneath this is black flow media; beneath this is blue Peel Ply.

Figure 3.42 Close up view of end of deck beneath vacuum bag. Note: the pieces of tacky tape atop the shear connectors aim prevent air leaks above 1 inch Brad nails.

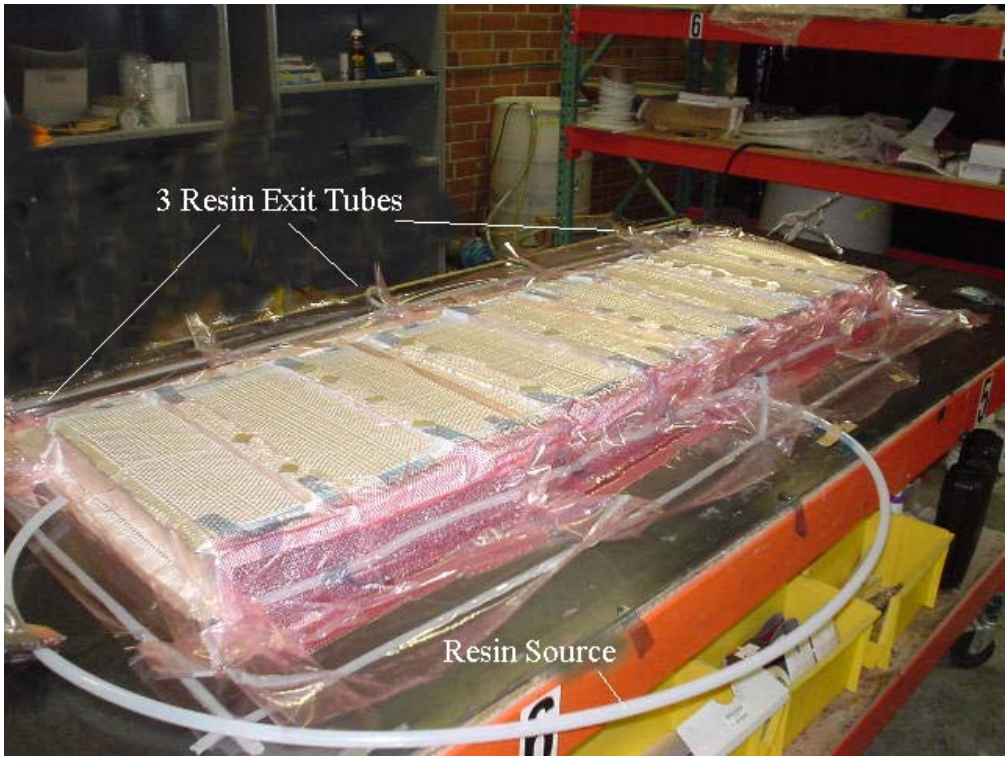

Figure 3.43 The entire infusion system beneath a vacuum bag.

Figure 3.44 Deck 3 completely cured with the bag removed. Note: the same epoxy resin system is used for each of the three decks; Jeffco Products did not dye this batch of resin red.

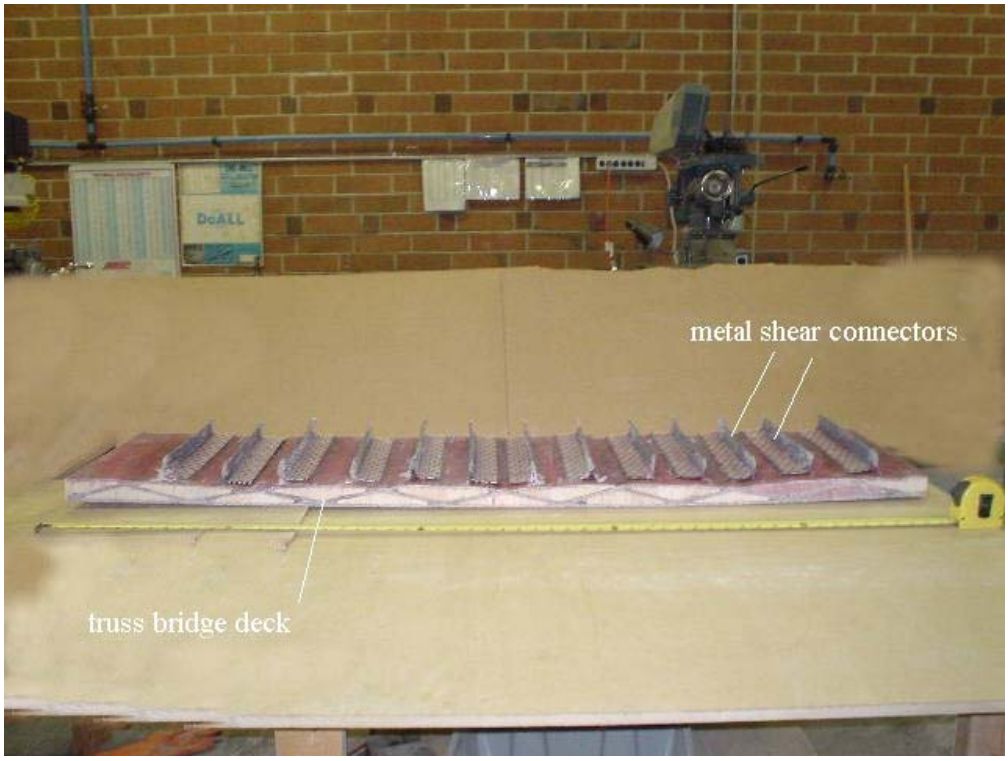

Figure 3.45 This figure illustrates Deck 1, first generation truss bridge deck, after having sides trimmed clean.

Figure 3.46 2 inch thickness of high/early concrete was cast atop Deck 1.

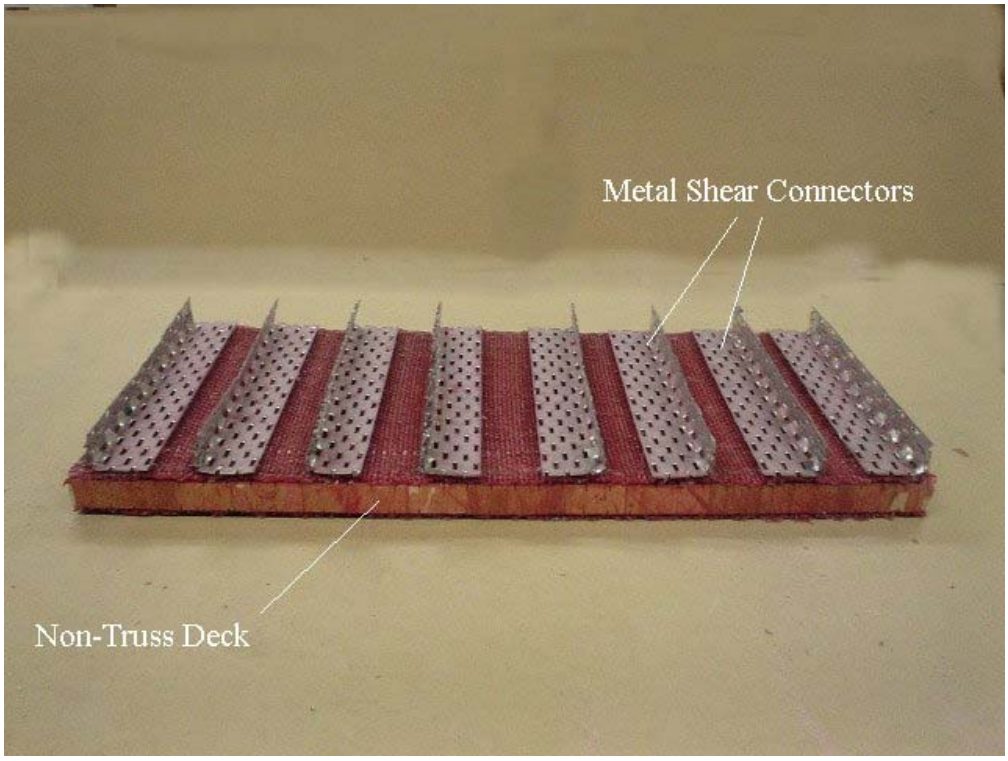

Figure 3.47 This figure illustrates 30 inch Deck 2 completely infused and cured. No sides needed to be trimmed.

Figure 3.48 2 inch thickness of concrete was cast atop 30 inch Deck 2.

Figure 3.49 This figure illustrates Deck 3 completely cured. Sides have been trimmed clean.

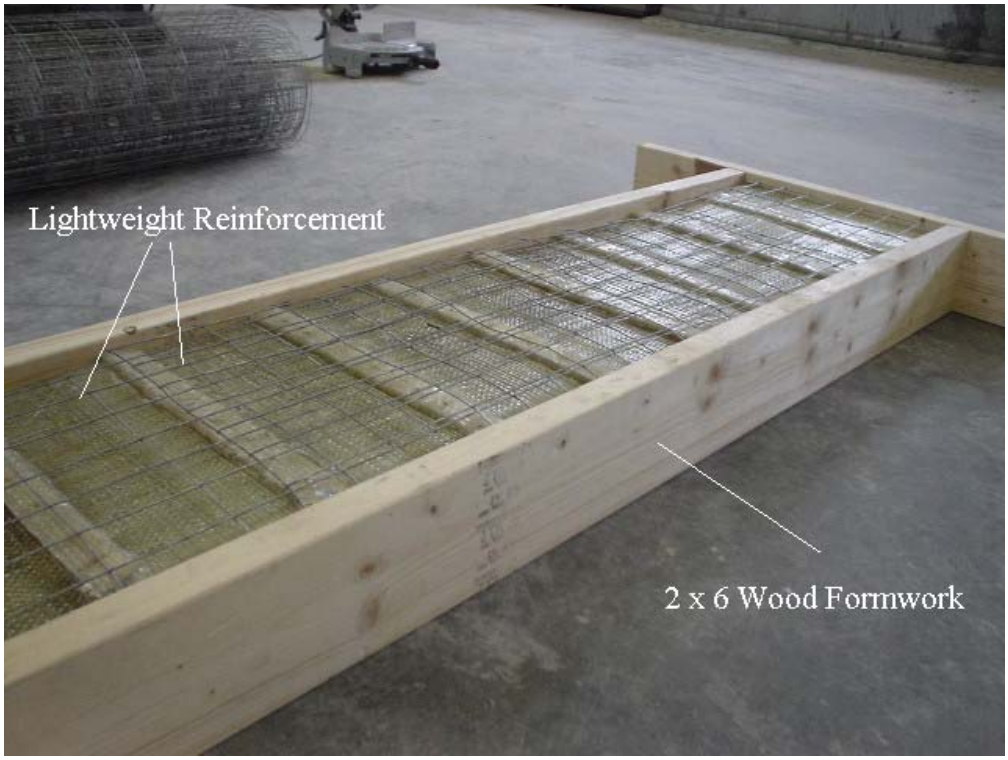

Figure 3.50 Lightweight reinforcement was set atop Deck 3 before casting concrete.

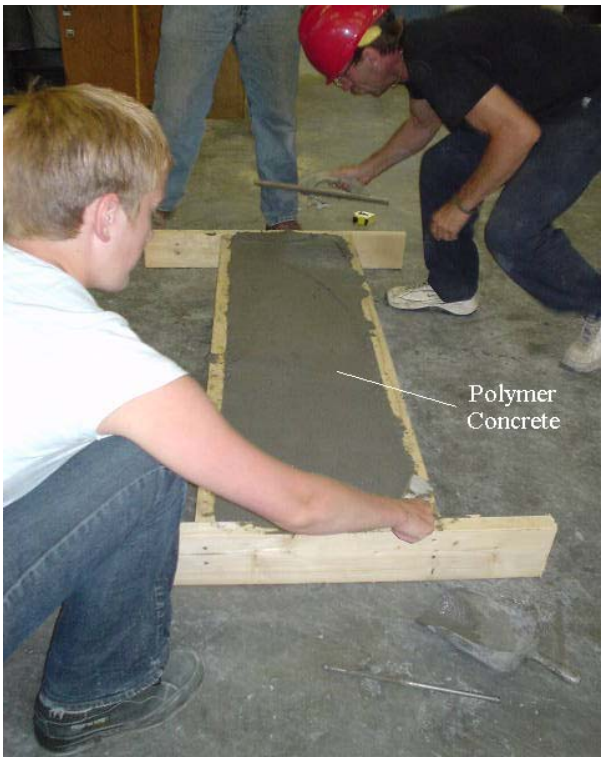

Figure 3.51 SikaTop^{R} 122 Plus concrete, a polymer concrete, was cast atop Deck 3.

Chapter 4: Characterization of Bridge Deck Panel Skins

4.1 Introduction

Three FRP deck skins were tested – P3W-062-12, P3W-063-12, P3W-064-12 (3TEX, Inc. Part Number). For Specimen 1 and Specimen 2, each skin was cut into six coupons of predetermined length, whereas Specimen 3 was cut into five coupons. The strength tests consisted of individually loading each coupon in uniaxial tension. The coupons were loaded until failure. The objective of experimentally characterizing the three fiber designs was to optimize the choice of fiber content to be used in the bridge deck.

4.2 Laboratory Test Setup

Identical test setups existed for each of the laboratory tests. Each fabricated deck skin was cut into five or six coupons 1.5" in width by 16" in length. The length of each coupon was consistent in direction with the warp (x-direction) of the composite skin. The dimensions of each coupon, including thickness, had minor variance and are presented in *Table 4.1*. A caliper was used for measurements. And an average of three measurements at distinct locations was used for width and thickness.

Metal end tabs were bonded to each end of the coupons using Epoxy MSEE2130. Though the ends of the coupon would be compressed within the hydraulic wedge grips of the Hydraulic Wedge Grip Machine, the epoxy was used for surety of grip (*Figure 4.2*).

Each end of the coupons was compressed between hydraulic grips at 1000 psi, and a tensile load was applied to the specimen. The load rate applied was .1 in/min.

4.3 Instrumentation

4.3.1 Introduction

Load was governed by the machine and recorded by TCS software on the data acquisition. The displacement was measured by the actuator and recorded as well. Strain gauges were not used. An extensiometer was unsuccessfully used as the rupture of the glass fibers would jolt the mechanism from feasible location. The strain of the coupons

would be calculated using Microsoft Excel by dividing the displacement of the coupon by its respective original length between metal end tabs ($\varepsilon = \frac{\Delta L}{L}$).

4.3.2 Skin 1 / P3W-062-12

P3W-062-12 consisted of 21 ppi of 103 yd/lb glass fiber in the warp (x-direction). These fibers spread across the 15" width panel. The Z-yarns were 7 ppi across the section and were of 618 yd/lb. The weft yarn (y-direction) was 208 yd/lb. and was 6 insertions each inch. Each filler insertion consisted of double yarn above and below the warp, giving a total of 4 strands each insertion.

4.3.3 Skin 2 / P3W-063-12

Skin 2 consisted of 14 ppi of 103 yd/lb, a reduction in warp from Skin 1 by 1/3. The Z-yarn and filler yarn remain the same in count as Skin 2, 7 ppi and 6 ppi respectively.

4.3.4 Skin 3 / P3W-064-12

Skin 3 consisted of the same reduced warp as Skin 2, 14 ppi across the 15" section. This third composite skin consisted of a reduced filler (y-direction) yarn by 1/3. Thus, this panel maintained 4 insertions per inch of fabrication. Each filler insertion was still a double insertion of yarn above and below the warp. This sustains a count of 16 strands of 218 yd/lb. each inch.

4.4 Laboratory Test Program

4.4.1 Introduction

Three batches of specimens were tested for strength. The first batch of coupons was from bridge deck Skin 1 (P3W-062-12). There were six coupons tested. The second batch of coupons was from bridge deck Skin 2 (P3W-063-12). There were six coupons

tested. The third batch of coupons tested was from bridge deck Skin 3 (P3W-064-12). There were five coupons tested. Each of the coupons was tested until failure.

4.4.2 Strength Tests

Each of the coupons was compressed between the hydraulic wedge grips at 1000 psi and loaded uniaxially in tension at a rate of .1 in/min. The coupons were only tested in the warp direction, or x-direction. The specimens were consistently placed within the grips such that the entire surface of the metal end tabs was in contact distributing a uniform load to the coupon. The rupture strength and modulus could then be calculated using the data recorded by the TCS and Excel software.

4.5 Results and Discussion

4.5.1 Introduction

It was with great effort that the fabrication and experimental characterization was conducted in order to confidently select the most efficient glass fiber-reinforced bridge deck skin for the development of the innovative 3" GFRP truss-like bridge deck. The strength of each of the three different bridge skins was investigated to keep safety and economics at the front of this research. These tests fully illustrate the effects of a reduced warp and filler, respectively, with regard to strength.

4.5.2 Skin 1

4.5.2.1 Strength Tests

Results of the Skin 1 coupon tests are shown in *Table 4.2*. The strength of each of the coupons was determined by dividing the ultimate rupture load by the area of the cross-section. This gives the strength in psi.

The average strength of Skin 1 is 86.2 ksi. The standard deviation of the six coupons is 3.78 ksi which is 4% of the strength.

The Modulus of Elasticity (E) of each specimen is determined from the stress-strain diagram. Given the following the equation $E = \sigma / \varepsilon$. The Modulus can be determined from the slope of the graph. The average Modulus of Elasticity is 1270 ksi.

4.5.3 Skin 2

4.5.3.1 Strength Tests

Results of the Skin 2 coupon tests are shown in *Table 4.3*.

The average strength of P3W-063-12 is 68.0 ksi. The standard deviation of the six coupons is 2.55 ksi which is 4% of the strength.

The Modulus of Elasticity (E) of each specimen is determined from the stress-strain diagram. The average modulus of elasticity is 1190 ksi.

4.5.4 Skin 3

4.5.4.1 Strength Tests

Results of the Skin 3 coupon tests are shown in *Table 4.4*.

The average strength of P3W-064-12 is 86.2 ksi. The standard deviation of the five coupons is 5.31 ksi which is 6% of the strength.

The modulus of elasticity of each specimen is determined from the stress-strain diagrams. The average modulus of elasticity is 1950 ksi.

4.5.5 Summary of Results

Skin 1 maintained the highest rupture load. The reduction of warp by 1/3 from Skin 1 to Skin 2 and Skin 3 stands to explain the reduction in ultimate load by approximately 1/3. The reduction in filler yarn by 1/3 from Skin 2 to Skin 3 has no apparent effect on the ultimate rupture load. From the strengths gathered in *Table 4.2* and *Table 4.3*, one can see that the most efficient bridge deck panel is Skin 1, the first panel specimen, followed by the third skin.

Economically, the second skin, P3W-063-12, contains 1/3 more filler than the third panel, P3W-064-12, yet demonstrates no more ultimate load capacity than the latter.

Thus, it is not a feasible solution. Its apparent less strength is derived from maintaining a same ultimate rupture load as the third skin while sustaining a larger cross-sectional area.

The third panel, P3W-064-12, though indicative of a panel with strength properties near the first panel, P3W-062-12, still maintains approximately 1/3 less ultimate load carrying capacity. Thus, with safety having precedence, it is with good conscience that the FRP composite Skin 1 is chosen for fabrication of the 3TEX GFRP Bridge Decks.

The experimental and predicted average modulus of elasticity for each of the three skins is illustrated in Table 4.5. The predicted modulus is higher for each of the three skins.

4.6 Tables and Figures

Table 4.1 Measured dimensions of GFRP coupons

Coupon Dimensions			
Specimen	**width (in.)**	**thickness(in.)**	**length (in.)**
1.1	1.480	0.183	5.410
1.2	1.484	0.187	4.884
1.3	1.484	0.192	4.827
1.4	1.484	0.191	4.902
1.5	1.490	0.192	5.000
1.6	1.490	0.192	5.000
2.1	1.489	0.158	4.858
2.2	1.489	0.155	4.717
2.3	1.486	0.162	4.813
2.4	1.486	0.161	4.916
2.5	1.490	0.162	4.973
2.6	1.486	0.162	4.720
3.1	1.476	0.122	4.938
3.2	1.486	0.127	4.745
3.3	1.485	0.120	4.800
3.4	1.485	0.121	4.765
3.5	1.486	0.131	4.984

Table 4.2 Results of coupon strength tests of panel skin P3W-062-12

Specimen	**Rupture Load (kips)**	**Strength (ksi)**
1.1	24.5	90.2
1.2	24.7	89.1
1.3	25.5	89.2
1.4	23.2	81.4
1.5	24.4	85.1
1.6	23.6	82.4
	Average	86.2
	Standard Deviation	3.78
	% Deviation	0.04

Table 4.3 Results of coupon strength tests of panel skin P3W-063-12

Specimen	Rupture Load (kips)	Strength (ksi)
2.1	15.8	67.0
2.2	16.7	72.2
2.3	16.5	68.3
2.4	15.7	65.5
2.5	15.9	65.7
2.6	16.7	69.4
	Average	68.0
	Standard Deviation	2.55
	% Deviation	0.04

Table 4.4 Results of coupon strength tests of panel skin P3W-064-12

Specimen	Rupture Load (kips)	Strength (ksi)
3.1	16.9	93.4
3.2	15.6	82.3
3.3	14.4	80.6
3.4	16.2	89.8
3.5	16.6	84.8
	Average	86.2
	Standard Deviation	5.31
	% Deviation	0.06

Table 4-5 Results of experimental and predicative moduli of elasticity for each of the three skins

Moduli of Elasticity - Warp Direction					
Skin	Experimental (ksi)	Voight (ksi)		Reuss (ksi)	
		50% Vf	60% Vf	50% Vf	60% Vf
1	1270	3858	4598	2271	2814
2	1190	3456	4130	1992	2478
3	1950	3851	3851	2265	2265

Figure 4.1 Coupons were tested until failure

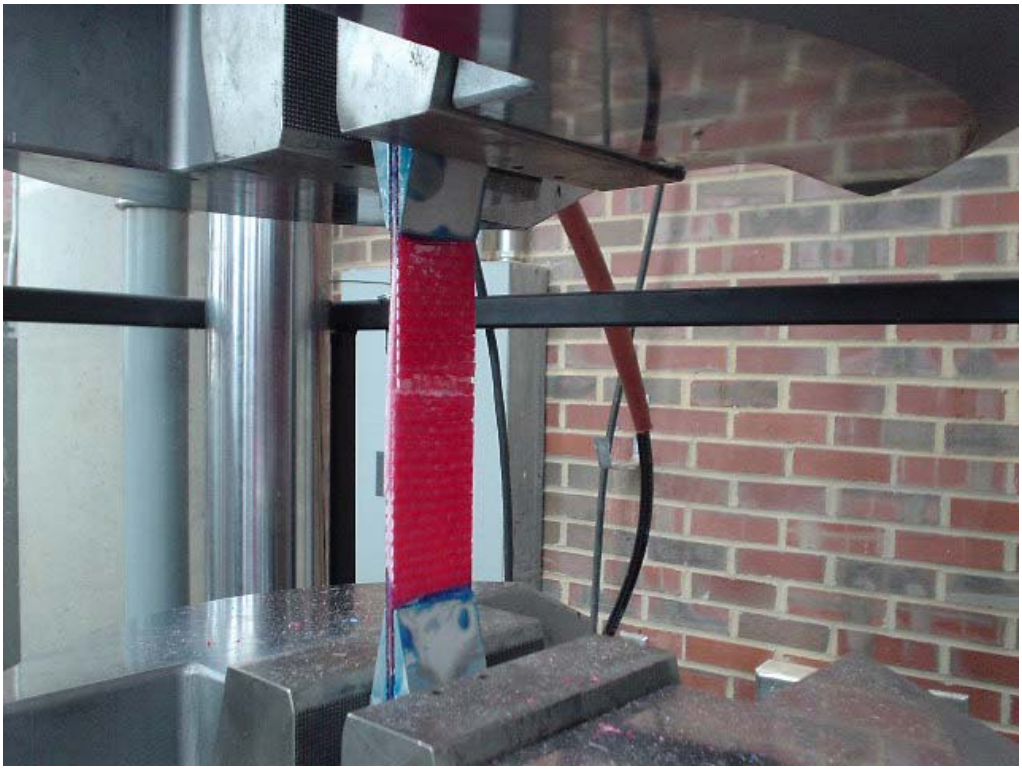

Figure 4.2 Ends of the coupon compressed within the hydraulic wedge grips of the machine

Chapter 5: Experimental Characterization of Bridge Decks

5.1 Introduction

The main objective of this experimental program is to investigate the structural behavior of a completely woven 3Weave™ GFRP bridge deck panel beneath an AASHTO HS20 wheel load.

Four FRP decks with Balsa core were tested: Deck 1 is the 3Weave™ truss-like bridge deck comprising a top and bottom skin with a core skin woven diagonally between them; Deck 2 is the control 3Weave™ deck consisting of a top and bottom skin without diagonal reinforcement through the core; Deck 3 is the second generation 3Weave™ truss-like bridge deck with twice the thickness of Deck 1; and Deck 4 comprised the undamaged half of Deck 3 after testing.

Each of the FRP deck specimens was tested under three-point loading. First test was for stiffness beneath a 20,800 lb (HS20 + 30% impact) point load. The second test was to load the specimen to ultimate strength.

5.2 Test Specimens

5.2.1 Introduction

Two styles of GFRP deck panels were manufactured by the author at 3TEX, Inc. in Cary N.C. Each of the specimens utilizes 3Weaving™ technology in the fabrication of its skins. The design fiber weight fraction and resulting fiber architecture are identical for each of the decks skins.

5.2.2 Design of Specimens

5.2.2.1 Deck 1

Three dry glass fiber skins are woven and interconnected in a truss-like manner. Metal L-shaped plates with protruding pins are hammered into the top of this dry preform (used as shear connectors), and the system is resin infused beneath a vacuum bag. A 2 inch layer of concrete was cast atop the deck to aid in the stiffness characteristic of the composite deck panel.

The length of the full composite deck is 58 inches and the breadth and depth of the deck are 14.25 inches and 3.5 inches, respectively. The depth of the infused composite panel before concrete is 1.5 inches (2 in. of concrete). Triangular cut Balsa wood cores fill the open-cell truss of the dry-fiber preform (placed before infusion). The ultimate height of each of these triangular shafts is 1 inch. The tested span of the deck is 40.5 inches.

5.2.2.2 Deck 2

Two dry glass fiber skins are woven separately with no interconnection. Metal L-shaped plates are used as shear connectors analogous to Deck 1. One skin is laid on the infusion table. A 1 inch thick rectangular Balsa wood core is placed atop the dry fiber preform skin. Then the top skin (including shear connectors) is laid atop the Balsa core, and the composite is resin infused beneath a vacuum bag. The skins and wood core are ultimately laminated together. A 2 inch layer of concrete was cast atop the deck to aid in the stiffness characteristic of the composite deck panel.

The length of the full composite deck is 28 inches and the breadth and depth of the deck are 12.5 inches and 3.5 inches, respectively. The depth of the infused composite panel before concrete is 1.5 inches (2 in. of concrete). The rectangular cut Balsa wood core is 1 inch thick and cut to the length and width of the dry fiber skins (placed before infusion). The tested span of the deck is 20 inches.

5.2.2.3 Deck 3

Deck 3 is a second generation truss deck that meets the 3" design specifications. Three dry glass fiber skins are woven and interconnected in a truss-like manner. Strips of 3D woven ¾ inch thick dry fiber fabric are nailed into the top of this dry preform (used as shear connectors), and the system is resin infused beneath a vacuum bag. A 2 inch layer of concrete was cast atop the deck to aid in the stiffness characteristic of the composite deck panel.

The length of the full composite deck is 58 inches and the breadth and depth of the deck are 15 inches and 4 inches, respectively. The depth of the infused composite panel before concrete is 3 inches (1 in. of concrete). Triangular cut Balsa wood cores fill

the open-cell truss of the dry-fiber preform (placed during weaving process). The ultimate height of each of these triangular shafts is 2.25 inch. The tested span of the deck is 41.5 inches.

5.2.2.4 Deck 4

As illustrated in Chapter 6, one half of Deck 3 was visually undamaged after testing. This half of the deck was tested at a 22 inch span beneath the same loading conditions and is herein referred to as Deck 4.

5.3 Material Properties

In this section, concrete and composite skin mechanical properties are reported based on experimental test results in accordance with American Society of Testing and Materials (ASTM) standards.

5.3.1 Concrete

5.3.1.1 Deck 1 and Deck 2

One batch of Quikcrete 5000 High-Early was used in this program to cast Deck 1 and Deck 2. Quick Crete Products Corporation (QCPC) assures this concrete to have a compressive strength of 3500 psi in 7 days and a nominal strength of 5000 psi in 28 days. The exact mixture proportions and additives are a trade secret, but QCPC maintains this product is a 5 bag mix and recommends a minimum 2 inch thickness when casting this concrete. Quikcrete 5000 High-Early is a concrete ready mix with a Portland cement base (Appendix D).

The target concrete compressive strength for the testing of the bridge decks is 4000 psi. The actual properties of the concrete are determined by compressive tests of four 4" x 8" concrete cylinders (ASTM C 39-03) prepared from the same batch of concrete as the top of the bridge decks. The hydraulic compressive machine continually exhibits a compressive load on the concrete cylinder until failure. The loading was applied at a constant rate of 0.05 inches per minute. The maximum load sustained by each specimen was obtained from the screen and recorded. The maximum compressive

strength was calculated by dividing the maximum recorded load by the area beneath the load.

Deck 1 was tested 12 days after concrete casting, and Deck 2 was tested 13 days after concrete casting. Figures 5.1-5.4 display the compressive failure associated with each cylinder. The compressive strength of each of the cylinders is listed in table 5.1. The average compressive strength of the concrete on Deck 1 is assumed to be 3600 psi; the average compressive strength of the concrete on Deck 2 is assumed to be 3900 psi.

5.3.1.2 Deck 3 and Deck 4

One batch of SikaTop® 122 Plus, a polymer-modified concrete with 3/8 inch aggregate, was used to cast the top of Deck 3. The aggregate is in accordance with ASTMC1260 per Sika® recommendations. Sika® assures this concrete to have a compressive strength of 5,500 psi in 7 days, and 7,000 psi in 28 days (see Appendix E). Two 4" x 8" cylinders were cast in conjunction with Deck 3 in order to approximate the value of the compressive strength at the time of deck testing (ASTM C 39-03). The maximum compressive strength was calculated by dividing the maximum recorded load by the area beneath the load. Figures 5.5-5.6 display the compressive failure associated with each cylinder. The compressive strength of each of the cylinders is listed in table 5.2. The cylinders and Decks 3 and 4 were tested 7 days after concrete casting. The estimated compressive strength of the concrete is 4800 psi.

5.3.2 Bridge Deck FRP Skins

Although the actual skins of the bridge decks were not tested for mechanical properties, replicas of these skins, i.e., the exact same fiber weight fraction and resin epoxy system, were experimentally characterized and were noted in chapter 4.

5.4 Instrumentation

5.4.1 Introduction

All three decks were completely instrumented to measure the applied loads on the decks, deflections associated with each loading, and strains in composite and concrete.

Strains were measured using 10 mm and 60 mm gauge length, uniaxial electrical strain gauges, model number PL-60-11-3L by Texas Measurements, Inc. Deflections recorded during the laboratory tests were measured using cable-extension position transducers also referred to as string-pots. Vertical displacements of the end of each deck, at the support, were measured using linear variable deflection transducers (LVDT) to account for the displacement in the neoprene pad.

A total of two strain gauges (SG) were placed on the bottom FRP composite skin of each deck (10 mm). SGB1 was placed at mid-span, and SGB2 was placed 1 ½ inches to the left of mid-span. The mid-span is the proposed location of maximum strain beneath a three point bend. One 60 mm strain gauge was placed at the interface of the concrete and composite skin (top skin). This gauge was placed at mid-span, on the concrete, and on the side of the bridge deck. This gauge is used to determine whether this portion of the concrete surface is in tension or compression.

String-pots measured vertical deflections at critical locations, quarter-points, along the deck span as well as out-of-plane deflections at three points along the mid-section. These measuring devices connect to eyebolts glued to the bottom of each deck. The center string-pot at mid-span measures the maximum deflection of the deck. The quarter-point deflections aid in interpolating a deflection curve for the composite bridge deck. One LVDT was placed on top of the deck at each support (LV1 and LV2) of the test span to determine the net recorded deflections by subtracting the deflection induced by the neoprene pads beneath the deck.

The strain gauges, cable-extension position transducers, linear variable deflection transducers, and load cell were connected to a data acquisition system and the data was recorded and stored on a computer at an interval of 1 second during loading.

5.5 Testing Procedure

5.5.1 Test Setup

The FRP decks 1, 2, 3, and 4 were tested under three-point loading with effective span lengths of 40 ½ inches, 20 inches, 41 ½ inches, and 22 inches respectively. Figure 5.8 illustrates a schematic of the test setup. The load was applied using a hydraulic MTS actuator of 440,000 lb capacity. The load is transmitted to the deck through a 3 inch steel

hollow box section atop a rectangular neoprene pad of size 15 inches x 3 inches x 1 ½ inches in order to represent an AASHTO HS20 standard truck wheel load. The rate of loading for each test was .1 in./min.

Each deck was positioned to span from one concrete block (support) to another. The size of each concrete block was 22 in. x 22 in. x 32 in. in width, length, and height. A ¾ inch neoprene pad was placed at the support between the deck and the concrete block. In addition to the weight of the blocks, 2 inch x 4 inch boards were bolted to the concrete blocks to prevent lateral movement.

5.5.2 Illustration of Test Setup

Figure 5.7 displays Deck 1 within the test setup, and figure 5.8 displays the string-pots (SP) oriented at quarter points and out-of-plane points beneath the deck. Figure 5.9 displays Deck 2 within the test setup, and Figure 5.10 displays the string-pots (SP) oriented at quarter points. Figure 5.11 displays Deck 3 within the test setup, and figure 5.12 displays the string-pots (SP) oriented at quarter points and out-of-plane points beneath the deck. Figure 5.13 displays Deck 4 within the test setup, and there is only one the string-pot (SP) oriented mid-span beneath the deck.

5.5.3 Preparation for Testing

With the deck specimen properly positioned, wires from strain gauges, string-pots, and LVDTs were connected to the data acquisition system. String-pots and LVDTs were manually checked to be functioning properly. With each of the measuring devices checked and plugged in, the data acquisition had to be calibrated.

5.6 Testing

5.6.1 Stiffness Tests

The stiffness tests for each deck were performed in a similar manner. In three-point bend, each deck was loaded gradually up to 2,000 lbs after which the load was removed. This operation was repeated before each test to ensure: 1) the loading edges

remained in proper contact with the specimen, 2) the sensors (strain gauges, string pots, LVDTs, and load actuator) were working properly, and 3) there were no loose connections. Observation of the deck's behavior under loading was also achieved.

The load steps were of the following order:

Step1: Load from zero to 2000 lb and release the load back to zero in order to establish a baseline curve.

Step2: Load from zero to prior load + 2,000 lbs and back to zero, and repeat this cycle up to 22,000 lbs. (20,800 lb load represents an AASHTO HS20 truck wheel load of 16,000 lb + 30% impact of 4,800 lb.)

Step3: Load from zero to failure (strength test).

5.6.2 Strength Tests

The deck is loaded for the strength test in the same manner as in the stiffness test. The only step in the load cycle is to continuously load the deck until failure. Pictures were taken to assess damage and to assess the failure mode. Both the stiffness tests and the strength tests were also filmed for documentation and analysis.

5.7 Figures and Tables

Table 5.1 Maximum loads and resulting compressive strengths of the concrete cylinders

QUIKRETE 5000 High Early Strength Concrete Cylinders					
	Cylinder	Maximum Load (lbs.)	Area (in^2)	Compressive Strength (psi)	Average (psi)
Deck 1	1	41,800	12.62	3310	3580
	2	48,800	12.72	3840	
Deck 2	3	47,000	12.66	3710	3870
	4	50,800	12.65	4020	

Table 5.2 Maximum loads and resulting compressive strengths of the polymer-modified concrete cylinders

SikaTop® 122 PLUS Concrete					
	Cylinder	Maximum Load (lbs.)	Area (in^2)	Compressive Strength (psi)	Average (psi)
Deck 3	1	61,400	12.67	4850	4830
	2	61,300	12.75	4810	

Note: Deck 4 maintained the same concrete surface as Deck 3.

Figure 5.1 Cylinder 1 failing in compression.

Figure 5.2 Cylinder 2 failing in compression.

Figure 5.3 Cylinder 3 failing in compression.

Figure 5.4 Cylinder 4 failing in compression.

Figure 5.5 Polymer concrete cylinder 1 failing in compression.

Figure 5.6 Polymer concrete cylinder 2 failing in compression.

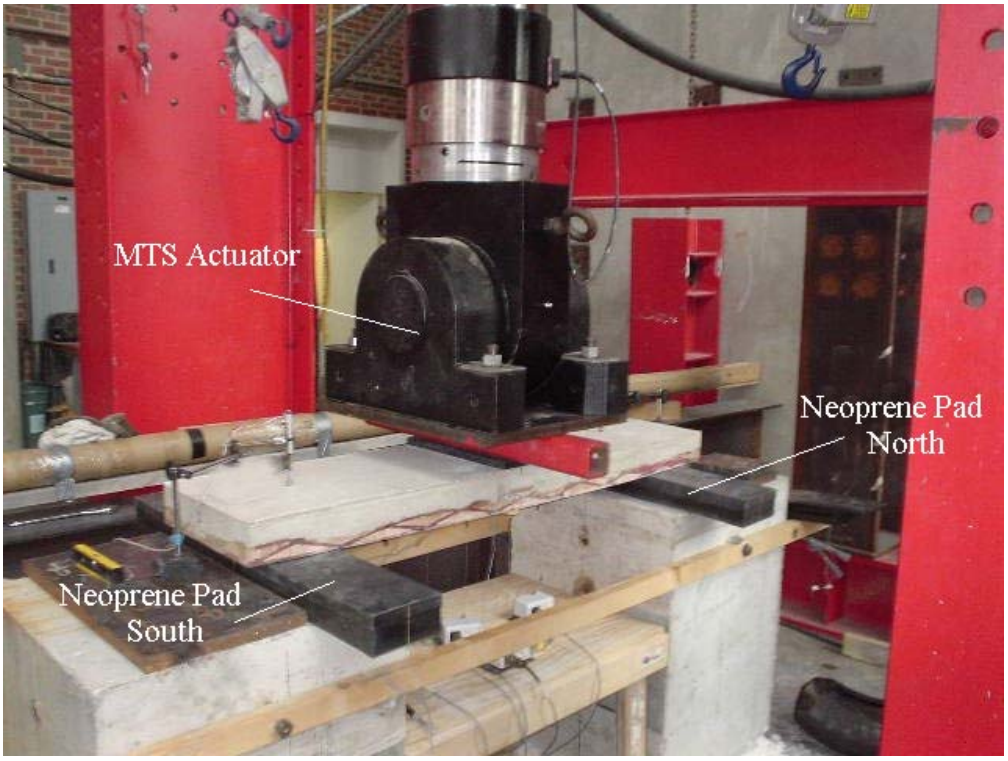

Figure 5.7 Deck 1 test setup for three-point bend.

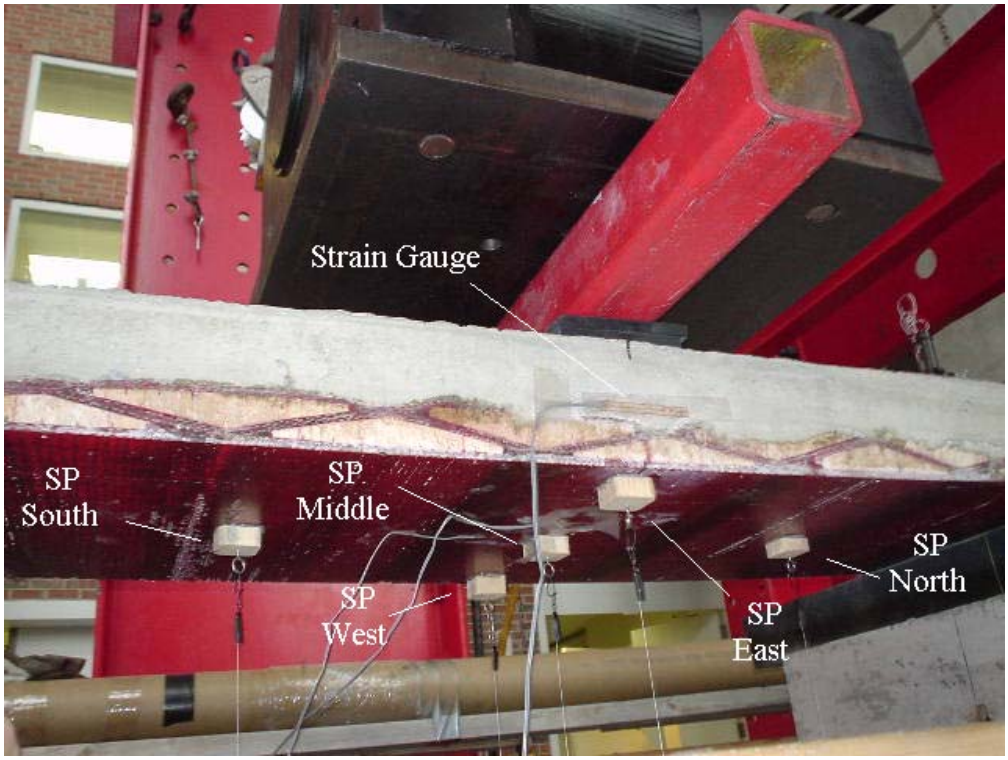

Figure 5.8 This figure illustrates the string-pots at quarter points and out-of-plane points for Deck 1. Note the strain gauge at the interface of concrete and top composite skin.

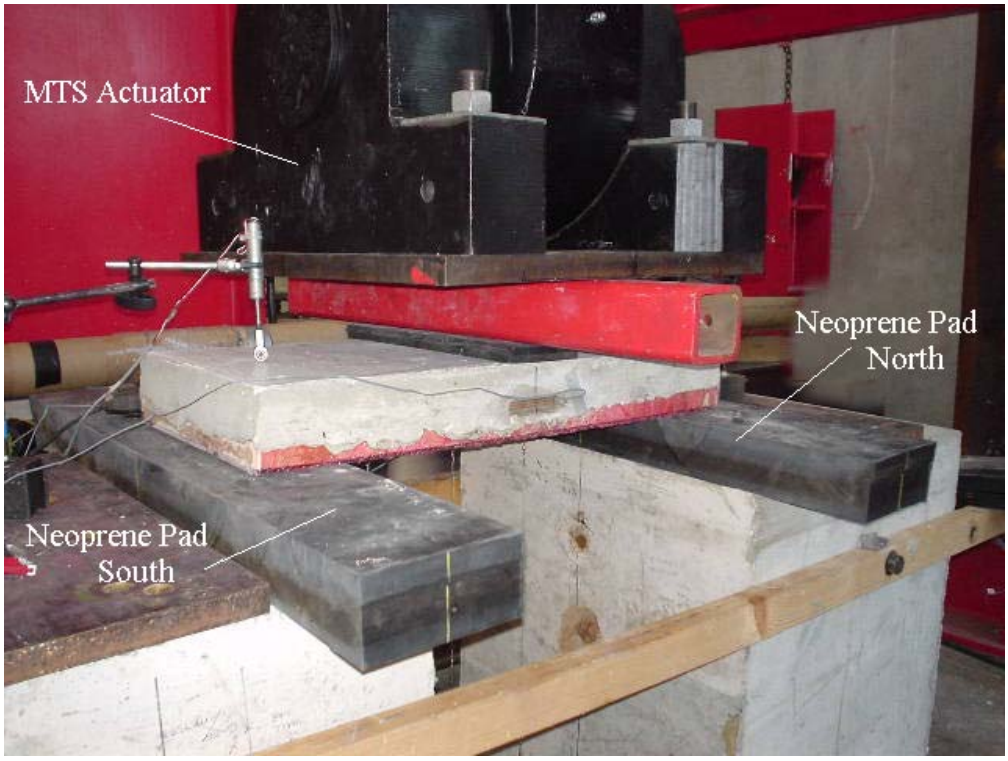

Figure 5.9 Deck 2 test setup for three-point bend.

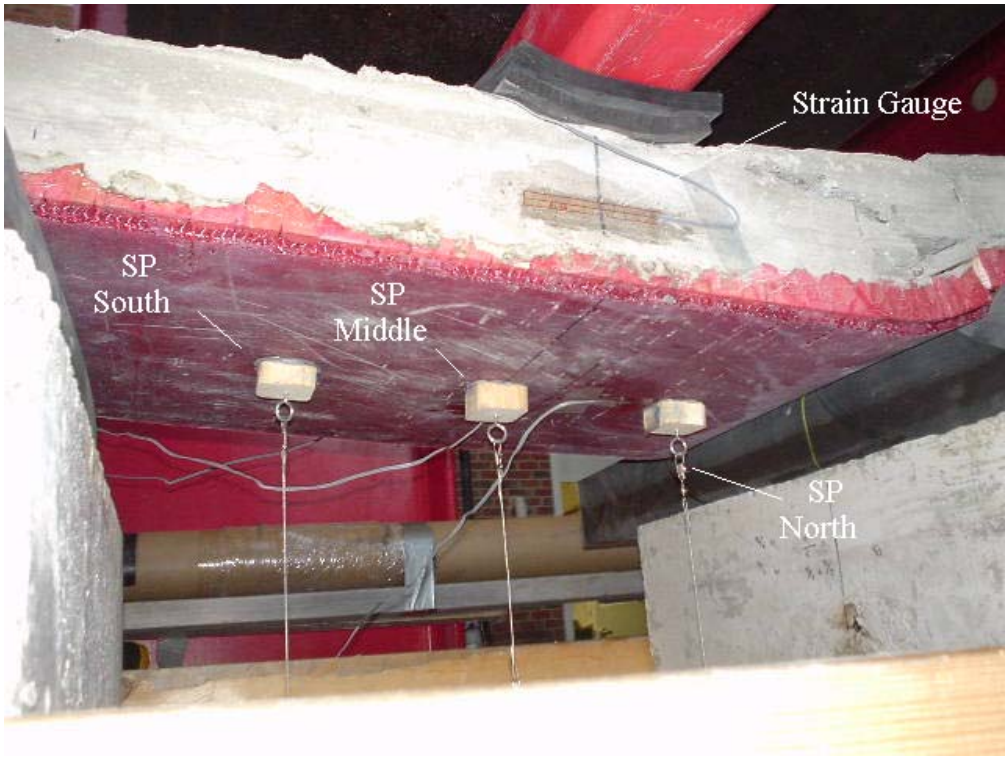

Figure 5.10 This figure illustrates the string-pots at quarter points for Deck 2. Note the strain gauge at the interface of concrete and top composite skin.

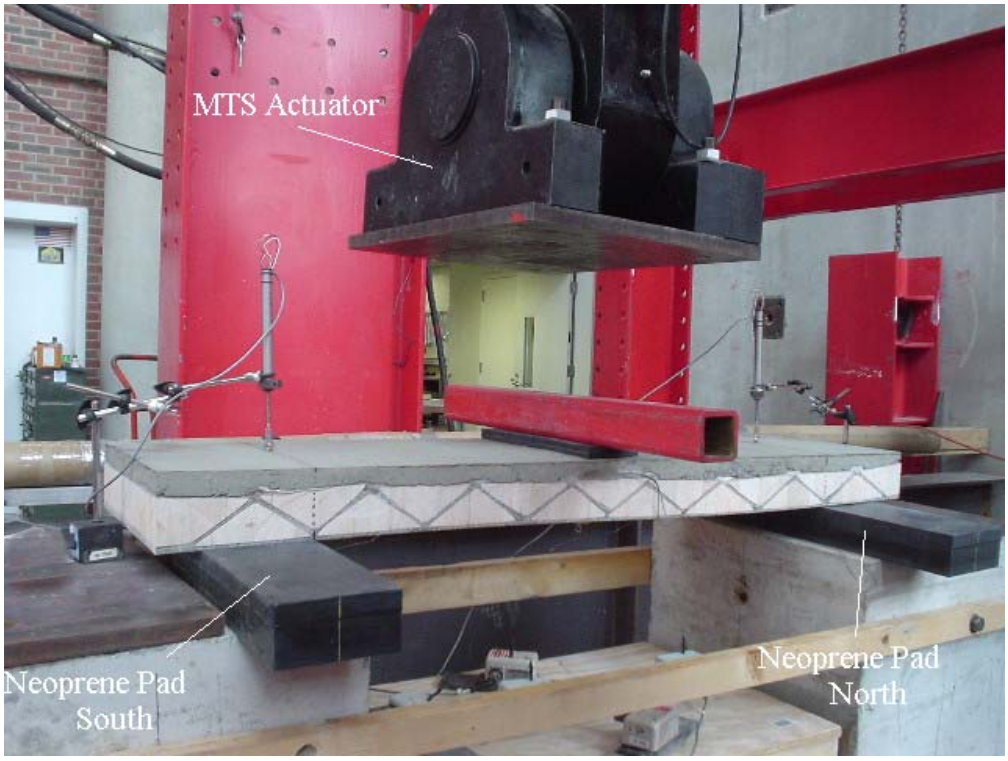

Figure 5.11 Deck 3 test setup for three-point bend.

Figure 5.12 This figure illustrates the string-pots at quarter points and out-of-plane points for Deck 3. Note the strain gauge at the interface of concrete and top composite skin.

Figure 5.13 Deck 4 test setup for three-point bend.

Chapter 6: Results and Discussion

6.1 Deck 1

6.1.1 Stiffness Test

Deck 1 sustained 10 cycles of loading at 2 kip increments before failure. Load vs. net-deflection graphs were plotted for each cycle, and linear regression analysis revealed the stiffness of the deck in each cycle. Figure 6.1 displays the load vs. net deflection at mid-span. Table 6.1 illustrates these stiffnesses. There was no apparent degradation in stiffness illustrated in the results. The average stiffness of Deck 1 was 63.5 kips/in.

The maximum deflection and strain in the deck at the peak of each cycle in loading steps are presented in Table 6.2. The deflection of Deck 1 beneath a 16.0 kip load (AASHTO HS20 Wheel Load) was .254 inches and beneath a 20.8 kip load (AASHTO HS20 Wheel Load plus Impact) was .439 inches. The strain gauge at the interface of the concrete and the top skin layer indicates this area is in tension. This defines the neutral axis of the deck to be above the interface. The indication that the top composite skin of the deck is below the neutral axis illustrates that this skin is tension. Thus, the laminate composite is not acting as a truss but as reinforcement for the concrete topping. This strain gauge data is graphed in figure 6.2.

6.1.2 Strength Test

The load vs. deflection curve for the failure load indicates that the specimen behaves linearly up to the failure load of 20.8 kips. The mode of failure was crushing of concrete. Figure 6.3 demonstrates the failure of Deck 1 beneath a 20.5 kip point load. Shortly after the release of the concrete, buckling of top skin was observed. Deck 1 did return to its original shape minus the crushed concrete.

6.2 Deck 2

6.2.1 Stiffness Tests

Deck 2 sustained 12 cycles of loading at 2 kip increments before failure. Load vs. net-deflection graphs were plotted for each cycle (figure 6.4), and Table 6.1 illustrates the stiffnesses obtained from linear regression analysis. There appears to be a slight increase

in stiffness of the deck, monotonically, through the cyclic loading and unloading. The average stiffness of Deck 2 is 151.9 kips/in.

The maximum deflection and strain in the deck at the peak of each cycle in loading steps are presented in Table 6.2. The deflection of Deck 2 beneath a 16.0 kip, 20.8 kip, and 21.8 kip load was .102 in., .130 in., and .138in., respectively. The strain gauge at the interface of the concrete and the top skin layer indicates this area was in tension (Figure 6.5). This was done as a comparison to the truss-like Deck 1 with the same thickness. Both decks maintain a neutral axis above the interface.

6.2.2 Strength Test

The load vs. deflection curve for the failure load indicates that the specimen behaves linearly up to the failure load of 21.8 kips. The mode of failure was concrete shearing. Figure 6.6 demonstrates the failure of Deck 2. At failure, the top composite skin preceded to delaminate from the Balsa core. The concrete pulled from the core with this skin (figure 6.7). The deck did not regain its original form after the load was released.

6.3 Deck 3

6.3.1 Stiffness Tests

Deck 3 sustained 9 cycles of loading at 2 kip increments before failure. Load vs. net-deflection graphs were plotted for each cycle (figure 6.8), and linear regression analysis revealed the stiffness of the deck in each cycle. Table 6.1 illustrates these stiffnesses. There appears to be no degradation in stiffness of the deck through the cyclic loading and unloading. The average stiffness of Deck 3 is 69.0 kips/in.

The maximum deflection and strain in the deck at the peak of each cycle in loading steps are presented in Table 6.2. The deflection of Deck 3 beneath a 16.0 kip (AASHTO HS20 Wheel Load) was .239 inches and at failure of 17.5 kips was .274 inches. The strain gauge at the interface of the concrete and the top skin layer indicates this area is in compression (figure 6.9). This supports the theory of truss analysis as opposed to a concrete slab with reinforcement.

6.3.2 Strength Test

The strength test for Deck 3 was in effect the 9th cycle of the stiffness test. The load vs. deflection curve for the failure load indicates that the specimen behaves linearly up to the failure load of 17.5 kips. There was no observed delamination of the truss composite before or shortly thereafter the first/primary failure.

At 17.5 kips, the south half of the concrete surface of Deck 3 debonded from the composite. Observation sustained the shear connectors were not adequate to maintain full composite action of the truss with the polymer concrete. This is illustrated in figure 6.10. The deck then accepted loading up to 15.0 kips and failed with the break of a core/skin connection thought due to shear stresses (Figure 6.11).

The deck was oriented on the supports in a truss-like manner such that the first diagonal member toward the loading was in compression. The adjacent diagonal supporting member (slanting downward) was in tension. Thus, this section of the deck was oriented to sustain high levels of shear stress. However, the next diagonal member is in compression and is thus oriented tangent to the principal shear stresses. Therefore, this section of the deck maintains a low level of shear stress resistance. As a result, the damage illustrated in figure 10 assents this mode of shear failure.

6.4 Deck 4

6.4.1 Strength Test

The load vs. deflection curve for the failure load indicates that the specimen behaves linearly up to the failure load of 40.5 kips (Figure 6.12). The mode of failure was delamination of concrete from composite surface and shear cracking of concrete. Figure 6.13 demonstrates the failure of Deck 4 beneath a 40.5 kip point load (.275 in. deflection at mid-span). Shortly after the release of the concrete, slight buckling of top skin was observed. The shear cracking is illustrated in figure 6.14. Deck 4 did return to its original shape. There was no delamination of the core from the outer skins.

6.5 Summary

The results of testing of the composite bridge decks provided positive feedback as to the potential of this new completely woven design. Future slight modifications can

prove exceptionally useful as they did from the design of Deck 1 to Deck 3. These future modifications and recommendations are stated in Chapter 7.

First, slight modification in the fabricated 3-D loom increased the 1 ½ inch composite thickness of Deck 1 to the 3 inch composite thickness of Deck 3 (see section 3.6.3). The results of this testing proved the increase in composite thickness (and subsequent decrease in concrete topping) not only resulted in an increased deck stiffness but also in a reduction of weight by 25%; with a 41 ½ inch span, Deck 3 maintained a 69.0 kips/in. stiffness, whereas with a 40 ½ inch span, Deck 1 maintained a 63 ½ kips/in. stiffness (8% less). In addition, Deck 3 exhibited a mid-span deflection of .274 inches at 17.5 kip loading while Deck 1 demonstrated a deflection of .307 inches beneath the same load. Additionally, the top skin of Deck 3 appeared to be above the neutral axis resulting in a truss-like action of the overall deck. This is realized by observing the compressive strain illustrated at the concrete/composite interface of Deck 3 under loading.

Second, light reinforcement in an enhanced concrete surface directly contributed to the compressive strength (above neutral axis) of Deck 3. Though, Deck 3 did not attain the ultimate load carrying capacity of Deck 1. This was due to a decrease in surface bond with the concrete. The shear connectors engaged in Deck 3 were ½ inch high and not nearly as efficient as the metal shear connectors of Deck 1 with 1 ¼ inch height. The composite truss of Deck 3 showed no signs of damage under the cyclic loading until the concrete debonded from the surface due to shear stresses. Thus, the load carrying capacity could be directly increased by means of better designed shear connection. After the loss of concrete surface, Deck 3 exhibited a break in core/outer-skin connection. This was unexpected but can be easily improved by simple manipulation of the weaving cycle.

Deck 4 was tested to illustrate the repeatability of the failure mode of Deck 3. The composite truss displayed no signs of delamination throughout the cyclic loading. At 40.5 kips, the concrete similarly debonded from the surface of the composite truss. Shortly after the loss of concrete surface, there was localized buckling atop the composite section directly beneath the debonded concrete. No core connections were lost. Deck 4 also performed like a truss with compressive forces in the upper skin; this was again realized from the strain gauge at concrete/skin interface. Observation of Deck 4

maintained the break in core connection of Deck 3 to be potentially a weak link, and not an overall illustration of the connections.

Deck 2 demonstrated the presumed delamination often displayed in composite bridge decks. Without direct reinforcement of the outer skin to the inner core, the upper skin delaminated from the Balsa core in a shearing manner.

6.6 Tables and Figures

Table 6.1 Cyclic stiffness provided by linear regression analysis of load vs. net displacement profiles

	Stiffness (kips/in.)			
Cycle	**Deck 1**	**Deck 2**	**Deck 3**	**Deck 4**
1	59.575	33.479	77.678	164.533
2	63.186	125.704	61.034	
3	65.928	115.945	66.395	
4	68.189	127.310	70.939	
5	69.995	140.650	71.462	
6	69.146	145.988	70.525	
7	66.591	151.254	68.987	
8	62.858	161.402	67.736	
9	58.319	169.589	66.243	
10	51.416	173.424		
11		181.805		
12		178.901		
average	**63.520**	**151.997**	**69.000**	**164.533**

Table 6.2 Mid-span deflection and corresponding strain of Decks 1-4 at significant loads

Deck	Load A/B/C (kips)	Deflection at Mid-Span (in.)	Deflection Index	FRP Strain at Mid-Span (%)	Concrete Strain at Interface (%)	Concrete Strain at Top (near mid-span) (%)	FRP Strain at Bottom (near mid-span) (%)
1	16	0.254	L/160	0.2608	0.0655	n/a	0.1596
	20.8	0.439	L/92	0.4522	0.0134	n/a	0.2292
	20.8	0.439	L/92	0.4522	0.0134	n/a	0.2292
2	16	0.102	L/196	0.1851	0.1361	-0.1119	0.1615
	20.8	0.130	L/154	0.2436	0.179	-0.1469	0.2163
	21.8	0.138	L/145	0.2739	0.1983	-0.1674	0.2519
3	16	0.239	L/174	0.315	-0.0409	-0.1553	0.3158
	20.8	n/a	n/a	n/a	n/a	n/a	n/a
	17.5	0.274	L/151	0.3567	-0.0482	-0.1754	0.3497
4	16	0.070	L/314	n/a	n/a	n/a	n/a
	20.8	0.091	L/242	n/a	n/a	n/a	n/a
	40.5	0.276	L/80	n/a	n/a	n/a	n/a

Load A = AASHTO HS20 Wheel Load
Load B = AASHTO HS20 Wheel Load plus Impact (30%)
Load C = Ultimate Load

Table 6.3 Average deck stiffness for deck orientation including mode of failure

	Span (in.)	Average Stiffness (kips/in.)	Total Thickness (in.)	Angle of Truss (degrees)	Ultimate Load (kips)	Mode of Failure
Deck 1	40.5	63.520	3.75	25	21.850	Conc. Crushing/Shearing
Deck 2	20	151.997	3.5	n/a	21.845	Conc. Shearing
Deck 3	41.5	69.000	3.75	43	17.565	Conc. Delamination
Deck 4	22	164.533	3.75	43	40.320	Conc. Delam./Shearing

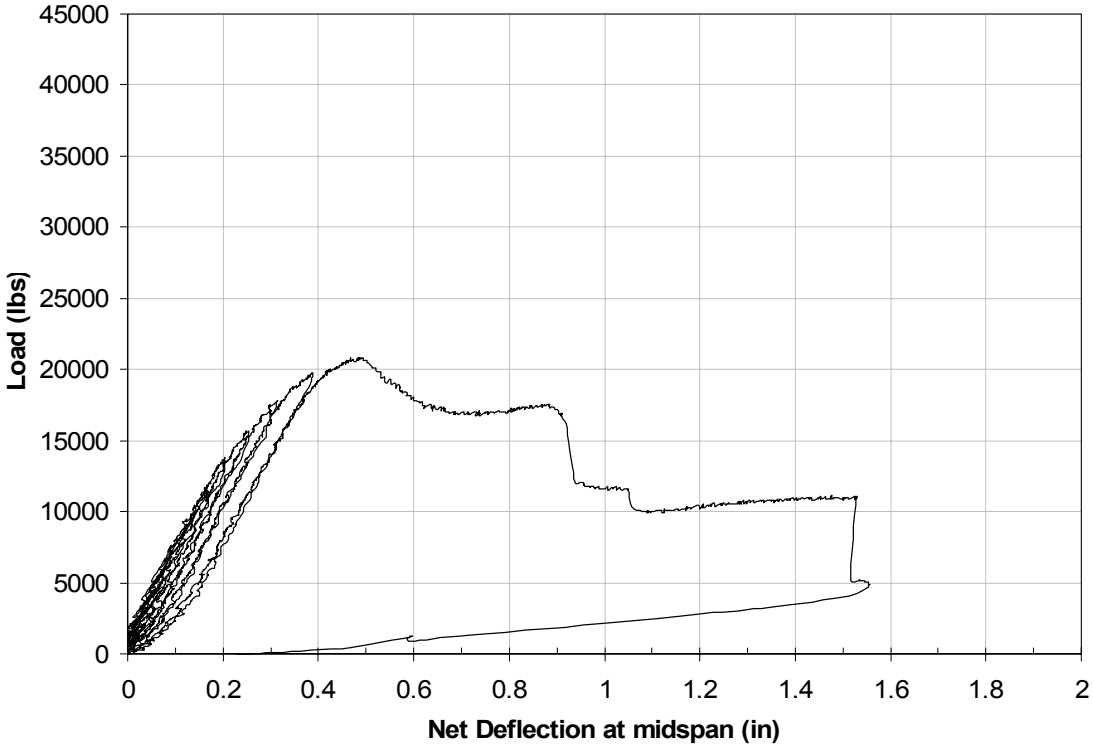

Figure 6.1 Load vs. Net-Deflection graph for Deck 1.

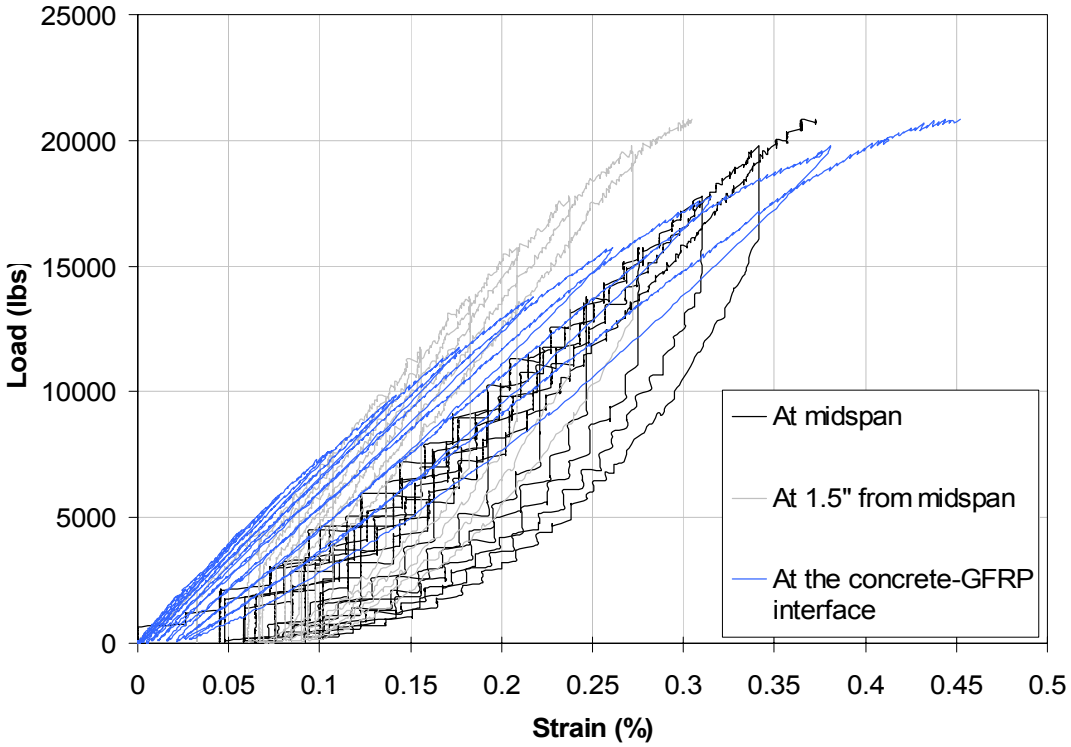

Figure 6.2 Load vs. Strain graph for Deck 1.

Figure 6.2

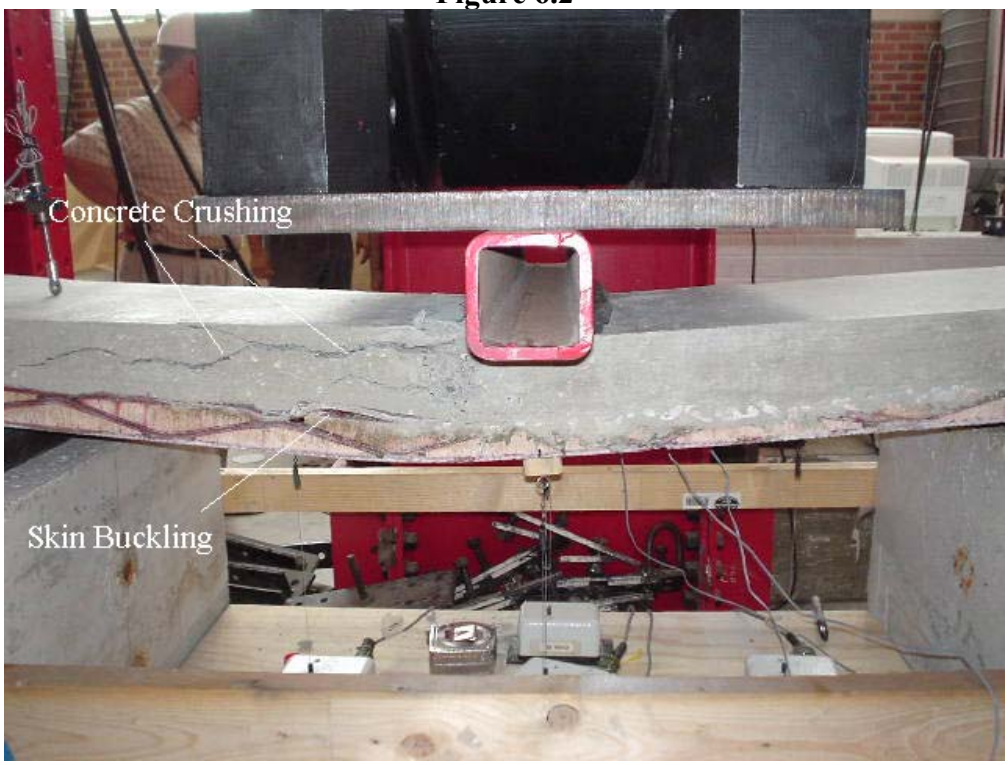

Figure 6.3 Failure of Deck 1 beneath 20.5 kip point load.

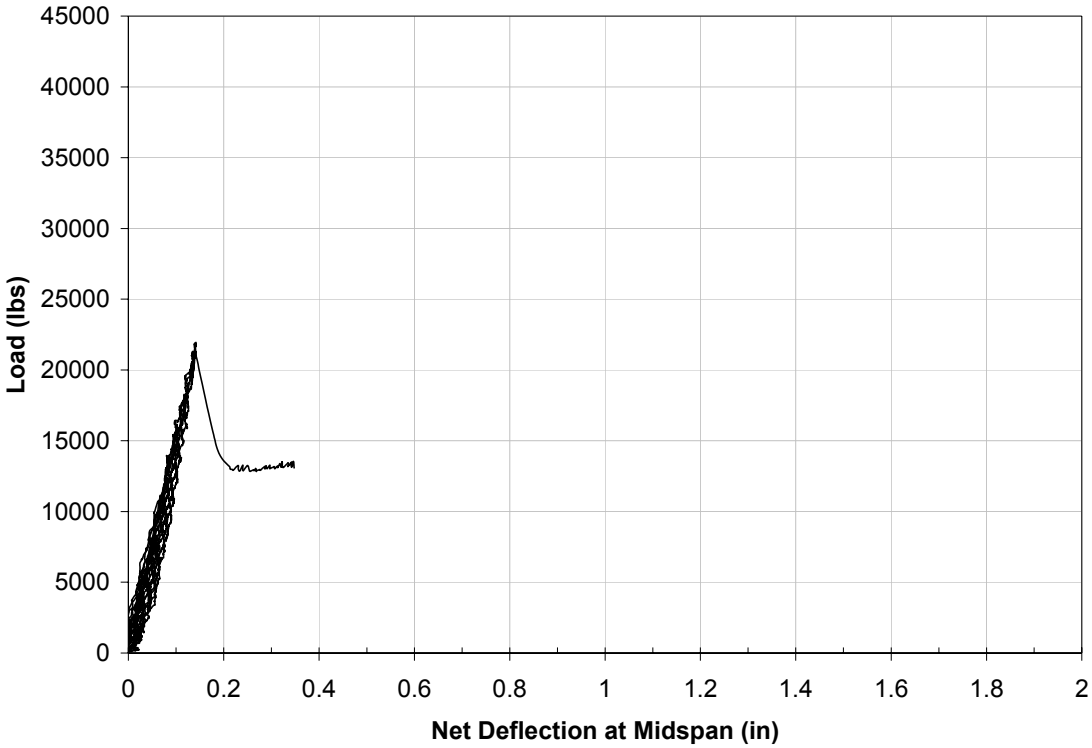

Figure 6.4 Load vs. Net-Deflection graph for Deck 2.

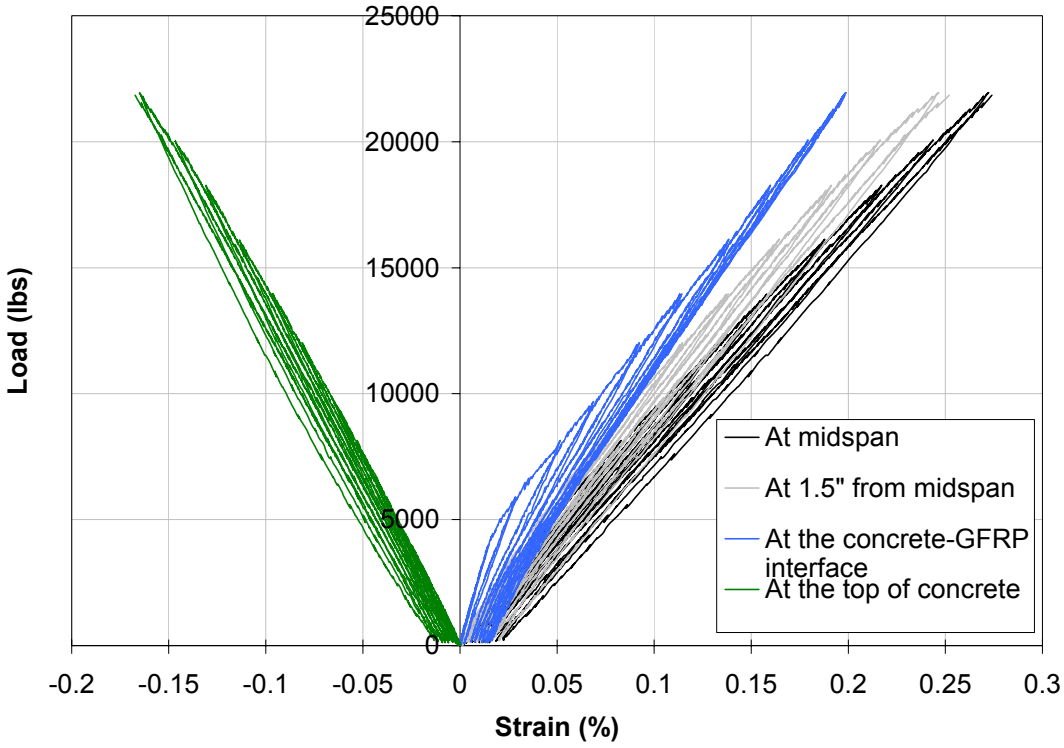

Figure 6.5 Load vs. Strain graph for Deck 2

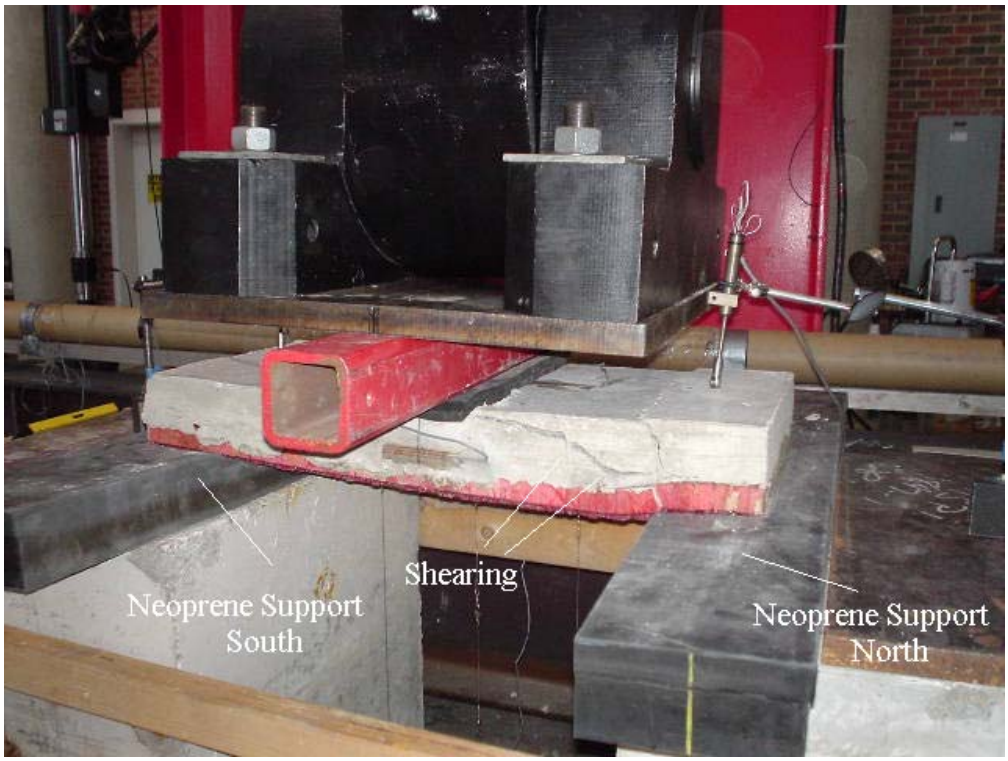

Figure 6.6 Failure of Deck 2. Concrete shearing.

Figure 6.7 Delamination of top skin from core (Deck 2).

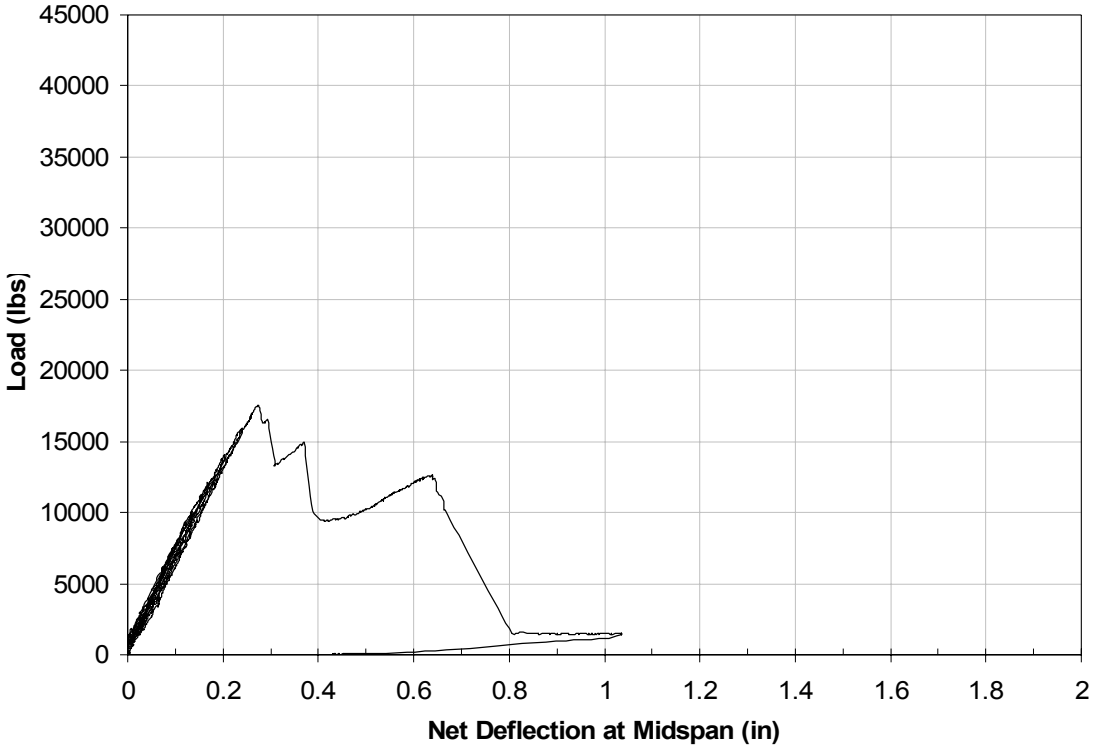

Figure 6.8 Load vs. Net-Deflection graph for Deck 3.

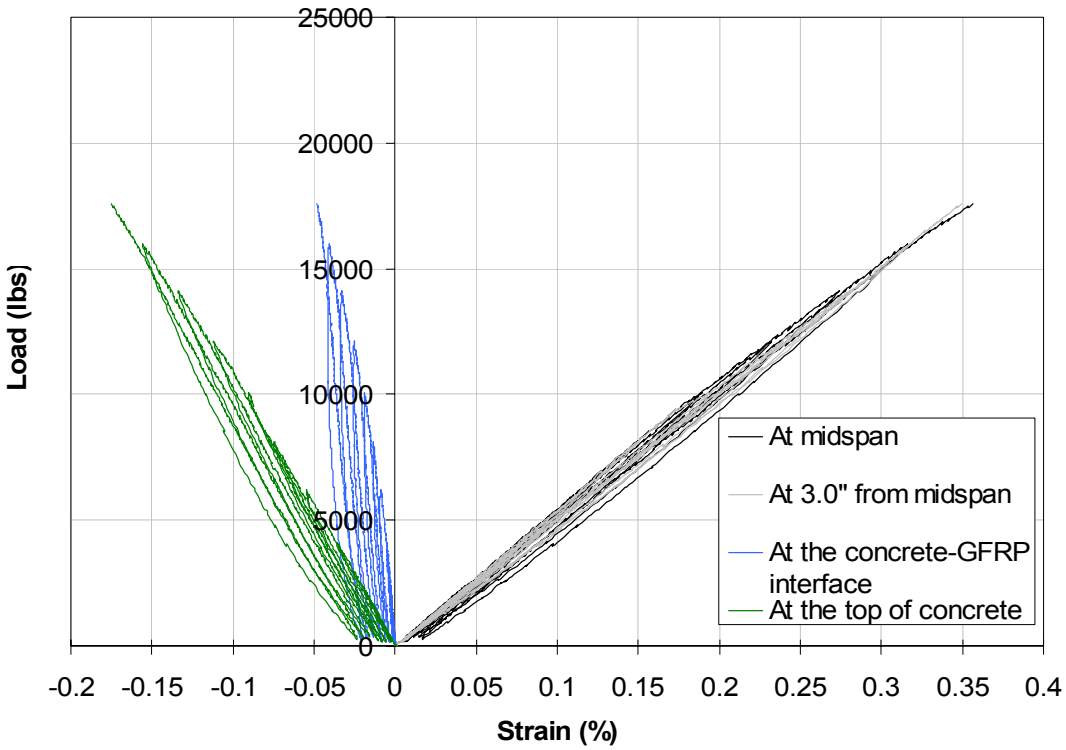

Figure 6.9 Load vs. Strain graph for Deck 3.

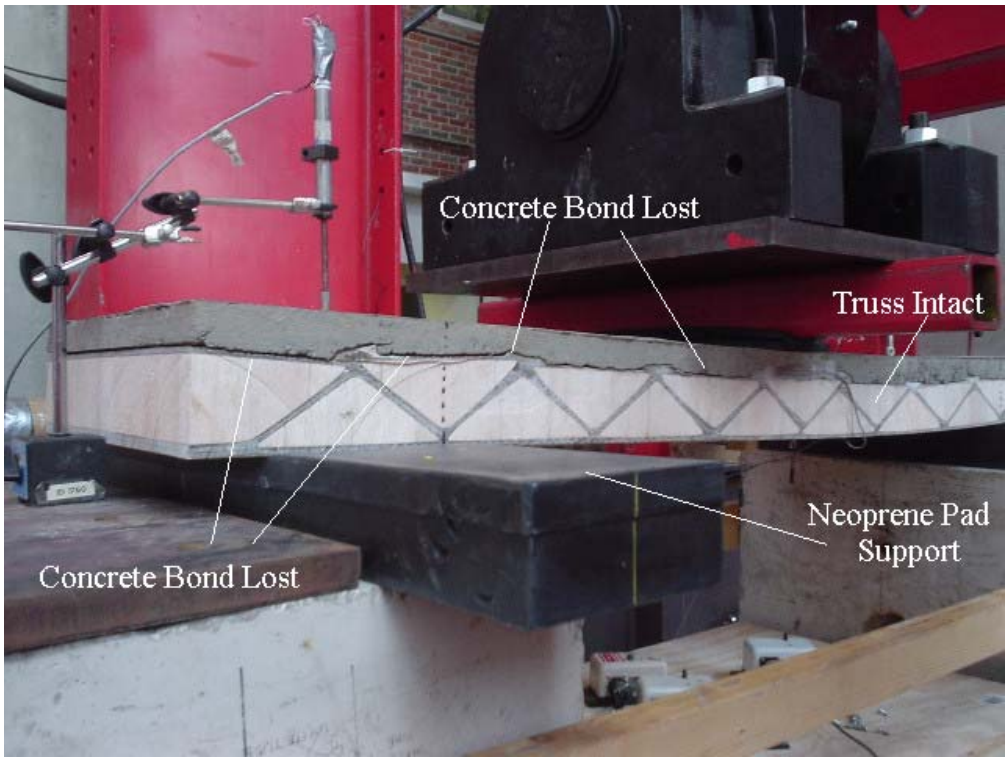

Figure 6.10 Concrete bond with composite truss is lost at 17.5 kips (Deck 3).

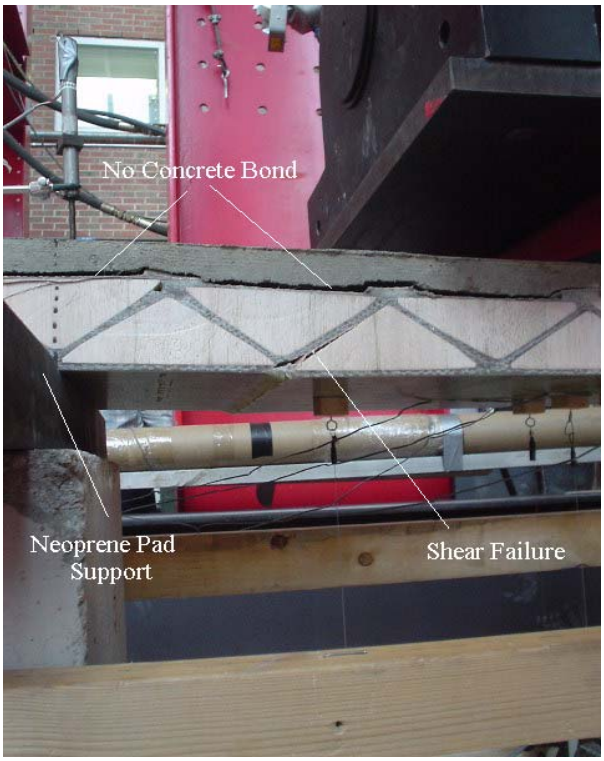

Figure 6.11 Shear failure in composite after bond lost with concrete (Deck 3).

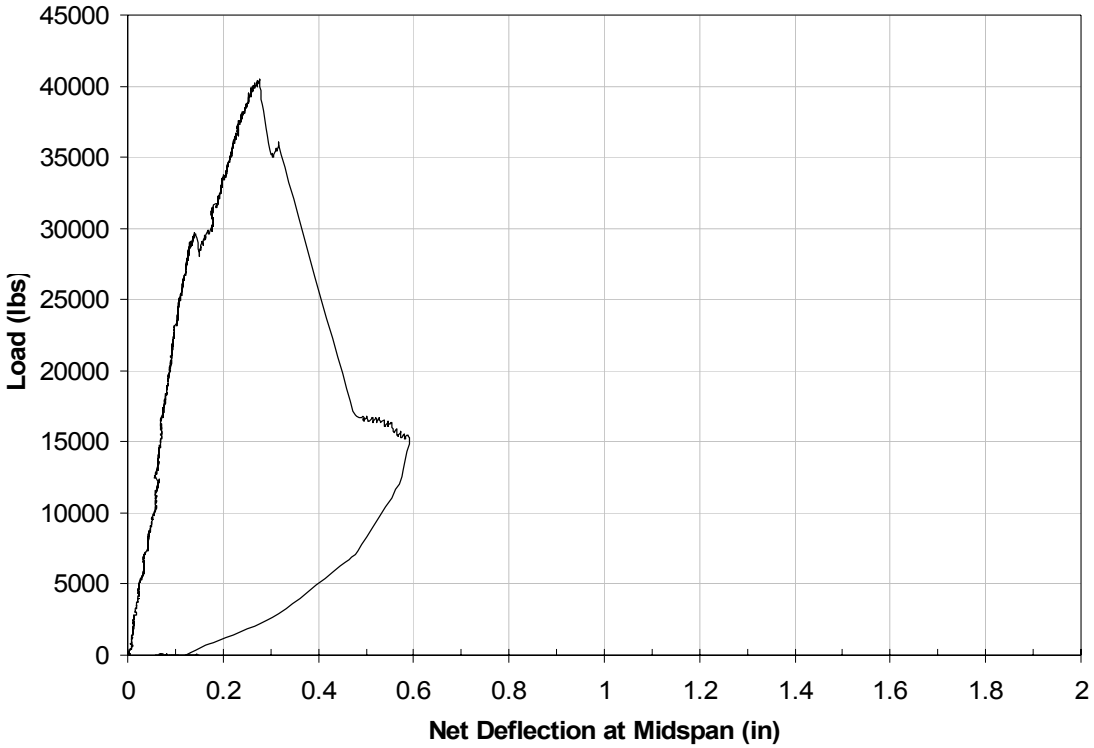

Figure 6.12 Load vs. Net-Deflection graph for Deck 4.

Figure 6.13 This figure illustrates the delamination of the concrete topping (Deck 4).

Figure 6.14 Cracking in concrete topping due to shear stress (Deck 4).

Chapter 7: Conclusions and Recommendations and Future Research

The ability to make simple and/or major modifications to the fabrication process due to the unique setup of the 3-D weaving machine, the observation of the failure modes within the structural components of the bridge deck, and the knowledge of the unique weaving process that creates these structural components are three significant tools that lead to the optimization of a sound future series of completely woven bridge decks.

- The break in the structural attachment of the core skin to the bottom skin in Deck 3 exemplifies the importance of a rigorous reinforcement through these connection points. And within Step 2 of the innovative weaving sequence, the core skin can attach to the outer skin for double or triple (4 or 6) the pick cycles by simple alteration of the weaving code. Even further attachment of the two skins could result in trapezoidal figures comprising the deck. If the intention is to maintain a sharp point of attachment for the triangular truss-like orientation, then the loom can simply not beat-up during these additional pick cycles.

- The shear connectors also deem an important aspect of the composite bridge deck. Observation revealed the bond of the concrete topping to the composite surface the limiting factor in ultimate load carrying capacity. The metal shear connectors posed useful but were difficult in the infusion process beneath a vacuum bag. The composite shear connectors were simple to infuse and maintained their bond with the composite deck but failed to prevent concrete debonding. Potentially, shear bolts could be drilled into the top surface of the composite deck after infusion to create better bonding with the concrete. 3TEX, Inc. promotes excellent pull-out values for bolts connected to their infused fabrics.

- The thickness of the woven composite appeared to directly affect the performance of the bridge deck. The potential of the unique 3-D loom is

to weave a 6-7 inch open cell thickness. Adjusting the weaving cycle to a 32 pick count as opposed to a 16 pick count for each step could produce a 6 ½ inch preform. The 15 inch reed is the limiting factor to maintaining appropriate shed orientation.

- Although Deck 2 displayed skin delamination near ultimate loading, the rapidity and cost effective manner in which is can be produced provides interest in pursuing thicker Balsa core composite decks with 3Weave^{TM} fabrics ultimately laminated together. 3TEX, Inc. continuously weaves economical hybrid fabrics as well as all carbon fabrics that could replace the bottom skin which maintains pure tension.

Appendix A
3 TEX, Inc. Proprietary Preform Product Specification

Figure A1 Preform product specification of bridge deck panel skin 1

PREFORM PRODUCT SPECIFICATION **3TEX, Inc. PROPRIETARY**

Code/#: P3W-GE062-12 Specification Date: 6/17/03

Preform Name: 3WEAVE™ Bridge Panel Revision Date/#:

Preform Description: 1.5-21/12@3/2/1 194-60/33/7

Issuer: Mahmoud Salama Reviewed by:

Preform Type: 3WEAVE Cross-sectional Shape: Flat

Drawing of Cross-Section Showing Sections/Areas of Different Architecture # of Sections: 1

Comments:

Preform Required Specifications:

			Units	Note: "Overall" is final width and includes selvedge
Width-in-Reed, W_R:	12.00	+/- 0.25	inch	
Overall Width, W_O:	13.50	+/- 0.25	inch	
Linear Density, Lp:	64.67	+/- 4.0%	oz/yd	
Areal Density, Ap:	194.00	+/- 4.0%	oz/sq. yd.	
Thickness, t:	0.21	+/-		
Other:		+/-		
Other:		+/-		

Section A

Fiber Type

Warp (0°): Hybon 2022 roving, 1 warp layers, 103 yield, 21 ends/in/layer (3 ends/dent)

Filling (90°): Hybon 2022 roving, 2 fill layers, 218 yield, 6 insertions/in (double insertion)

Z (Thickness): Hybon 2022 roving, 675 yld 2 harnesses, plain weave pattern, 7 ends/in.

Nominal Architectural Parameters		Units	Comments:
Width-end-to-end, W_{e-e}:	12.00	inch	
Linear Weight, Lp:	64.67	oz/yd	
Areal Weight, Ap:	194.00	oz/sq. yd.	
Thickness, t:	0.21		

	Weight Fraction	Fiber Vol. Fraction
Warp (0°):	60.3%	27.9%
Filling (90°):	32.7%	15.1%
Z (Thickness):	7.0%	3.3%
Total:	100.0%	46.3%

FigureA2 Preform product specification of bridge deck panel skin 2

PREFORM PRODUCT SPECIFICATION **3TEX, Inc. PROPRIETARY**

Code/#: P3W-GE063-12 Specification Date: 6/17/03

Preform Name: 3WEAVE™ Bridge Panel Revision Date/#:

Preform Description: 1.5-14/12@2/2/1 154-51/41/8

Issuer: Mahmoud Salama Reviewed by:

Preform Type: 3WEAVE Cross-sectional Shape: Flat

Drawing of Cross-Section Showing Sections/Areas of Different Architecture # of Sections: 1

Comments:

Preform Required Specifications:

				Units	Note: "Overall" is final width and includes selvedge
Width-in-Reed, W_R:	12.00	+/-	0.25	inch	
Overall Width, W_O:	13.50	+/-	0.25	inch	
Linear Density, Lp:	51.19	+/-	4.0%	oz/yd	
Areal Density, Ap:	153.57	+/-	4.0%	oz/sq. yd.	
Thickness, t:	0.17	+/-		inch	
Other:		+/-			
Other:		+/-			

Section A

Fiber Type

Warp (0°): Hybon 2022 roving, 1 warp layers, 103 yield, 14 ends/in/layer (2 ends/dent)

Filling (90°): Hybon 2022 roving, 2 fill layers, 218 yield, 6 insertions/in (double insertion)

Z (Thickness): Hybon 2022 roving, 675 yld 2 harnesses, plain weave pattern, 7 ends/in.

Nominal Architectural Parameters		Units
Width-end-to-end, W_{e-e}:	12.00	inch
Linear Weight, Lp:	51.19	oz/yd
Areal Weight, Ap:	153.57	oz/sq. yd.
Thickness, t:	0.17	inch

	Weight Fraction	Fiber Vol. Fraction
Warp (0°):	50.8%	23.0%
Filling (90°):	41.3%	18.7%
Z (Thickness):	7.9%	3.6%
Total:	100.0%	45.3%

Comments:

Figure A3 Preform product specification of bridge deck panel skin 3

PREFORM PRODUCT SPECIFICATION **3TEX, Inc. PROPRIETARY**

Code/#: P3W-GE064-12 Specification Date: 6/17/03

Preform Name: 3WEAVE™ Bridge Panel Revision Date/#:

Preform Description: 1.5-14/8@2/2/1 130-60/33/7

Issuer: Mahmoud Salama Reviewed by:

Preform Type: 3WEAVE Cross-sectional Shape: Flat

Drawing of Cross-Section Showing Sections/Areas of Different Architecture # of Sections: 1

Comments:

Preform Required Specifications:

			Units	Note: "Overall" is final width and includes selvedge
Width-in-Reed, W_R:	12.00	+/- 0.25	inch	
Overall Width, W_O:	13.50	+/- 0.25	inch	
Linear Density, L_P:	43.27	+/- 4.0%	oz/yd	
Areal Density, A_P:	129.80	+/- 4.0%	oz/sq. yd.	
Thickness, t:	0.15	+/-	inch	
Other:		+/-		
Other:		+/-		

Section A

Fiber Type

Warp (0°): Hybon 2022 roving, 1 warp layers, 103 yield, 14 ends/in/layer (2 ends/dent)

Filling (90°): Hybon 2022 roving, 2 fill layers, 218 yield, 4 insertions/in (double insertion)

Z (Thickness): Hybon 2022 roving, 675 yld 2 harnesses, plain weave pattern, 7 ends/in.

Nominal Architectural Parameters		Units
Width-end-to-end, W_{e-e}:	12.00	inch
Linear Weight, L_P:	43.27	oz/yd
Areal Weight, A_P:	129.80	oz/sq. yd.
Thickness, t:	0.15	inch

	Weight Fraction	Fiber Vol. Fraction
Warp (0°):	60.1%	26.7%
Filling (90°):	32.6%	14.5%
Z (Thickness):	7.3%	3.3%
Total:	100.0%	44.4%

Comments:

Appendix B
JEFFCO 1401-12/4101-17 Epoxy System for Infusion

Figure B1 JEFFCO PRODUCTS technical information and recommendations

JEFFCO PRODUCTS

5252 Kearny Villa Way
San Diego, CA. 92123
(858) 576-9900
FAX (858) 576-7093

JEFFCO 1401-12/4101-17

Epoxy System for Infusion

System SKU: 1401-12/4101-17
System Category: Epoxy System

DESCRIPTION:
Multifunctional epoxy and cycloaliphatic-amine blend hardener for high performance composite parts. Very long pot life, with fast cure development at standard molding temperatures. Excellent combination that provides good thermal resistance, excellent fatigue and inter-laminar shear strength with rapid wetting of E-glass fiber reinforcements. Jeffco 1401-12 Epoxy Resin is colored transparent ruby red for visual indication of infusion progress. Jeffco 1401-12 Epoxy Resin is formulated for highly increased E-glass fiber compatibility. Low toxicity, low odor system. No VOC's, 100% solids.

APPLICATIONS:
Resin infused composite rotor blades, other large fiberglass reinforced structures.

SUGGESTIONS FOR USE:
Condition epoxy resin and hardener to between 24ºC and 38ºC (75ºF to 100ºF) to ensure proper mixed viscosity. Introduce mixed material into part to be infused keeping mold temperature between 35ºC and 40ºC (95ºF to 104ºF). Place or position injection ports to introduce material as needed to ensure injection within two hours. Under moderate vacuum, inject material for up to 120 minutes at the above temperature parameters. Once injection is complete, increase mold temperature to between 50ºC and 60ºC (122ºF to 140ºF). Hold at this temperature for between 12 and 14 hours. A final post cure of 2 hours at 85º C (185ºF) will bring the infused composite to full cure. Cure temperatures may be from 50°C to 85°C to accomplish maximum HDT. Optimum cure time(s) versus temperature(s) will depend on parameters such as part thickness or size.

REINFORCEMENT TYPES:
Jeffco 1401-12 Epoxy Resin is specially formulated for highly increased compatibility with E-glass reinforcements. For carbon fiber laminates, Jeffco 1401-14 Epoxy Resin should be used. When using E-glass / carbon fiber hybrid fabrics or reinforcements, Jeffco 1401-16 Epoxy Resin is recommended. All three Epoxy Resins are compatible and recommended with Jeffco 4101-17 Epoxy Hardener. Please refer to the specific Jeffco Epoxy Resin product bulletin for more information.

ADVANTAGES OF JEFFCO:
As discussed previously, Jeffco 1401-12 Epoxy Resin is formulated to improve the intimate bond between the epoxy resin and E-glass fiber reinforcements. This formulation technique results in increased physical properties as follows:

¨ Fiber Pull-Out Strength
¨ Tensile Strength and Modulus
¨ Flexural Strength and Modulus

¨ Compressive Strength
¨ Impact Resistance
¨ Inter-Laminar Shear Strength

Of equal, if not greater significance is the retention of the above properties after exposure to heat, cycle fatigue, water, expected adverse environmental reagents such as salt spray, acid rain, etc. The formulation of Jeffco 1401-12 Epoxy Resin results in minimal degradation of the cured composite's physical properties as compared to epoxy resin systems not containing the proprietary formulation constituents of Jeffco 1401-12 Epoxy Resin. Similar results with carbon reinforced composites are obtained with Jeffco 1401-14 Epoxy Resin and carbon / E-glass hybrids with Jeffco 1401-16 Epoxy Resin.
The benefit to the composite fabricator is obvious and clear: Increased product life and confidence!

PROPERTIES OF 1401-12/4101-17 SYSTEM LIQUID PROPERTIES (77°F):	Minimum	Maximum
Resin Viscosity (Part "A") (cps) @ 77°F	**900**	**1,000**
Hardener Viscosity (Part "B")	**10**	**10**
Mixed Viscosity	**140**	**140**
Mix Ratio , Resin to Hardener (by weight)	**100:30**	**100:30**
Gel Time, minutes @ 77°F	**70**	**75**
Weight Per Gallon, Resin (lbs.)	**9.4**	**9.5**
Weight Per Gallon, Hardener (lbs.)	**7.9**	**8.0**
Color, Resin	**Transparent Ruby Red**	
Color, Hardener	**Clear - Amber**	

CURED PHYSICAL PROPERTIES OF NEAT RESIN:
Jeffco 1401-12 Epoxy Resin, 100 parts, Jeffco 4101-17 Epoxy Hardener, 30 parts. Cured 2 hours at 35°C + 14 hours at 50°C + 2 hours at 85°C.

NEAT RESIN CURED PROPERTIES OF 1401-12/4101-17 SYSTEM:	Minimum	Maximum
Shore D Hardness	**87D**	**87D**
Tensile Strength	**83,000**	**83,000**
Flexural Strength	**86,000**	**86,000**
Compressive Strength	**14,500**	**14,500**
HDT, °F	**188**	**188**
Elongation	**7.5**	**8.5**

HOW SUPPLIED:
['Pails', 'Drums', 'Tote Bins']

Appendix C
PPG Industries Product Description of HYBON 2022 ROVING

Figure C HYBON 2022 Product Description

PPG Fiber Glass

Hybon® 2022 Roving

(Revised 9/03)

APPLICATION

Hybon 2022 *roving is a single end roving for filament winding and weaving/knitting applications and is made of electrical (E) glass fiber. This roving is compatible with polyester, vinyl ester, epoxy, and phenolic resin systems. 2022 roving is designed for applications which require maximum wet-out and wet-out consistency together with good abrasion resistance and processing characteristics. It is suitable for applications such as piping in oil-field CO_2 gathering systems and pressure cylinders.*

USER BENEFITS

- Provides strand hardness without sacrificing rapid and complete wet-out
- Excellent payout and package transfer
- Low resin demand during processing
- Excellent package transfer efficiency through the use of an outer adhesive film
- Product is manufactured in conformance to ISO 9002 requirements
- Supported by experienced Customer Liaison Services Representatives

PRODUCT DESCRIPTION

Property	Unit	Minimum Average Value			ASTM Method
		Polyester	Epoxy	Vinyl Ester	
Apparent Horizontal Shear Strength	MPa	55/44*	62/56*	55/44*	D2344
	ksi	8/6.4*	9/8.1 *	8/6.4*	
	kg/cm^2	562/450*	633/569	562/450	

*Strength after immersion in boiling water for six hours.

PRODUCT DESCRIPTION

Type of Fiber													
Roving Yields, nominal ±7% (yd/lb)	103	206	218	225	250	288	330	413	450	675	827	1200	1800
TEX, nominal ±7% (g/km)	4800	2400	2275	2200	1985	1722	1500	1200	1100	735	600	413	276
Fiber Diameter, nominal	T	MN	MN	T	M	LM	Q	MN	MN	K	K or MN	K or MN	K
Micrometers, µm	24	17	17	24	16	15	20	17	17	13	13 or 17	13 or 17	13
Type of Sizing	Silane	Silane	Silane	Silane	Silane	Silane	Silane	Silane	Silane	Silane	Silane	Silane	Silane
Percent of Sizing, (by wt. of glass)	.55	.55	.55	.55	.55	.55	.55	.55	.55	.55	.55	.55	.55

PALLETIZING & PACKAGING DATA

Packaging Option 1:

- Yields: 103, 206, 413 & 827
- 48 packages/pallet
- Pallet weight: 980 kg
- Package weight: 20.4 kg

Packaging Option 2:

- Yields: 218, 225, 250, 288, 330, 450, 675, 1200, & 1800
- 60 packages/pallet
- Pallet weight: 1,225 kg
- Package weight: 20.4 kg

Caution: To avoid possibility of potential injury, maintain column stability by limiting pallet stacking to two or three high as noted on individual shipping container.

Appendix D
Reed Construction Data for QUIKRETE® 5000 High Early Strength Concrete Mix Specification Data

Figure D1 QUIKRETE® 5000 High Early Strength Concrete Mix Specification Data

SPEC DATA

STRUCTURAL CONCRETE 03310

The QUIKRETE Companies

QUIKRETE

1. Product Name
QUIKRETE® 5000 High Early Strength Concrete Mix #1007

2. Manufacturer
The QUIKRETE Companies
One Securities Centre
3490 Piedmont Rd., NE, Suite 1300
Atlanta, GA 30305
(404) 634-9100
Fax: (404) 842-1424
www.quikrete.com

3. Product Description

BASIC USE

For any concrete use requiring high early strength and rapid strength gains. QUIKRETE 5000 sets quickly, making it ideal for cold weather applications. It has a walk-on time of 10 - 12 hours. QUIKRETE 5000 can be used for any application requiring concrete in a minimum thickness of 2" (51 mm), such as slabs, footings, steps, columns, walls and patios.

COMPOSITION & MATERIALS

QUIKRETE 5000 consists of a uniformly blended, properly proportioned mixture of stone or gravel, sand, Portland cement and other ingredients approved for use in concrete.

SIZES

- 60 lb (27.2 kg) bags
- 80 lb (36.3 kg) bags

YIELD

An 80 lb (36.3 kg) bag yields approximately 0.60 cu ft (17 L). A 60 lb (27.2 kg) bag yields approximately 0.45 cu ft (12.7 L).

LIMITATIONS

When used in structural elements, comply with the steel reinforcing and additional requirements of applicable building codes.

4. Technical Data

APPLICABLE STANDARDS

ASTM International - ASTM C387 Standard Specification for Packaged, Dry, Combined Materials for Mortar and Concrete

PHYSICAL/CHEMICAL PROPERTIES

QUIKRETE 5000 High Early Strength Concrete Mix exceeds the compressive strength requirements of ASTM C387, as shown in Table 1.

TABLE 1 TYPICAL PROPERTIES OF QUIKRETE 5000 CONCRETE MIX [1]

Cure time	Compressive strength
1 day	1500 psi (10.3 MPa)
3 day	2500 psi (17.2 MPa)
7 days	3500 psi (24.1 MPa)
28 days	5000 psi (34.5 MPa)
Slump range	2" - 3" (51 - 76 mm)

[1] Tested under standard laboratory conditions in accordance with ASTM C387.

5. Installation

MACHINE MIXING

- QUIKRETE 5000 can be mixed in a barrel-type concrete mixer or a mortar mixer. Choose the mixer size most appropriate for the size of the job to be done. Allow at least 1 cu ft (28 L) of mixer capacity for each 80 lb (36.3 kg) bag of QUIKRETE 5000 to be mixed at 1 time
- For each 80 lb (36.3 kg) bag of QUIKRETE 5000 to be mixed, add approximately 6 pt (2.8 L) of fresh water to the mixer. Turn on the mixer and begin adding the bags of concrete to the mixer
- If the material becomes too difficult to mix, add additional water until a workable mix is obtained
- If a slump cone is available, adjust water to achieve a 2" - 3" (51 - 76 mm) slump

Note - Final water content should be approximately 6 - 10 pt (2.8 - 4.7 L) per 80 lb (36.3 kg) bag and 4.5 - 7 pt (2.1 - 3.3 L) per 60 lb (27.2 kg) bag.

HAND MIXING

- Empty bags into a suitable mixing container
- Add approximately 6 pt (2.8 L) of clean water for each 80 lb (36.3 kg) bag
- Work the mix with a shovel, rake or hoe and add water as needed until a stiff, moldable consistency is achieved
- Do not exceed a total volume of 10 pt (4.7 L) per 80 lb (36.3 kg) bag or 7 pt (3.3 L) per 60 lb (27.2 kg) bag
- Be sure all material is wet; do not leave unabsorbed puddles of water

QUIKRETE® 5000 High Early Strength Concrete Mix #1007

TEMPERATURE OF WATER

Set times will fluctuate in extremely hot or cold weather. Use cold water or water mixed with ice cubes in severely hot weather; use hot water when mixing in severely cold weather.

SITE PREPARATION

Stake out the area and remove sod or soil to the desired depth. Nail and stake forms securely in place. Tamp the subbase until firm.

APPLICATION

- Dampen the subgrade before concrete is placed. Do not leave standing puddles
- Shovel or place the concrete into the form. Fill to the full depth of the form
- After the concrete has been compacted and spread to completely fill the forms, strike off and float immediately
- To strike off, use a straight board (screed), moving the edge back and forth with a saw-like motion to smooth the surface. Then use a darby or bull float to float the surface. This helps level any ridges and fill voids left by the straight edge
- Cut the concrete away from the forms by running an edging tool or trowel along the forms to compact the slab edges
- Cut 1" (25.4 mm) control joints into the slab every 6' - 8' (1.8 - 2.4 m) using a grooving tool
- Allow the concrete to stiffen slightly, waiting until all water has evaporated from the surface before troweling or applying a broom finish

Note - For best results, do not overwork the material.

CURING

General

Curing is one of the most important steps in concrete construction. Proper curing increases the strength and durability of concrete, and a poor curing job can ruin an otherwise well-done project. Proper water content and temperature are essential for good curing. In near freezing temperatures, the hydration process slows considerably. When weather is too hot, dry or windy, water is lost by evaporation from the concrete and hydration stops resulting in finishing difficulties and cracks. The ideal circumstances for curing are ample moisture and moderate temperature and wind conditions.

Curing should be started as soon as possible and should continue for a period of 5 days in warm weather, 70 degrees F (21 degrees C) or higher, or 7 days in colder weather, 50 - 70 degrees F (10 - 21 degrees C).

Specific Curing Methods

QUIKRETE Acrylic Concrete Cure & Seal provides the easiest and most convenient method of curing concrete.

- Apply by sprayer or roller after the final finishing operation when the surface is hard. The surface may be damp, but not wet, when applying curing compound. Complete coverage is essential
- Other methods of providing proper curing include covering the surface with wet burlap, keeping the surface wet with a lawn sprinkler and sealing the concrete surface with plastic sheeting
- If burlap is used, it should be free of chemicals that could weaken or discolor the concrete. New burlap should be washed before use. Place it when the concrete is hard enough to withstand surface damage and sprinkle it periodically to keep the concrete surface continuously moist
- Water curing with lawn sprinklers or hoses must be continuous to prevent interruption of the curing process
- Curing with plastic sheets is convenient. They must be laid flat, thoroughly sealed at joints and anchored carefully along edges

PRECAUTIONS

- Curing compounds should not be applied if rain or temperatures below 50 degrees F (10 degrees C) are expected within 24 hours
- Curing with plastic or burlap can cause patchy discoloration in colored concrete. For colored concrete, wet curing or chemical curing compounds are recommended
- Use of Acrylic Concrete Cure and Seal or other curing compounds is not recommended during late fall in northern climates on surfaces where de-icers will be used to melt ice and snow. Using curing compounds at that time may prevent proper air curing of the concrete, which is necessary to enhance its resistance to damage caused by deicers
- Protect concrete from freezing during the first 48 hours. Plastic sheeting and insulation blankets should be used if temperatures are expected to fall below 32 degrees F (0 degrees C)

6. Availability

QUIKRETE 5000 is available at leading concrete construction supply houses and distributors. Contact QUIKRETE Construction Products for the name of the nearest dealer.

7. Warranty

The QUIKRETE Companies warrant this product to be of merchantable quality when used or applied in accordance with the instructions herein. The product is not warranted as suitable for any purpose or use other than the general purpose for which it is intended. Liability under this warranty is limited to the replacement of its product (as purchased) found to be defective or, at the shipping companies' option, to refund the purchase price. In the event of a claim under this warranty, notice must be given to The QUIKRETE Companies in writing. This limited warranty is issued and accepted in lieu of all other express warranties and expressly excludes liability for consequential damages.

8. Maintenance

None required.

9. Technical Services

The QUIKRETE Companies maintain technical field representatives throughout the country. Contact a local distributor for the name and number of the nearest representative, or call QUIKRETE Construction Products.

10. Filing Systems

- First Source™
- Additional product information is available from the manufacturer.

6943-59

D2 QUIKRETE® 5000 High Early Strength Concrete Mix

THE QUIKRETE COMPANIES

Material Safety Data Sheet
[OSHA 29 CFR 1910.1200]

The QUIKRETE® Companies
One Securities Centre
3490 Piedmont Road, Suite 1300
Atlanta, GA 30329

Emergency Telephone Number
(770) 216-9580

Information Telephone Number
(770) 216-9580

Revision: July 2003

MSDS J

SECTION I: PRODUCT IDENTIFICATION

Product Types: QUIKRETE® DRY PACKAGED PORTLAND CEMENT BASED PRODUCTS (SERIES 1)

QUIKRETE® Product Name	Code #	QUIKRETE® Product Name	Code #
CONCRETE MIX	1101	FENCE POST MIX	1005
FIBER REINFORCED CONCRETE	1006	CRACK RESISTANT CONCRETE	1006-80
QUIKRETE® 5000	1007	LIGHT WEIGHT CONCRETE	1008
FAST SETTING CONCRETE	1004	RIP RAP	1129
SAND MIX	1103	VINYL CONCRETE PATCHER	1133, 1132
BASIC CONCRETE MIX	1015-60	HANDI-CRETE CONCRETE	1141
LIGHT WEIGHT SAND MIX	1103-51	HANDI-CRETE SAND MIX	1143
HIGH YIELD CONCRETE	1100	B-CRETE	1101-81
COMMERCIAL GRADE FASTSET™ CEMENT			1124-92
COMMERCIAL GRADE FASTSET™ NON SHRINK GROUT			1585-09
COMMERCIAL GRADE FASTSET™ REPAIR MORTAR			1241-60
COMMERCIAL GRADE FASTSET™ CONCRETE			1004-51
COARSE & FINE CORE FILL GROUTS (MASONRY GROUTS)			SR-9003, SR-9006
(ALSO APPLIES TO CUSTOM BLENDED AND PRIVATE LABEL CONCRETES AND MORTARS)			

SECTION II - HAZARDOUS INGREDIENTS/IDENTITY INFORMATION

Hazardous Components	CAS No.	PEL (OSHA) mg/M^3	TLV (ACGIH) mg/M^3
Silica Sand, crystalline	14808-60-7	$\frac{10}{\% SiO_2 + 2}$	0.05 (respirable)
Portland Cement	65997-15-1	5	5
Lime	01305-62-0	5	5
May contain one or more of the following:			
Amorphous Silica (From Fly Ash)	07631-86-9	$\frac{80\ mg/M^3}{\% SiO_2}$	10
Alumina (From Fly Ash)	01344-28-1	5	5
Limestone Dust	01317-65-3	5	5
Calcium Sulfate	10101-41-4 or 13397-24-5	5	5
Calcium Sulfo Aluminate	65997-16-2	15	10

Other Limits: NIOSH has recommended that the permissible exposure limit be changed to 50 micrograms respirable free silica per cubic meter of air (50 ug/M^3) averaged over a work shift of up to 10 hours per day, 40 hours per week. The NIOSH Criteria Document for Crystalline Silica should be consulted for more detailed information.

SECTION III - PHYSICAL/CHEMICAL CHARACTERISTICS

Appearance: Gray to gray-brown colored powder. Some products contain coarse aggregate. (QUIKRETE Vinyl Concrete Patcher available in white)

Specific Gravity:	2.6 to 3.15	**Melting Point:**	>2700 °F	**Boiling Point:**	>2700 °F
Vapor Pressure:	None	**Vapor Density:**	None	**Evaporation Rate:**	None
Solubility in Water:	Slight	**Odor:**	None	**Solubility in Water:**	Slight

SECTION IV - FIRE AND EXPLOSION HAZARD DATA

Non combustible and not explosive.

SECTION V - REACTIVITY DATA

Stability: Stable.
Incompatibility (Materials to Avoid): Contact of silica with powerful oxidizing agents such as fluorine, chlorine trifluoride, manganese trioxide, oxygen difluoride, may cause fires.
Hazardous Decomposition or Byproducts: Silica will dissolve in Hydrofluoric Acid and produce a corrosive gas - silicon tetrafluoride.
Hazardous Polymerization: Will not occur.
Condition to Avoid: Keep dry until used to preserve product utility.

SECTION VI - HEALTH HAZARD DATA

Route(s) of Entry:	Inhalation?	Yes
	Skin?	Yes
	Ingestion?	Yes

Acute Exposure: Product becomes alkaline when exposed to moisture. Exposure can dry the skin, cause alkali burns and effect the mucous membranes. Dust can irritate the eyes and upper respiratory system. Toxic effects noted in animals include, for acute exposures, alveolar damage with pulmonary edema.
Chronic Exposure: Dust can cause inflammation of the lining tissue of the interior of the nose and inflammation of the cornea. Hypersensitive individuals may develop an allergic dermatitis. Respirable crystalline silica (quartz) can cause silicosis, a fibrosis (scarring) of the lungs and possibly cancer. There is evidence that exposure to respirable silica or the disease silicosis is associated with an increased incidence of Scleroderma, tuberculosis and kidney disorders.

Carcinogenicity Listings:	NTP:	Known carcinogen
	OSHA:	Not listed as a carcinogen
	IARC Monographs:	Group 1 Carcinogen
	California Proposition 65:	Known carcinogen

NTP: The National Toxicology Program, in its "Ninth Report on Carcinogens" (released May 15, 2000) concluded that "Respirable crystalline silica (RCS), primarily quartz dusts occurring in industrial and occupational settings, is *known to be a human carcinogen*, based on sufficient evidence of carcinogenicity from studies in humans indicating a causal relationship between exposure to RCS and increased lung cancer rates in workers exposed to crystalline silica dust (reviewed in IAC, 1997; Brown *et al*., 1997; Hind *et al*., 1997)

IARC: The International Agency for Research on Cancer ("IARC") concluded that there was "*sufficient evidence* in humans for the carcinogenicity of crystalline silica in the forms of quartz or cristobalite from occupational sources", and that there is "*sufficient evidence* in experimental animals for the carcinogenicity of quartz or cristobalite." The overall IARC evaluation was that "crystalline silica inhaled in the form of quartz or cristobalite from occupational sources is *carcinogenic to humans (*Group 1)." The IARC evaluation noted that "carcinogenicity was not detected in all industrial circumstances or studies. Carcinogenicity may be dependent on inherent characteristics of the crystalline silica or on external factors affecting its biological activity or distribution of its polymorphs." For further information on the IARC evaluation, see IARC Monographs on the Evaluation of carcinogenic Risks to Humans, Volume 68, "Silica, Some Silicates..." (1997)

Signs and Symptoms of Exposure: Symptoms of excessive exposure to the dust include shortness of breath and reduced pulmonary function. Excessive exposure to skin and eyes especially when mixed with water can cause caustic burns as severe as third degree.

Medical Conditions Generally Aggravated by Exposure: Individuals with sensitive skin and with pulmonary and/or respiratory disease, including, but not limited to, asthma and bronchitis, or subject to eye irritation, should be precluded from exposure.

Emergency First Aid Procedures:

Eyes: Immediately flush eye thoroughly with water. Continue flushing eye for at least 15 minutes, including under lids, to remove all particles. Call physician immediately.

Skin: Wash skin with cool water and pH-neutral soap or a mild detergent. Seek medical treatment if irritation or inflammation develops or persists. Seek immediate medical treatment in the event of burns.

Inhalation: Remove person to fresh air. If breathing is difficult, administer oxygen. If not breathing, give artificial respiration. Seek medical help if coughing and other symptoms do not subside. Inhalation of large amounts of portland cement require immediate medical attention.

Ingestion: Do not induce vomiting. If conscious, have the victim drink plenty of water and call a physician immediately.

SECTION VII - PRECAUTIONS FOR SAFE HANDLING AND USE

Spills: If spilled, use dustless methods (vacuum) and place into covered container for disposal or use if not contaminated or wet. Use adequate ventilation.

Waste Disposal Method: The packaging and material may be land filled; however, material should be covered to minimize generation of airborne dust. This product is not classified as a hazardous waste under RCRA or CERCLA.

SECTION VIII - CONTROL MEASURES

Inhalation: DO NOT BREATHE DUST. In dusty environments, the use of an OSHA, MSHA or NIOSH approved respirator is recommended. Local exhaust can be used, if necessary, to control airborne dust levels.

Eyes: Wear tight fitting goggles.

Skin: The use of barrier creams or impervious gloves, boots and clothing to protect the skin from contact is recommended. Following work, workers should shower with soap and water. Precautions must be observed because burns occur with little warning -- little heat is sensed.

WARN EMPLOYEES AND/OR CUSTOMERS OF THE HAZARDS AND REQUIRED OSHA PRECAUTIONS ASSOCIATED WITH THE USE OF THIS PRODUCT.

NOTE: The information and recommendations contained herein are based upon data believed to be correct. However, no guarantee or warranty of any kind, express or implied, is made with respect to the information contained herein. We accept no responsibility and disclaim all liability for any harmful effects, which may be caused by exposure to silica contained in our products.

Appendix E

Sika® Construction Products Catalog Technical Information and Recommendations

Figure E1 SikaTop®122 Plus Technical Information and Recommendations

Construction

Product Data Sheet
Edition 8.2003
Identification no. 189
SikaTop 122 *Plus*

SikaTop® 122 *PLUS*

Two-component, polymer-modified, cementitious, trowel-grade mortar plus FerroGard 901 penetrating corrosion inhibitor

Description	SikaTop 122 *PLUS* is a two-component, polymer-modified, portland-cement, fast-setting, trowel-grade mortar. It is a high performance repair mortar for horizontal and vertical surfaces and offers the additional benefit of FerroGard 901, a penetrating corrosion inhibitor.
Where to Use	▪ On grade, above, and below grade on concrete and mortar. ▪ On horizontal surfaces. ▪ As a structural repair material for parking structures, industrial plants, walkways, bridges, tunnels, dams, and ramps. ▪ To level concrete surfaces. ▪ As an overlay system for topping/resurfacing concrete. ▪ Overlay in cathodic protection systems.
Advantages	▪ High compressive and flexural strengths. ▪ High early strengths. Opens to traffic fast: foot in 4-6 hours, pneumatic tire in 8-12 hours. ▪ High abrasion resistance. ▪ Increased freeze/thaw durability and resistance to deicing salts. ▪ Compatible with coefficient of thermal expansion of concrete - Passes ASTM C-884 (modified). ▪ Increased density - improved carbon dioxide resistance (carbonation) without adversely affecting water vapor transmission (not a vapor barrier). ▪ Enhanced with FerroGard 901, a penetrating corrosion inhibitor - reduces corrosion even in the adjacent concrete. ▪ Not flammable, non-toxic. ▪ Conforms to ECA/USPHS standards for surface contact with potable water. ▪ USDA approved for food industry. ▪ ANSI/NSF Standard 61 potable water approved.
Yield	0.51 cu. ft./unit mortar; 0.75 cu. ft./unit concrete; (SikaTop 122 + 42 lbs. 3/8 pea gravel)
Packaging	**Component 'A'** - 1-gal. plastic jug; 4/carton. **Component 'B'** - 61.5-lb. multi-wall bag.

Typical Data *(Material and curing conditions @ 73°F (23°C) and 50% R.H.)*

Shelf Life	One year in original, unopened packaging.
Storage Conditions	Store dry at 40°-95°F. **Condition material to 65°-75°F before using.** Protect Component 'A' from freezing. If frozen, discard.
Color	Concrete gray when mixed.
Mixing Ratio	Plant-proportioned kit, mix entire unit.
Application Time	Approximately 30 minutes.
Finishing Time	50-120 minutes

Note: All times start after adding Component 'B' to Component 'A' and are highly affected by temperature, relative humidity, substrate temperature, wind, sun and other job site conditions.

Density (wet mix) 136 lbs./cu. ft. (2.18 kg./l)
Flexural Strength (ASTM C-293) 28 days 2,000 psi (13.8 MPa)
Splitting Tensile Strength (ASTM C-496) 28 days 750 psi (5.2 MPa)
Bond Strength* (ASTM C-882 modified) 28 days 2,200 psi (15.2 MPa)
Compressive Strength (ASTM C-109)
1 day 3,000 psi (20.7 MPa)
7 days 5,500 psi (37.9 MPa)
28 days 7,000 psi (48.3 MPa)
Permeability (AASHTO T-277) 28 days Approx. 500 Coulombs. Electrical resistivity (ohm-cm) 28,000
Freeze/Thaw Resistance (ASTM C-666) 300 cycles 98%
Corrosion Testing for FerroGard 901
Cracked Beam Corrosion Tests:
Reduced corrosion rates 63% versus control specimens
ASTM G109 modified after 400 days

* Mortar scrubbed into substrate.

How to Use

Substrate Concrete, mortar, and masonry products.

Surface Preparation - Concrete/Mortar: Remove all deteriorated concrete, dirt, oil, grease, and all bond-inhibiting materials from surface. Be sure repair area is not less than 1/8 inch in depth. Preparation work should be done by high pressure water blast, scabbler, or other appropriate mechanical means to obtain an exposed aggregate surface with a minimum surface profile of ±1/16 inch (CSP-5). Saturate surface with clean water. Substrate should be saturated surface dry (SSD) with no standing water during application.

Reinforcing Steel: Steel reinforcement should be thoroughly prepared by mechanical cleaning to remove all traces of rust. Where corrosion has occurred due to the presence of chlorides, the steel

Construction

should be high-pressure washed with clean water after mechanical cleaning. For priming of reinforcing steel use Sika Armatec 110 EpoCem (consult Technical Data Sheet).

Priming

Concrete Substrate: Prime the prepared substrate with a brush or sprayed applied coat of Sika Armatec 110 EpoCem (consult Technical Data Sheet). Alternately, a scrub coat of SikaTop 122 Plus can be applied prior to placement of the mortar. The repair mortar has to be applied into the wet scrub coat before it dries.

Mixing

Pour approximately 7/8 of Component 'A' into the mixing container. Add Component 'B' (powder) while mixing continuously. Mix mechanically with a low-speed drill (400- 600 rpm) and mixing paddle or mortar mixer. Add remaining Component 'A' (liquid) to mix if a more loose consistency is desired. Mix to a uniform consistency, maximum 3 minutes. Thorough mixing and proper proportioning of the two components is necessary.

For SikaTop 122 *PLUS* concrete: Pour all of Component 'A' into mixing container. Add all of Component 'B' while mixing, then introduce 3/8 inch coarse aggregate at desired quantity. Mix to uniform consistency, maximum 3 minutes. Addition rate is 42 lbs. per bag (approx. 3.0 to 3.5 gal. by loose volume). The aggregate must be non-reactive (reference ASTMC1260, C227 and C289), clean, well-graded, saturated surface dry, have low absorption and high density, and comply with ASTM C 33 size number 8 per Table 2.

Note: Variances in the quality of the aggregate will affect the physical properties of SikaTop 122 *PLUS*. The yield is increased to 0.75 cu. ft./unit with the addition of the aggregate (42 lbs.). Do not use limestone aggregate.

Application & Finish

SikaTop 122 *PLUS* **must be scrubbed** into the substrate, filling all pores and voids. Force material against edge of repair, working toward center. After filling repair, consolidate, then screed. Allow mortar or concrete to set to desired stiffness, then finish with wood or sponge float for a smooth surface, or broom or burlap-drag for a rough finish.

Curing

As per ACI recommendations for portland cement concrete, curing is required. Moist cure with wet burlap and polyethylene, a fine mist of water or a water based* compatible curing compound. Curing compounds adversely affect the adhesion of following layers of mortar, leveling mortar or protective coatings. Moist curing should commence immediately after finishing. Protect newly applied material from direct sunlight, wind, rain and frost.

*Pretesting of curing compound is recommended.

Limitations

Application thickness:	Min.	Max. in one lift
Neat	1/8 inch (3 mm)	1 inch (25 mm)
Extended	1 inch (25 mm)	4 inches (100 mm)

- Minimum ambient and surface temperatures 45°F (7°C) and rising at time of application.
- Addition of coarse aggregates may result in variations of the physical properties of the mortar.
- Do not use solvent-based curing compound.
- Size, shape and depth of repair must be carefully considered and consistent with practices recommended by ACI. For additional information, contact Technical Service.
- For additional information on substrate preparation, refer to ICRI Guideline No.03732 Coatings, and Polymer Overlays.
- If aggressive means of substrate preparation is employed, substrate strength should be tested in accordance with ACI 503 Appendix A prior to the repair application.
- As with all cement based materials, avoid contact with aluminum to prevent adverse chemical reaction and possible product failure. Insulate potential areas of contact by coating aluminum bars, rails, posts etc. with an appropriate epoxy such as Sikadur Hi-Mod 32.

Caution

Component 'A' - Irritant - May cause skin/eye/respiratory irritation. Avoid breathing vapors. Use with adequate ventilation. Avoid skin and eye contact. Safety goggles and rubber gloves are recommended.

Component 'B' - Irritant; suspect carcinogen - Contains portland cement and sand (crystalline silica). Skin and eye irritant. Avoid contact. Dust may cause respiratory tract irritation. Avoid breathing dust. Use only with adequate ventilation. May cause delayed lung injury (silicosis). IARC lists crystalline silica as having sufficient evidence of carcinogenicity in laboratory animals and limited evidence of carcinogenicity in humans. NTP also lists crystalline silica as a suspect carcinogen. Use of safety goggles and chemical resistant gloves is recommended. If PELs are exceeded, an appropriate, NIOSH approved respirator is required. Remove contaminated clothing.

First Aid

In case of skin contact, wash thoroughly with soap and water. For eye contact, flush immediately with plenty of water for at least 15 minutes, and contact a physician. For respiratory problems, remove person to fresh air.

Clean Up

In case of spillage, scoop or vacuum into appropriate container, and dispose of in accordance with current, applicable local, state and federal regulations. Keep container tightly closed and in an upright position to prevent spillage and leakage. **Mixed components:** Uncured material can be removed with water. Cured material can only be removed mechanically.

KEEP CONTAINER TIGHTLY CLOSED — KEEP OUT OF REACH OF CHILDREN
NOT FOR INTERNAL CONSUMPTION — FOR INDUSTRIAL USE ONLY
CONSULT MATERIAL SAFETY DATA SHEET FOR MORE INFORMATION

Sika warrants this product for one year from date of installation to be free from manufacturing defects and to meet the technical properties on the current technical data sheet if used as directed within shelf life. User determines suitability of product for intended use and assumes all risks. Buyer's sole remedy shall be limited to the purchase price or replacement of product exclusive of labor or cost of labor.

NO OTHER WARRANTIES EXPRESS OR IMPLIED SHALL APPLY INCLUDING ANY WARRANTY OF MERCHANTABILITY OR FITNESS FOR A PARTICULAR PURPOSE. SIKA SHALL NOT BE LIABLE UNDER ANY LEGAL THEORY FOR SPECIAL OR CONSEQUENTIAL DAMAGES.

Visit our website at www.sikausa.com — **1-800-933-SIKA NATIONWIDE**

Regional Information and Sales Centers. For the location of your nearest Sika sales office, contact your regional center.

Sika Corporation
201 Polito Avenue
Lyndhurst, NJ 07071
Phone: 800-933-7452
Fax: 201-933-6225

Sika Canada Inc.
601 Delmar Avenue
Pointe Claire
Quebec H9R 4A9
Phone: 514-697-2610
Fax: 514-694-2792

Sika Mexicana S.A. de C.V.
Carretera Libre Celaya Km. 8.5
Corregidora, Queretaro
C.P. 76920 A.P. 136
Phone: 52 42 25 0122
Fax: 52 42 25 0537

QUALITY ISO 9001 9002 ACHIEVEMENT

Figure E2 Spec Component

CONCRETE RESTORATION SYSTEMS

Spec Component: SC-025-0300
SikaTop 122 Plus

DIVISION 3 - CONCRETE

Section - 03550 Concrete Toppings
03720 Concrete Resurfacing
03730 Concrete Rehabilitation

Part 1 – General

1.01 Summary

A. This specification describes the patching or overlay of interior and/or exterior horizontal surfaces with a polymer-modified, portland cement mortar/concrete.

1.02 Quality Assurance

A. Manufacturing qualifications: The manufacturer of the specified product shall be ISO 9001 certified and have in existence a recognized ongoing quality assurance program independently audited on a regular basis.

B. Contractor qualifications: Contractor shall be qualified in the field of concrete repair and protection with a successful track record of 5 years or more. Contractor shall maintain qualified personnel who have received product training by a manufacturer's representative

C. Install materials in accordance with all safety and weather conditions required by manufacturer or as modified by applicable rules and regulations of local, state and federal authorities having jurisdiction. Consult Material Safety Data Sheets for complete handling recommendations.

1.03 Delivery, Storage, and Handling

A. All materials must be delivered in original, unopened containers with the manufacturer's name, labels, product identification, and batch numbers. Damaged material must be removed from the site immediately.

B. Store all materials off the ground and protect from rain, freezing or excessive heat until ready for use.

C. Condition the specified product as recommended by the manufacturer.

1.04 Job Conditions

A. Environmental Conditions: Do not apply material if it is raining or snowing or if such conditions appear to be imminent. Minimum application temperature 45ºF (7ºC) and rising.

B. Protection: Precautions should be taken to avoid damage to any surface near the work zone due to mixing and handling of the specified material.

1.05 Submittals

A. Submit two copies of manufacturer's literature, to include: Product Data Sheets, and appropriate Material Safety Data Sheets (MSDS).

1.06 Warranty

A. Provide a written warranty from the manufacturer against defects of materials for a period of five (5) years, beginning with date of substantial completion of the project.

Part 2 - Products

2.01 Manufacturer

A. **SikaTop 122 Plus**, as manufactured by Sika Corporation, is considered to conform to the requirements of this specification.

2.02 Materials

A. Polymer-modified Portland cement mortar:

1. Component A shall be a liquid polymer emulsion of an acrylic copolymer base and additives.
   a. pH: 4.5-6.5
   b. Film Forming Temperature: 73°F max.
   c. Tear Strength: 950-psi min.
   d. Elongation at Break: 500% min.
   e. Particle Size: less than 0.1 micron
2. Component A shall contain an organic, penetrating corrosion inhibitor which has been independently proven to reduce corrosion in concrete via ASTM G3 (half-cell potential tests). The corrosion inhibitor shall not be calcium nitrite, and shall have a minimum of 5 years of independent field testing to document performance on actual construction projects.
3. Component B shall be a blend of selected portland cements, specially graded aggregates, admixtures for controlling setting time, water reducers for workability, and an organic accelerator.
4. The materials shall be non-combustible, both before and after cure.
5. The materials shall be supplied in a factory-proportioned unit.
6. The polymer-modified, portland cement mortar must be placeable from 1/8-in. to 1-in. in depth per lift for horizontal applications.

B. To prepare a polymer-modified portland cement concrete: aggregate shall conform to ASTM C-33. The factory-proportioned unit shall be extended with 42-lb. max. of a 3/8 in. (No.8 distribution per ASTM C-33, Table II) clean, well-graded, saturated surface dry aggregate, having low absorption and high density. Aggregate must be approved for use by the Engineer.

2.03 Performance Criteria

A. Typical Properties of the mixed polymer-modified, portland cement mortar:

1. Working Time: Approximately 30 minutes
2. Finishing Time: 50-120 minutes
3. Color: concrete gray

B. Typical Properties of the cured polymer-modified, portland cement mortar:

1. Compressive Strength (ASTM C-109 Modified)
   a. 1 day: 3000 psi min. (20.7 MPa)
   b. 7 day: 5500 psi min. (37.9 MPa)
   c. 28 day: 7000 psi min. (48.3 MPa)
2. Flexural Strength (ASTM C-293) @ 28 days: 2000 psi (13.8 MPa)
3. Splitting Tensile Strength (ASTM C-496) @ 28 days 750 psi (5.2 MPa)
4. Bond Strength (ASTM C-882 Modified) @ 28 days: 2200 psi (15.2 MPa)
5. The portland cement mortar shall not produce a vapor barrier.
6. Density(wet mix): 136 lbs. / cu. ft. (2.18 kg/l)
7. Permeability (AASHTO T-277 @ 28 days Approximately 500 Coulombs)

Note: Tests above were performed with the material and curing conditions @ 71°F – 75°F and 45-55% relative humidity.

Part 3 – Execution

3.01 Surface Preparation

A. Areas to be repaired must be clean, sound, and free of contaminants. All loose and deteriorated concrete shall be removed by mechanical means. Mechanically prepare the concrete substrate to obtain a surface profile of +/- 1/16" (CSP 5 or greater as per ICRI Guidelines) with a new exposed aggregate surface. Area to be patched shall not be less than 1/8" in depth.

B. Where reinforcing steel with active corrosion is encountered, sandblast the steel to a white metal finish to remove all contaminants and rust. Where corrosion has occurred due to the presence of chlorides, the steel shall be high pressure washed after mechanical cleaning. Prime steel with 2 coats of Sika Armatec 110 EpoCem as directed by manufacturer. (See Spec Component SC-201-0699)

3.02 Mixing and Application

A. Mechanically mix in appropriate sized mortar mixer or with a Sika jiffy paddle and low speed (400-600 rpm) drill. Pour approximately 4/5 gal Component A into the mixing container. Add Component B while continuing to mix. Mix to a uniform consistency for a maximum of three minutes. Add remaining Component A to mix if a more loose consistency is desired. Should smaller quantities be needed, be sure the components are measured in the correct ratio and that the Component B is uniformly blended before mixing the components together. Mix only that amount of material that can be placed in 30 minutes. Do not retemper material.

B. Mixing of the polymer-modified portland cement concrete: Pour all (1-gallon) of Component A into the mixing container. Add Component B while continuing to mix. Add correct amount of the pre-approved coarse aggregate, and continue mixing to a uniform consistency. Mixing time should be 3 minutes maximum.

C. Placement Procedure: At the time of application, the substrate should be saturated surface dry with no standing water. Mortar and/or concrete must be scrubbed into substrate filling all pores and voids. While the scrub coat is still plastic, force material against edge of repair, working toward center. If repair area is too large to fill while scrub coat is still wet use Sika Armatec 110 EpoCem in lieu of scrub coat (See Spec Component SC-200). After filling, consolidate, then screed. Allow mortar or concrete to set to desired stiffness, then finish with trowel, manual or power, for smooth surface. Broom or burlap drag for rough surface. Areas where the depth of the repair is less than 1-inch shall be repaired with polymer-modified portland cement mortar. In areas where the depth of the repair is greater than 1 inch, the repair shall be made with polymer-modified portland cement concrete.

D. As per ACI recommendations for portland cement concrete, curing is required. Moist cure with wet burlap and polyethylene, a fine mist of water or a water-based* compatible curing compound. Moist curing should commence immediately after finishing and continue for 48 hours. Protect newly applied material from rain, sun, and wind until compressive strength is 70% of the 28-day compressive strength. To prevent from freezing cover with insulating material. Setting time is dependent on temperature and humidity.

*Pretesting of curing compound is recommended.

E. Adhere to all procedures, limitations and cautions for the polymer-modified portland cement mortar in the manufacturers current printed technical data sheet and literature.

3.05 Cleaning

A. The uncured polymer-modified portland cement mortar can be cleaned from tools with water. The cured polymer - modified portland cement mortar can only be removed mechanically.

B. Leave finished work and work area in a neat, clean condition without evidence of spillovers onto adjacent areas.

Figure E3 Material Safety Data Sheet for SikaTop122® Plus Part A

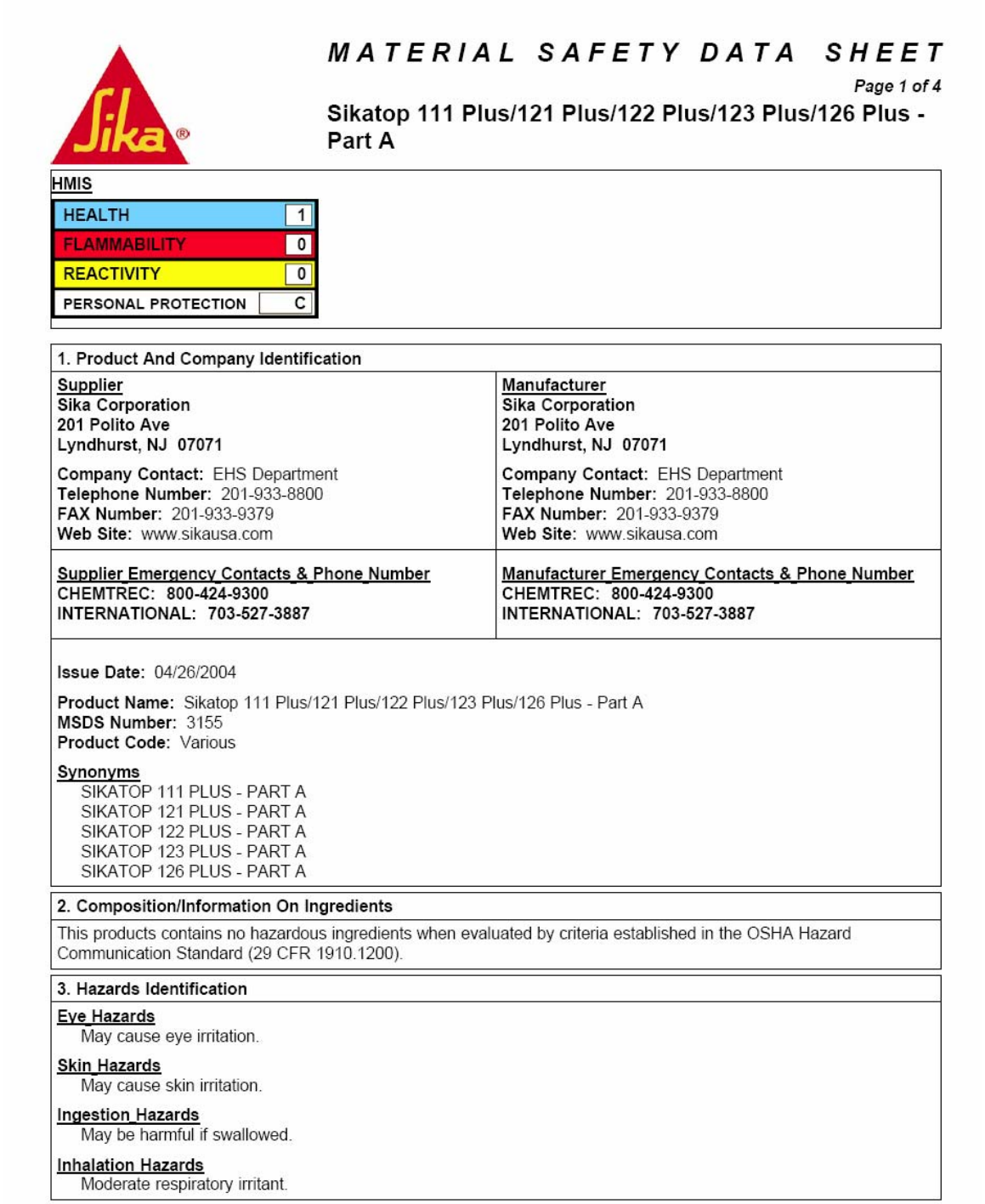

MATERIAL SAFETY DATA SHEET

Sikatop 111 Plus/121 Plus/122 Plus/123 Plus/126 Plus - Part A

HMIS

HEALTH	1
FLAMMABILITY	0
REACTIVITY	0
PERSONAL PROTECTION	C

1. Product And Company Identification

Supplier
Sika Corporation
201 Polito Ave
Lyndhurst, NJ 07071

Company Contact: EHS Department
Telephone Number: 201-933-8800
FAX Number: 201-933-9379
Web Site: www.sikausa.com

Manufacturer
Sika Corporation
201 Polito Ave
Lyndhurst, NJ 07071

Company Contact: EHS Department
Telephone Number: 201-933-8800
FAX Number: 201-933-9379
Web Site: www.sikausa.com

Supplier Emergency Contacts & Phone Number
CHEMTREC: 800-424-9300
INTERNATIONAL: 703-527-3887

Manufacturer Emergency Contacts & Phone Number
CHEMTREC: 800-424-9300
INTERNATIONAL: 703-527-3887

Issue Date: 04/26/2004

Product Name: Sikatop 111 Plus/121 Plus/122 Plus/123 Plus/126 Plus - Part A
MSDS Number: 3155
Product Code: Various

Synonyms
SIKATOP 111 PLUS - PART A
SIKATOP 121 PLUS - PART A
SIKATOP 122 PLUS - PART A
SIKATOP 123 PLUS - PART A
SIKATOP 126 PLUS - PART A

2. Composition/Information On Ingredients

This products contains no hazardous ingredients when evaluated by criteria established in the OSHA Hazard Communication Standard (29 CFR 1910.1200).

3. Hazards Identification

Eye Hazards
May cause eye irritation.

Skin Hazards
May cause skin irritation.

Ingestion Hazards
May be harmful if swallowed.

Inhalation Hazards
Moderate respiratory irritant.

Sikatop 111 Plus/121 Plus/122 Plus/123 Plus/126 Plus - Part A

4. First Aid Measures

Eye
In case of contact, hold eyelids apart and immediately flush eyes with plenty of tepid water for at least 15 minutes. Get medical attention immediately if irritation develops and persists.

Skin
In case of contact, immediately flush skin with soap and plenty of tepid water for at least 15 minutes. Get medical attention immediately if irritation (redness, rash, blistering) develops and persists.

Ingestion
If victim is fully conscious, give one or two cups of water or milk to drink. Call a physician if necessary.

Inhalation
Remove to fresh air. If not breathing, give artificial respiration. Call a physician if needed.

5. Fire Fighting Measures

Flash Point: >220 °F

Fire And Explosion Hazards
Material may splatter above 212F. Polymer film can burn.

Extinguishing Media
In case of fire, use water spray (fog) foam, dry chemical, or CO2.

Fire Fighting Instructions
In the event of a fire, firefighters should wear full protective clothing and NIOSH-approved self-contained breathing apparatus with a full facepiece operated in the pressure demand or other positive pressure mode.

6. Accidental Release Measures

Avoid release to the environment. Use appropriate Personal Protective Equipment (PPE). Contain spill and collect with absorbent material and transfer into suitable containers. Do not flush to sewer or allow to enter waterways. Ventilate enclosed area.

7. Handling And Storage

Handling And Storage Precautions
Keep out of reach of children. Store in a cool, dry, well ventilated area. Keep containers tightly closed.

Work/Hygienic Practices
Wash thoroughly with soap and water after handling.

8. Exposure Controls/Personal Protection

Engineering Controls
Use with adequate general and local exhaust ventilation. Refer to the current edition of "Industrial Ventilation: A Manual of Recommended Practice" published by the American Conference of Governmental Industrial Hygienists for information on the design, installation, use, and maintenance of exhaust systems.

Eye/Face Protection
Faceshield over safety glasses or goggles.

Skin Protection
Wear long sleeve shirt, long pants, chemical resistant gloves.

Respiratory Protection
A respirator protection program that meets 29 CFR 1910.134 requirement must be followed whenever workplace conditions warrant a respirator's use.

Sikatop 111 Plus/121 Plus/122 Plus/123 Plus/126 Plus - Part A

9. Physical And Chemical Properties

Appearance
Green Liquid

Odor
Acrylic smell

Chemical Type: Mixture
Physical State: Liquid
Percent VOCs: 0%
Packing Density: 8.5 pounds/gallon
Vapor Density: >AIR
Evaporation Rate: Slower then ether

10. Stability And Reactivity

Stability: Stable
Hazardous Polymerization: Will not occur

Conditions To Avoid (Stability)
Avoid Freezing

Incompatible Materials
None Known

Hazardous Decomposition Products
None Known

Conditions To Avoid (Polymerization)
None Known

11. Toxicological Information

Conditions Aggravated By Exposure
None Known

12. Ecological Information

No Data Available...

13. Disposal Considerations

Dispose in accordance with applicable federal, state and local government regulations. Waste generators must determine whether a discarded material is classified as a hazardous waste. USEPA guidelines for the classification determination are listed in 40 CFR Parts 261.3. Additionally, waste generators must consult state and local hazardous waste regulations to ensure complete and accurate classification.

14. Transport Information

Proper Shipping Name
Not Regulated by the USDOT.

15. Regulatory Information

U.S. Regulatory Information
All ingredients of this product are listed or are excluded from listing under the U.S. Toxic Substances Control Act (TSCA) Chemical Substance Inventory.

SARA Section 313 Notification
This product does not contain any ingredients regulated under Section 313 of the Emergency Planning and Community Right-To-Know Act of 1986 or 40 CFR 372.

Sikatop 111 Plus/121 Plus/122 Plus/123 Plus/126 Plus - Part A

16. Other Information

HMIS Rating
Health: 1
Fire: 0
Reactivity: 0
PPE: C

Revision/Preparer Information
MSDS Preparer: EHS Department
This MSDS Supercedes A Previous MSDS Dated: 12/16/2003

Disclaimer

Although reasonable care has been taken in the preparation of this document, we extend no warranties and make no representations as to the accuracy or completeness of the information contained therein, and assume no responsibility regarding the suitablility of this information for the user's intended purposes or for the consequences of its use. Each individual should make a determination as to the suitability of the information for their particular purposes(s).

SIKA CORPORATION

Figure E4 Material Safety Data Sheet for SikaTop122® Plus Part B

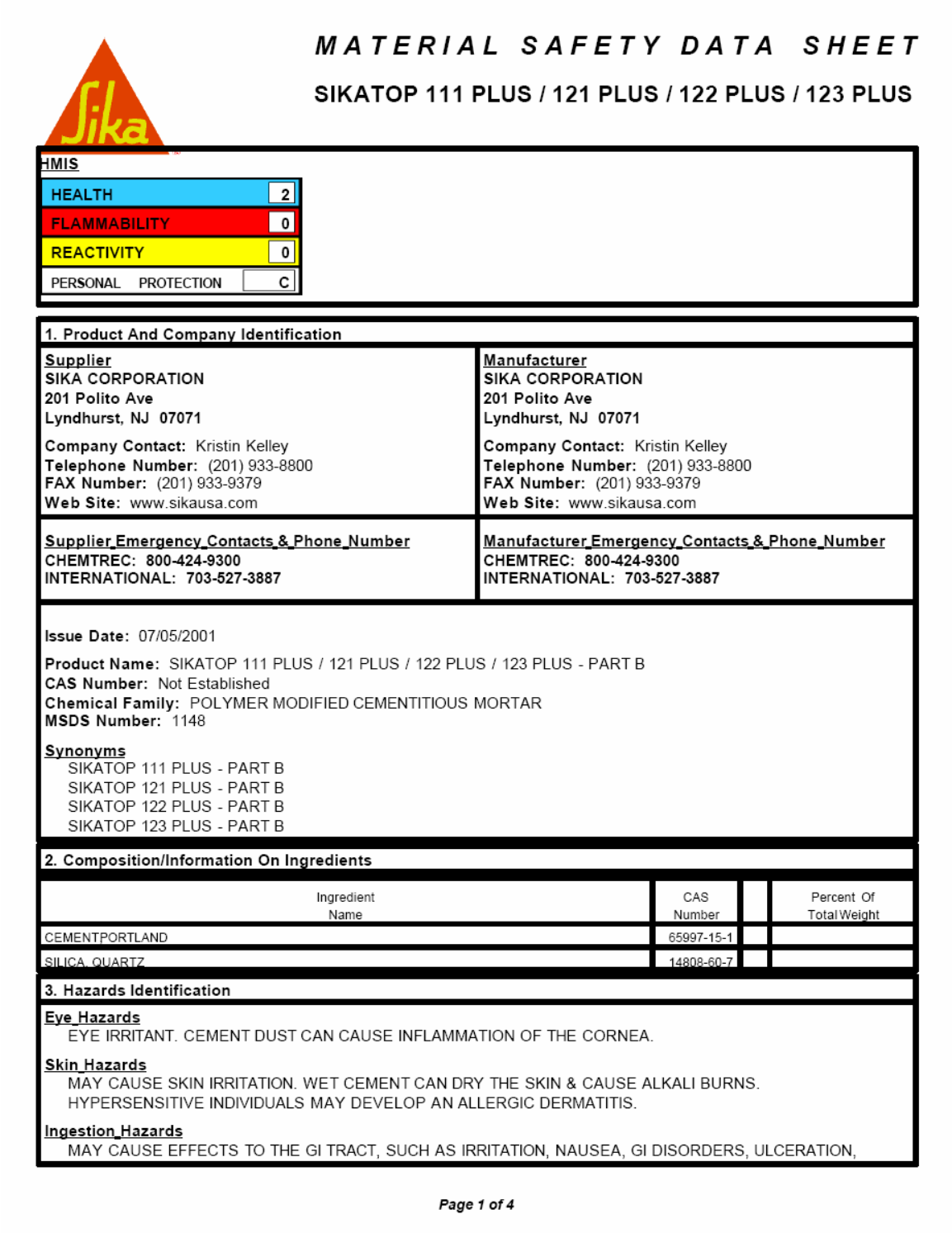

MATERIAL SAFETY DATA SHEET

SIKATOP 111 PLUS / 121 PLUS / 122 PLUS / 123 PLUS

HMIS

HEALTH	2
FLAMMABILITY	0
REACTIVITY	0
PERSONAL PROTECTION	C

1. Product And Company Identification

Supplier
SIKA CORPORATION
201 Polito Ave
Lyndhurst, NJ 07071

Company Contact: Kristin Kelley
Telephone Number: (201) 933-8800
FAX Number: (201) 933-9379
Web Site: www.sikausa.com

Manufacturer
SIKA CORPORATION
201 Polito Ave
Lyndhurst, NJ 07071

Company Contact: Kristin Kelley
Telephone Number: (201) 933-8800
FAX Number: (201) 933-9379
Web Site: www.sikausa.com

Supplier Emergency Contacts & Phone Number
CHEMTREC: 800-424-9300
INTERNATIONAL: 703-527-3887

Manufacturer Emergency Contacts & Phone Number
CHEMTREC: 800-424-9300
INTERNATIONAL: 703-527-3887

Issue Date: 07/05/2001

Product Name: SIKATOP 111 PLUS / 121 PLUS / 122 PLUS / 123 PLUS - PART B
CAS Number: Not Established
Chemical Family: POLYMER MODIFIED CEMENTITIOUS MORTAR
MSDS Number: 1148

Synonyms
SIKATOP 111 PLUS - PART B
SIKATOP 121 PLUS - PART B
SIKATOP 122 PLUS - PART B
SIKATOP 123 PLUS - PART B

2. Composition/Information On Ingredients

Ingredient Name	CAS Number		Percent Of Total Weight
CEMENT PORTLAND	65997-15-1		
SILICA, QUARTZ	14808-60-7		

3. Hazards Identification

Eye Hazards
EYE IRRITANT. CEMENT DUST CAN CAUSE INFLAMMATION OF THE CORNEA.

Skin Hazards
MAY CAUSE SKIN IRRITATION. WET CEMENT CAN DRY THE SKIN & CAUSE ALKALI BURNS.
HYPERSENSITIVE INDIVIDUALS MAY DEVELOP AN ALLERGIC DERMATITIS.

Ingestion Hazards
MAY CAUSE EFFECTS TO THE GI TRACT, SUCH AS IRRITATION, NAUSEA, GI DISORDERS, ULCERATION,

Page 1 of 4

3. Hazards Identification - Continued

Ingestion Hazards - Continued
DIARRHEA OR CONSTIPATION.

Inhalation Hazards
MAY CAUSE RESPIRATORY TRACT IRRITATION. CEMENT DUST CAN CAUSE INFLAMMATION OF THE LINING TISSUE OF THE INTERIOR OF THE NOSE. PROLONGED OR EXCESSIVE EXPOSURE TO RESPIRABLE SILICA CAN CAUSE SILICOSIS.

4. First Aid Measures

Eye
RINSE EYES THOROUGHLY WITH WATER FOR AT LEAST 15 MINUTES. CONSULT PHYSICIAN.

Skin
WASH SKIN THOROUGHLY WITH SOAP AND WATER. REMOVE CONTAMINATED CLOTHING. IF SYMPTOMS PERSIST, CONSULT PHYSICIAN.

Ingestion
DILUTE WITH WATER. CONSULT PHYSICIAN.

Inhalation
REMOVE TO FRESH AIR. IF BREATHING HAS STOPPED, INSTITUTE ARTIFICIAL RESPIRATION. CONSULT WITH PHYSICIAN.

5. Fire Fighting Measures

Flash Point: >200 °F

Fire And Explosion Hazards
NONE KNOWN

Extinguishing Media
In case of fire, use water spray (fog) foam, dry chemical, or CO2.

Fire Fighting Instructions
Firefighters should wear self-contained breathing apparatus and full protective gear.

6. Accidental Release Measures

SCOOP OR VACUUM UP AND PLACE INTO CLOSABLE CONTAINERS FOR LATER DISPOSAL.

7. Handling And Storage

Handling And Storage Precautions
STORE IN COOL DRY AREA.

Work/Hygienic Practices
Wash thoroughly with soap and water after handling.

8. Exposure Controls/Personal Protection

Engineering Controls
Use with adequate general and local exhaust ventilation.

Eye/Face Protection
Safety glasses with side shields or goggles.

8. Exposure Controls/Personal Protection - Continued

Skin Protection
AVOID SKIN CONTACT. WEAR LONG SLEEVE SHIRT AND LONG PANTS. CHEMICAL RESISTANT RUBBER OR PLASTIC GLOVES.

Respiratory Protection
In areas where the P.E.L.s are exceeded, use a properly fitted NIOSH-approved respirator.

Other/General Protection

Ingredient(s) - Exposure Limits
CEMENT, PORTLAND
ACGIH TLV-TWA - 10 mg/m3
OSHA PEL -TWA - 15 mg/m3 (total dust)
OSHA PEL - TWA - 5 mg/m3 (respirable dust)
SILICA, QUARTZ
ACGIH TLV-TWA 0.1 mg/m3 (Notice of Intended Change)
ACGIH TLV-TWA 0.05 mg/m3 (Proposed)
OSHA PEL-TWA 30/%SiO2+2 mg/m3
OSHA PEL-TWA 10/%SiO2+2 mg/m3
OSHA PEL-TWA 250/%SiO+5 mppcf

9. Physical And Chemical Properties

Appearance
GRAY MORTAR

Odor
NO ODOR

Chemical Type: Mixture
Physical State: Solid
Solubility: SOLUBLE

10. Stability And Reactivity

Stability: STABLE
Hazardous Polymerization: WILL NOT OCCUR

Conditions To Avoid (Stability)
NONE KNOWN

Incompatible Materials
NONE KNOWN

Hazardous Decomposition Products
NONE KNOWN

11. Toxicological Information

Conditions Aggravated By Exposure
EYE DISEASE, SKIN DISORDERS, CHRONIC RESPIRATORY CONDITIONS

Ingredient(s) - Carginogenicity
SILICA, QUARTZ
NTP - Listed On The National Toxicology Program
Listed In The IARC Monographs

12. Ecological Information

No Data Available...

13. Disposal Considerations

Dispose in accordance with applicable federal, state and local government regulations.

14. Transport Information

Proper Shipping Name
NOT REGULATED UNDER D.O.T.

15. Regulatory Information

U.S. Regulatory Information
All ingredients of this product are listed or are excluded from listing under the U.S. Toxic Substances Control Act (TSCA) Chemical Substance Inventory.

SARA Hazard Classes
Acute Health Hazard
Chronic Health Hazard

SARA Section 313 Notification
This product does not contain any ingredients regulated under Section 313 of the Emergency Planning and Community Right-To-Know Act of 1986 or 40 CFR 372.

State Regulations
WARNING: This product contains a chemical known to the State of California to cause cancer, birth defects, or other reproductive harm.

Ingredient(s) - State Regulations
SILICA, QUARTZ
New Jersey - Workplace Hazard
Pennsylvania - Workplace Hazard
California - Proposition 65
Massachusetts - Hazardous Substance

16. Other Information

HMIS Rating
Health: 2
Fire: 0
Reactivity: 0
PPE: C

Disclaimer

The data in this Material Safety Data Sheet relates only to the specific material herein and does not relate to use in combination with any other materialor in any process. The information set forth herein is based on technical da ta that Sika believes to be reliable as of the date hereof. Since conditions of use are outside our control, we make no warranties, express or implied andassume no liability in connection with any use of this information. Nothing herein is to be taken as a license to operate under or a recommendation to infringe any patents.

SIKA CORPORATION

Cited References

Acosta Costa, F.J. (1999). "Experimental characterization of the mechanical and structural properties of fiber reinforced polymeric bridge deck components." PhD Dissertation, Georgia Institute of Technology, Atlanta, U.S.

American Association of State Highway and Transportation Officials (AASHTO) LRFD Bridge Design Specifications (1998). Second Edition, Vol. 1.

Bathe, K., E. Wilson, and F. Peterson, SAP-IV: A Structural Analysis Program for Static and Dynamic Response of Linear Systems, Report No. EERC 73-11, College of Engineering, University of California, Berkeley, June 1973, Revised April 1974.

Brown, R.T. and Zureick, A. (1999). "Lightweight composite truss section decking." 3rd International Workshop on Very Large Floating Structures, Honolulu, Hawaii, U.S., paper 7-1-3

Bogdanovich, Alexander E. and Pastore, C. M. (1996). "Material-Smart Analysis of Textile Reinforced Structures," *Composites Science and Technology*, Vol. 56, pp. 291-309.

Bogdanovich, Alexander E. and Pastore, C. M. (1996). "Mechanics of Textile and Laminated Composites with Applications to Structural Analysis," Chapman & Hall.

Bogdanovich, Alexander E. and Mungalov, Dmitri. (2002). "Recent Advancements in Manufacturing 3-D Braided Preforms and Composites." *Proceedings of ACUN-4 "Composite Systems – Macrocomposites, Microcomposites, Nanocomposites,"* UNSW, Sydney, Australia, July 21-25, pp. 61-72.

Dickinson, L. C., G. L. Farley, M. K. Hinders (1999). "Translaminar Reinforced Composites: A Review," *Journal of Composites Technology & Research*, Vol. 21, No. 1, pp. 3-15.

Harik, I., Alagusundaramoorthy, P., Siddiqui, R., Lopez-Anido, R., Morton, S. Dutta, P., Dutta, P., and Sharooz, B. (1999). "Static testing on FRP bridge deck panels." Proceedings of the 44th International Sampe Symposium and Exhibition, Long Beach, California, U.S., pp. 1643-1654.

Henry, J.A. (1985). "Deck-girder systems for highway bridges using fiber reinforced plastics." M.S. Thesis, North Carolina State University, Raleigh, U.S.

Karbhari, V. M., Seible, F., Hegemier, G. A., and Zhao, L. (1997). "Fiber Reinforced Composite Decks for Infrastructure Renewal-Results and Issues." *Proceedings of the International Composites Expo'97*, Composite Institute, Nashville, TN, pp. 3-C(1-6)

Lopez-Anido, R., and GangaRao, H. V. S. (1997). "Design and Construction of Composite Material Bridges." *Recent Advances in Bridge Engineering*, Urs Meier and Raimondo Betti (Eds), pp. 269-276

Lopez-Anido, R., GangaRao, H. V. S., Vedam, V., and Overby, N. (1997a). "Design and Evaluation of a Modular FRP Bridge Deck." *Proceedings of the InternationalComposites Expo'97*, Composite Institute, Nashville, TN, pp. 3-E(1-6)

Lopez-Anido, R., GangaRao, H. V. S., Trovillion, J., and Busel, J. (1997b). "Development and Demonstration of a Modular FRP Deck for Bridge Construction and Replacement." *Proceedings of the International Composites Expo'97*, Composite Institute, Nashville, TN, pp.16-D(1-6)

Mohamed, Mansour H. (1996). "Weaving for Composites," in Textiles Used in Structural Composites, a Symposium sponsored by SAMPE and the Industrial Fabrics Association, March 25.

Mohamed, Mansour H., Bogdanovich, Alexander E., Ing, Habil., Dickinson, Larry., Singletary, James N., Lienhart, R. Bradley. (2001). "A New Generation of 3D Woven Fabric Preforms and Composites." *SAMPE Journal*, Vol. 37, No. 3, May/June, pp. 8-17.

Mohamed, Mansour H. and Dickinson, Larry C. (2000). "Recent Advances In 3D Weaving For Textile Preforming." *Proceedings of the ASME Aerospace Division*, The American Society of Mechanical Engineers, New York, NY, AD-Vol. 63, Book No. H01214, pp. 3-8.

Pastore, C. M., Bogdanovich, Alexander E., and Y. A. Gowayed, "Applications of a Meso-Volume Based Analysis for Textile Composite Structures," *Composites Engineering*, Vol. 3, No. 2, pp. 181-194.

U.S. Pat. 5,085,252 (Feb. 4, 1994) Mohamed, Mansour H. and Zhang, Z. (to North Carolina State University).

Singletary, J.N. and Bogdanovich, Alexander E. (2001). "Processing and Characterization of Novel 3-D Woven Composites," *Proceedings of SAMPE 2001 Conference*, Long Beach, CA, May 6-10.

Shih, Ban-Jwu (1995). On the Analysis of Fiber-Reinforced Polymeric Bridge Components. Ph.D. Thesis, Georgia Institute of Technology

Zureick, Abdul-Hamid., Shih, Ban-Jwu., Munley, E. (1995). "Fiber-Reinforced Polymeric Bridge Decks." *Structural Engineering Review*, Vol. 7, No. 3, pp. 257-266.